Open access • Report • DOI:10.2172/7142250

Spectra and optics of synchrotron radiation — Source link

G.K. Green

Published on: 15 Apr 1976

Topics: Synchrotron Radiation Source, Synchrotron radiation, Particle accelerator, Bremsstrahlung and Electromagnetic radiation

BNL 50522
(Particle Accelerators and
High-Voltage Machines - TID 4500)

SPECTRA AND OPTICS OF SYNCHROTRON RADIATION

G.K. Green

April 15, 1976

ACCELERATOR DEPARTMENT
BROOKHAVEN NATIONAL LABORATORY
ASSOCIATED UNIVERSITIES, INC.
UPTON, NEW YORK 11973

under contract No. E(30-1)-16 with the
UNITED STATES ENERGY RESEARCH AND DEVELOPMENT ADMINISTRATION

DISCLAIMER

NOTICE

PRINTED IN THE UNITED STATES OF AMERICA
Available from
National Technical Information Service
U.S. Department of Commerce
5285 Port Royal Road
Springfield, VA 22161

Price: Domestic $5.00
Foreign $7.50
Microfiche $2.25

Printed: June 1976 350 Copies

ABSTRACT

Sect. I The spectra, angular distribution and polarization functions of synchrotron radiation are tabulated in parametric form. Numerous graphs of the functions are included, and can be used for rapid estimation of photon flux as a function of the various parameters.

Sect. II The extended synchrotron radiation source is described and the exact, but unintegrable, equations are derived. Properties of this source depend upon at least nine parameters. An approximation of the source accurate enough for estimating flux in optical instruments is developed.

Sect. III Power and power density in the radiation beam are described and convenient approximations are developed.

Sect. IV Simple optical transformations are used to illustrate some of the important properties of the extended source described in Sect. II.

Appendix A Brief description and short table of the Bessel functions used.

Appendix B Outline of the properties of electron orbits in a storage ring.

Appendix C Description and short table of integrating function ef(a,Y).

I. Synchrotron Radiation Spectra

The basic equations of synchrotron radiation were published by Schwinger[1] and by Sokolov and Ternov.[2] Quantitative measurements of the radiation were given by Tomboulian and Hartman.[3] However, there is no reasonably complete numerical compendium of the spectra in the literature, and the required Bessel functions are not easily available in tables. (They are now readily generated by the large scientific computers.) Numerous review papers have been published, of which Mack,[4] Codling,[5] Rowe[6] and the Orsay Group[7] are good examples. The CEA internal report by Mack[4] is parametric in terms of flux per eV but is not now easy to obtain (see Appendix A). The Orsay Group paper has the most complete published survey of the spectra but the many graphs and tables apply specifically to the ACO and DCI rings. If one can find it (E.M. Rowe kindly sent me a copy) there is a useful report by Ellis and Stevenson[8] which tabulates $K_{1/3}$, $K_{2/3}$, $K_{5/3}$ and G(x).

This section is an attempt to summarize the characteristics of synchrotron radiation in parametric form. Tables and graphs are arranged to give values to two or three figures by inspection, or by use of a hand calculator.

1. Fundamental Equations

If an electron is moving with velocity v the quantity β is defined by

$$\beta = v/c$$

and the total energy of the electron is

$$E = \frac{m_o c^2}{\sqrt{1-\beta^2}} = \gamma\, m_o c^2 \qquad (1)$$

with m_o the electron rest mass and c the velocity of light. Since the rest energy of the electron is 0.5110 MeV

$$\gamma = 1957\ E_{GeV}$$

and at large values of γ we can put E as either total energy or kinetic energy with very small error. (Particle energy in accelerators is usually quoted as kinetic energy).

Since
$$\beta = (1 - 1/\gamma^2)^{\frac{1}{2}} \simeq 1 - 1/2\gamma^2 \qquad (2)$$

and even at $\gamma = 1000$ is less than 1 by only 1/2 part per million, β will be set equal to 1 and will not be explicitly included in the equations.

If the electron is moving in a circular path in magnetic field B the radius of curvature is

$$\rho = pc/eB = m_o \beta \gamma c^2/eB \tag{3}$$

and the energy radiated per turn is (Ref. 1, Eq. I.10)*

$$\delta E = 4\pi e^2 \gamma^4/3\rho \tag{4}$$

Schwinger[1] (Eq. II.16) derives the power per unit angular frequency of the radiation, ω, per electron, per unit time

$$P(\omega,t) = \frac{3^{3/2} e^2}{4\pi \rho} \gamma^4 \frac{\omega_o \omega}{\omega_c^2} \int_{\omega/\omega_o}^{\infty} K_{5/3}(\eta)\, d\eta \tag{5}$$

with $\omega_o = c/\rho$ and $\omega_c = \frac{3}{2} \omega_o \gamma^3 = 3c\gamma^3/2\rho$

Using $\frac{dX}{dw} = \frac{dX}{dv}\frac{dv}{dw}$ and the relationships

$$\omega = 2\pi\nu = 2\pi c/\lambda$$

$$\lambda_c = 2\pi c/\omega_c = 4\pi\rho/3\gamma^3$$

$$\lambda = (\lambda/\lambda_c)\, 4\pi\rho/3\gamma^3$$

$$\epsilon = h\nu = h\omega/2\pi = hc/\lambda$$

$$\omega/\omega_c = \nu/\nu_c = \epsilon/\epsilon_c = \lambda_c/\lambda = y$$

and defining the resolution by $k = \Delta\lambda/\lambda$; the power P and number of photons per sec N radiated into all space per electron are:

$$P(\lambda,t) = \frac{3^{5/2}}{16\pi^2} \frac{e^2 c \gamma^7}{\rho^3} \left(\frac{\lambda_c}{\lambda}\right)^3 \int_y^{\infty} K_{5/3}(\eta) d\eta \qquad \text{per unit } \lambda$$

$$N(\lambda,t) = \frac{3^{3/2}}{4\pi} \frac{e^2 \gamma^4}{h\rho^2} \left(\frac{\lambda_c}{\lambda}\right)^2 \int_y^{\infty} K_{5/3}(\eta) d\eta \qquad \text{per unit } \lambda \tag{6}$$

$$N_k(\lambda,t) = 3^{\frac{1}{2}} \frac{ke^2\gamma}{h\rho} \left(\frac{\lambda_c}{\lambda}\right) \int_y^{\infty} K_{5/3}(\eta) d\eta \qquad \text{per } k\lambda$$

*cgs units are used in accordance with Refs. 1 and 2.

$$N_{\Delta\varepsilon}(\varepsilon,t) = \frac{4\pi}{3^{\frac{1}{2}}} \frac{e^2 \Delta\varepsilon}{hc^2 \gamma^2} \int_y^\infty K_{5/3}(\eta)d\eta \qquad \text{per } \Delta\varepsilon$$

The ring current in amperes is related to the number of electrons and to the revolution frequency by

$$\frac{I}{10} = n \frac{e}{c} f = \frac{ne}{2\pi\rho} \tag{7}$$

(In a ring with field free sections the circumference C is greater than $2\pi\rho$ and $I/10 = ne/C$. But the number radiating is the fraction $2\pi\rho/C$ of the total so $n = 2\pi\rho I/10e$ in agreement with (7)). If the formuli of (6) are multiplied by n and by $\theta/2\pi$ the result is radiation in all vertical angles per current I and arc θ;*

$$P(\lambda,t) = \frac{3^{5/2}}{160\pi^2} \frac{ec\theta I\gamma^7}{\rho^2} \left(\frac{\lambda_c}{\lambda}\right)^3 \int_y^\infty K_{5/3}(\eta)d\eta \qquad \text{per unit } \lambda$$

$$N(\lambda,t) = \frac{3^{3/2}}{40\pi} \frac{e\theta I\gamma^4}{h\rho} \left(\frac{\lambda_c}{\lambda}\right)^2 \int_y^\infty K_{5/3}(\eta)d\eta \qquad \text{per unit } \lambda$$

$$N_k(\lambda,t) = \frac{3^{\frac{1}{2}}}{10} \frac{ke\theta I\gamma}{h} \left(\frac{\lambda_c}{\lambda}\right) \int_y^\infty K_{5/3}(\eta)d\eta \qquad \text{per } k\lambda \tag{8}$$

$$N_{\Delta\varepsilon}(\varepsilon,t) = \frac{4\pi}{10 \cdot 3^{\frac{1}{2}}} \frac{e\Delta\varepsilon\theta I}{h^2 c} \frac{\rho}{\gamma^2} \int_y^\infty K_{5/3}(\eta)d\eta \qquad \text{per } \Delta\varepsilon$$

$$\text{or} \qquad = \frac{3^{\frac{1}{2}}}{10} \frac{e\Delta\varepsilon\theta I}{h^2 c} \gamma\lambda_c \int_y^\infty K_{5/3}(\eta)d\eta \qquad \text{per } \Delta\varepsilon$$

The power radiated at all wavelengths as a function of angle ψ to the orbit is (Ref. 1, Eq. II.36)

$$P(\psi,t) = \frac{ce^2}{\rho^2} \gamma^5 \left\{ (1 + \gamma^2\psi^2)^{-5/2} \left[\frac{7}{16} + \frac{5}{16} \frac{\gamma^2\psi^2}{1 + \gamma^2\psi^2}\right] \right\} \tag{9}$$

$$\text{or} \qquad P(\psi,t) = \frac{ce\theta I}{10\rho} \gamma^5 F(\gamma\psi) \quad \text{per rad } \psi \qquad \text{ergs/sec}$$

*I in amps, θ in radians, ρ in cm, other units see p. 7.

2. Angular and Polarization Functions

Synchrotron radiation is normally generated over an orbital arc θ much larger than the radiation angle of emission, and is usually collected in such a manner as to sum over the angles in the orbital plane. We are then justified in taking the radiation from arc θ as $\theta/2\pi$ times the total from a complete circular orbit. The variation with angle ψ, relative to the orbital plane, is directly observable and is a complex function of γ, ρ, λ/λ_c and ψ.

Sokolov and Ternov[2] have examined the polarization in considerable detail. They compute that, if $\beta \approx 1$, the $\parallel$ polarized component of the radiation (electric vector parallel to the orbital plane) contains 7/8 of the total radiated power, and the $\perp$ component only 1/8. The proportion varies with wavelength. If W is the energy (per sec) radiated into all angles then (Ref. 2, p. 32)

$$dW_i = W\varphi_i(y)dy \qquad \text{with } y = \lambda_c/\lambda = \epsilon/\epsilon_c$$

$$\varphi_i(y) = \frac{9\sqrt{3}}{16\pi}\, y \left\{(\ell_2^2 + \ell_3^2) \int_y^\infty K_{5/3}(\eta)d\eta + (\ell_2^2 - \ell_3^2)\, K_{2/3}(y)\right\} \tag{10}$$

$\ell_2 = 1$, $\ell_3 = 0$ for $\parallel$ linear polarization; $\ell_2 = 0$, $\ell_3 = 1$ for $\perp$ linear polarization. If we could observe the radiation from a short segment of arc, $\Delta\theta \ll 1/\gamma$, the total $\perp$ component of radiation would appear to be four lobes, the axis of each lying at angle $1/2\gamma$ relative to the orbital plane, and $1/2\gamma$ relative to the normal plane through the tangent. Since only the most critical optics could resolve the θ angular structure, it is convenient to express the functions of ψ as an average over θ.

The power radiated by a single electron in solid angle $d\Omega$ is given by Sokolov and Ternov[2] (Eq. 5.17)

$$dP_i(\theta,\nu) = \frac{ce^2}{\rho^2}\frac{\nu^2}{6\pi^3}\left\{\ell_2 \epsilon K_{2/3}(\tfrac{\nu}{3}\epsilon^{2/3}) + \ell_3 \cos\theta \sqrt{\epsilon}\, K_{1/3}(\tfrac{\nu}{3}\epsilon^{3/2})\right\}^2 d\Omega$$

in which their θ is the complement of ψ. Harmonic order ν defines $\omega = \nu\omega_o = \nu c/\rho$

$$\omega_c = \frac{3\omega_o}{2}\gamma^3 \qquad \epsilon = 1 - \beta^2 \sin^2\theta \doteq \frac{1 + \gamma^2\psi^2}{\gamma^2}$$

and $\ell_2 = 1$, $\ell_3 = 0$ for $\parallel$; $\ell_2 = 0$, $\ell_3 = 1$ for $\perp$ polarization. If we set $\frac{dP}{d\psi} = 2\pi \frac{dP}{d\Omega}$ and substitute for ψ and ω

$$\frac{dP_i}{d\psi} = \frac{3e^2}{4\pi^2\rho}\left(\frac{\omega}{\omega_c}\right)^2 \gamma^2 \left\{(1+\gamma^2\psi^2)\left[\ell_2 K_{2/3}(\xi) + \ell_3\gamma\psi(1+\gamma^2\psi^2)^{-\frac{1}{2}} K_{1/3}(\xi)\right]\right\}^2$$

$$\xi = \frac{\omega}{2\omega_c}(1+\gamma^2\psi^2)^{3/2} = \frac{\lambda_c}{2\lambda}(1+\gamma^2\psi^2)^{3/2} \qquad (11)$$

or $$\frac{dP_i}{d\psi} = \frac{3e^2}{4\pi^2\rho}\left(\frac{\omega}{\omega_c}\right)^2 \gamma^2 F(\lambda_c/2\lambda, \gamma\psi)$$

If the two components are summed this equation is identical with Schwinger's angular distribution equation[1] II.34. Making the substitutions of the previous section gives the radiation per I amperes, arc θ and per radian of ψ;

$$P(\psi,\lambda,t) = \frac{27}{320\pi^3}\frac{ec\theta I\gamma^8}{\rho^2}\left(\frac{\lambda_c}{\lambda}\right)^4 F(\lambda_c/2\lambda,\gamma\psi) \quad \text{per unit } \lambda$$

$$N(\psi,\lambda,t) = \frac{9}{80\pi^2}\frac{e\theta I\gamma^5}{h\rho}\left(\frac{\lambda_c}{\lambda}\right)^3 F \quad \text{per unit } \lambda \qquad (12)$$

$$N_k(\psi,\lambda,t) = \frac{3ke\theta I\gamma^2}{20\pi\, h}\left(\frac{\lambda_c}{\lambda}\right)^2 F \quad \text{per } k\lambda$$

$$N_{\Delta\epsilon}(\psi,\lambda,t) = \frac{2\Delta\epsilon\; e\theta I\rho}{10h^2\, c\,\gamma}\left(\frac{\lambda_c}{\lambda}\right) F \quad \text{per } \Delta\epsilon$$

$$N_{\Delta\epsilon}(\psi,\epsilon,t) = \frac{8\pi}{30}\frac{\Delta\epsilon\; ec\theta I\,\rho^2}{h^3\, c^2\,\gamma^4} F \quad \text{per } \Delta\epsilon$$

At $\psi = 0$

$$F(\lambda_c/2\lambda,\ o) \equiv F_{\parallel}(0) = K^2_{2/3}(\lambda_c/2\lambda)$$

At angle ψ

$$F_{\parallel}(\psi) = (1 + \gamma^2\psi^2)^2 \, K^2_{2/3}\left[\frac{\lambda_c}{2\lambda}(1 + \gamma^2\psi^2)^{3/2}\right]$$
$$F_{\perp}(\psi) = \gamma^2\psi^2(1 + \gamma^2\psi^2) \, K^2_{1/3}\left[\frac{\lambda_c}{2\lambda}(1 + \gamma^2\psi^2)^{3/2}\right] \qquad (13)$$

for convenient normalization set

$$N_{\parallel}(\psi,\lambda) = N_{\parallel}(0) \, F_{\parallel}(\psi)/F_{\parallel}(0)$$
$$N_{\perp}(\psi,\lambda) = N_{\parallel}(0) \, F_{\perp}(\psi)/F_{\parallel}(0) \quad \text{and} \quad N = N_{\parallel} + N_{\perp} \qquad (14)$$

expressed as functions of γ, λ_c/λ and $\gamma\psi$

The degree of linear polarization is then

$$P = \frac{F_{\parallel} - F_{\perp}}{F_{\parallel} + F_{\perp}} \qquad (15)$$

In the orbital plane the polarization is linear and parallel. Out of the plane it is elliptical; the expressions are given by Sokolov and Ternov.[2] One rather remarkable feature of this elliptical polarization is a phase difference between components always $\pm \pi/2$, so that the axes of the polarization ellipse are always $\parallel$ and $\perp$ to the orbital plane.

3. Numerical Values

Both Schwinger and Sokolov and Ternov use cgs units in their equations. Substituting

$$e = 4.803 \times 10^{-10} \text{ esu}$$
$$c = 2.9979 \times 10^{10} \text{ cm/sec}$$
$$h = 6.6256 \times 10^{-27} \text{ erg sec}$$
$$1 \text{ ev} = 1.6021 \times 10^{-12} \text{ erg}$$
$$1 \text{ Å} = 10^{-8} \text{ cm}$$

(3) $\quad B\rho - 1704\,\gamma \text{ gauss cm} = 33.35\, E_{GeV} \text{ kgauss-m}$

(4) $\delta E = 88.5\ E^4_{GeV}/\rho_m$ kev per turn

(7) $n = 1.308 \times 10^{11} \rho_m I_a$ electrons radiating (16)

(5) $\lambda_c = 5.59\ \rho_m/E^3_{GeV} = 186.4/B_{kg}E^2_{GeV}$ Å

With ρ in meters, λ and λ_c in Å, ϵ in eV, I in amps and θ in radians

$$\epsilon_c = 2218\ E^3_{GeV}/\rho \text{ eV}$$

(8) $$P(\lambda,t) = 1.421 \times 10^{-13} \frac{\theta I \gamma^7}{\rho^2} \left(\frac{\lambda_c}{\lambda}\right)^3 \int_{y=\lambda_c/\lambda}^{\infty} K_{5/3}(\eta)d\eta \text{ ergs/Å sec} \quad \text{all } \psi$$

$$N(\lambda,t) = 2.998 \times 10^5 \frac{I\theta\gamma^4}{\rho} \left(\frac{\lambda_c}{\lambda}\right)^2 \int_y^{\infty} K_{5/3}(\eta)d\eta \text{ photons/Å sec} \quad \text{all } \psi \qquad (17)$$

$$N_k(\lambda,t) = 1.256 \times 10^{16} kI\theta\gamma \left(\frac{\lambda_c}{\lambda}\right) \int_y^{\infty} K_{5/3}(\eta)d\eta \text{ ph/k}\lambda \text{ sec} \quad \text{all } \psi$$

$$N_{\Delta\epsilon}(\lambda,t) = 4.242 \times 10^{22} \frac{I\theta\rho}{\gamma^2} \int_y^{\infty} K_{5/3}(\eta)d\eta$$

$$= 1.013 \times 10^{12} \gamma\lambda_c \int_y^{\infty} K_{5/3}(\eta)d\eta \text{ ph/eV sec} \quad \text{all } \psi$$

(9) $$P = 1.440 \times 10^{-15} \frac{\gamma^5 I}{\rho} F(\gamma\psi) \text{ w/mrad } \theta, \text{ mrad } \psi \qquad (18)$$

(12) $$P(\psi,\lambda,t) = 3.918 \times 10^{-14} \frac{\theta I \gamma^8}{\rho^2} \left(\frac{\lambda_c}{\lambda}\right)^4 F(\lambda_c/2\lambda, \gamma\psi) \text{ ergs/Å sec rad } \psi$$

$$N(\psi,\lambda,t) = 8.263 \times 10^4 \frac{\theta I \gamma^5}{\rho} \left(\frac{\lambda_c}{\lambda}\right)^3 F \text{ ph/Å sec rad } \psi$$

$$N_k(\psi,\lambda,t) = 3.461 \times 10^{15} k\theta I \gamma^2 \left(\frac{\lambda_c}{\lambda}\right)^2 F \text{ ph/k}\lambda \text{ sec rad } \psi \qquad (19)$$

$$N_{\Delta\epsilon}(\psi,\lambda,t) = 1.169 \times 10^{22} \frac{\theta I \rho}{\gamma} \left(\frac{\lambda_c}{\lambda}\right) F \text{ ph/eV sec rad } \psi$$

$$N_{\Delta\varepsilon}(\psi,\varepsilon,t) = 3.951 \times 10^{28} \frac{\varepsilon\theta I\rho^2}{\gamma^4} F \qquad \text{ph/eV sec rad } \psi$$

The function G was defined by Tomboulian and Hartman[3] as

$$G = y^3 \int_y^\infty K_{5/3}(\eta)d\eta$$

This can be generalized to

$$G_i = y^i \int_y^\infty K_{5/3}(\eta)d\eta \quad \text{with } i = 0,1,2,3 \tag{20}$$

Also let $H_i(y,o) = y^i K^2_{2/3}(y/2)$ (21)

We can now write (17) and (19) in power and photons per sec per ma and per mrad of θ and ψ (where applicable)

with $y = \lambda_c/\lambda = \varepsilon/\varepsilon_c$

(8)
$$P(\lambda) = 1.421 \times 10^{-19} \frac{\gamma^7}{\rho^2} G_3(y) \quad \text{ergs/Å, sec, ma, mrad } \theta, \text{ all } \psi$$

$$N(\lambda) = 2.998 \times 10^{-1} \frac{\gamma^4}{\rho} G_2(y) \quad \text{ph/Å, sec, ma, mrad } \theta \text{ all } \psi \tag{22}$$

$$N_k(\lambda) = 1.256 \times 10^{10} k\gamma G_1(y) \quad \text{ph/k}\lambda\text{, sec, ma, mrad } \theta \text{ all } \psi$$

$$N_{\Delta\varepsilon}(\lambda) = 4.24 \times 10^{16} \frac{\rho}{\gamma^2} G_o(y)$$

$$= 1.013 \times 10^6 \gamma\lambda_c G_o(y) \text{ ph/eV, sec, ma, mrad } \theta \text{ all } \psi$$

and at $\psi = 0$

(12)
$$P(\lambda,0) = 3.918 \times 10^{-23} \frac{\gamma^8}{\rho^2} H_4(y,0) \text{ ergs/Å, sec, ma, mrad } \theta, \text{ mrad } \psi$$

$$N(\lambda,0) = 8.263 \times 10^{-5} \frac{\gamma^5}{\rho} H_3(y,o) \text{ ph/Å, sec, ma, mrad } \theta, \text{ mrad } \psi \tag{23}$$

$$N_k(\lambda,o) = 3.461 \times 10^6 k\gamma^2 H_2(y,o) \text{ ph/k}\lambda\text{, sec, ma, mrad } \theta, \text{ mrad } \psi$$

$$N_{\Delta\epsilon}(\lambda,o) = 1.169 \times 10^{13} \frac{\rho}{\gamma} H_1(y,o) \quad \text{ph/eV, sec, ma, mrad } \theta\text{, mrad } \psi$$

$$N_{\Delta\epsilon}(\epsilon,o) = 3.951 \times 10^{19} \frac{\epsilon\rho^2}{\gamma^4} H_o(y,o) \quad \text{ph/eV, sec, ma, mrad } \theta\text{, mrad } \psi$$

Of the above functions the ones most useful in optics and spectroscopy are N_k and $N_{\Delta\epsilon}$. N_k, with k small, is directly related to the resolution of monochromators and spectrometers. $N_{\Delta\epsilon}$ can be directly applied to level widths and level density and so seems preferable to N per $\Delta\epsilon/\epsilon$, although $N_{\Delta\epsilon}$ is misleading at small ϵ just as N is misleading at small λ. $N(\lambda)$ is the function most often seen in the literature, although its usefulness is limited to those instruments which have constant rather than proportional resolution.

The flux functions of (22) and (23) are listed in Table I in terms of functions F_i. These functions are simply, as a matter of convenience, the numerical constant combined with the Bessel function. A short table of the Bessel functions is included in Appendix A. The functions F_o through F_6 are graphed in Figs. 1 through 7. For estimating flux it is then only necessary to select the multiplier from Table I and to apply it to the selected point of the corresponding curve. These log-log graphs are convenient because their shape remains fixed while the axes are translated by the multipliers.* $N_k(\lambda)$ and $N_k(\lambda,o)$ seem particularly useful because, for a given ratio of λ_c/λ, the flux is proportional only to γ or to γ^2 respectively. The parameter γ has been used, rather than E, because the angular functions are expressed more neatly in terms of γ.

A simple-minded log-log family of λ_c values is drawn in Figs. 8 and 9 for constant B and constant ρ. These families can be scanned for ranges of values, and are handy for sketching "tuning curves".

The fraction of power radiated at all wavelengths greater than λ is

$$\int_{\lambda}^{\infty} P(\lambda)d\lambda / P_{total}$$

and the number of photons at all wavelengths greater than λ is

*This is not true for Fig. 7 or for any function whose multipliers contain λ or ϵ explicitly,

TABLE I

General Relations
$\gamma = 1957\ E_{GeV}$
$B\rho = 1704\ \gamma$ gauss cm $= 33.35\ E_{GeV}$ kgauss-m
$\delta E = 88.5\ E^4_{GeV}/\rho_m$ kev per turn
$n = 1.308 \times 10^{11}\ \rho_m\ I_a$ electrons radiating
$\lambda_c = 5.59\ \rho_m/E^3_{GeV} = 186.4/B_{kg}E^2_{GeV}$ Å
$\lambda_c = 4.189 \times 10^{10}\ \rho_m/\gamma^3$ Å
$\epsilon = 12{,}398/\lambda$ eV, Å
$\epsilon_c = 2218\ E^3_{GeV}/\rho_m = 2.960 \times 10^{-7}\ \gamma^3/\rho_m$ eV
$y = \lambda_c/\lambda = \epsilon/\epsilon_c$

Flux in photons per sec, ma, mrad θ	
$N(\lambda) = \gamma^4/\rho\ F_o(\lambda_c/\lambda)$	per Å, all ψ
$N_k(\lambda) = k\gamma F_1(\lambda_c/\lambda)$	per kλ, all ψ
$N_{\Delta\epsilon}(\lambda) = (\rho/\gamma^2)F_2(\lambda_c/\lambda)$	
$= \gamma\lambda_c F_3(\lambda_c/\lambda)$	per eV, all ψ
$N_k(\lambda,0) = k\gamma^2 F_4(\lambda_c/\lambda,0)$	per kλ, mrad ψ at $\psi = 0$
$N_{\Delta\epsilon}(\lambda,0) = (\rho/\gamma)F_5(\lambda_c/\lambda,0)$	per eV, mrad ψ at $\psi = 0$
$N_{\Delta\epsilon}(\epsilon,0) = (\epsilon\rho^2/\gamma^4)F_6(\lambda_c/\lambda,0)$	per eV, mrad ψ at $\psi = 0$

$$\int_{\lambda}^{\infty} N(\lambda)d\lambda \Big/ \int_{o}^{\infty} N(\lambda)d\lambda$$

These two functions are plotted in Figs. 10 and 11 as % vs. λ/λ_c.

The power radiated (at all λ) as a function of ψ is derived from (9)

$$P(\psi) = 1.44 \times 10^{-18} \, (\gamma^5/\rho_m) \, F(\gamma\psi) \quad \text{w/ma, mrad } \theta, \text{ mrad } \psi$$

or

$$P(\psi) - (\gamma^5/\rho) \, F_7 \, (\gamma\psi) \tag{24}$$

with $F(\gamma\psi)$ and F_7 plotted in Fig. 12.

Linear polarization components vary with wavelength. The function of (10)

$$\varphi_i(y) = 0.3101 \, y \left\{(\ell_2^2 + \ell_3^2) \, G_o(y) + (\ell_2^2 - \ell_3^2) \, K_{2/3}(y)\right\}$$

is plotted in Fig. 13 for the $\parallel$ component ($\ell_2 = 1$, $\ell_3 = 0$), the $\perp$ component ($\ell_2 = 0$, $\ell_3 = 1$), and the total, vs. $\lambda/\lambda_c = 1/y$. The percentages* of $\parallel$ and of $\perp$ components radiated into all angles are plotted in Fig. 14.

At a given wavelength λ the flux varies with vertical angle ψ (13) as:

$$F_{\parallel}(\psi) = \left[1 + (\gamma\psi)^2\right]^2 K_{2/3}^2 \left\{\frac{\lambda_c}{2\lambda}\left[1 + (\gamma\psi)^2\right]^{3/2}\right\}$$

$$F_{\perp}(\psi) = (\gamma\psi)^2 \left[1 + (\gamma\psi)^2\right] K_{1/3}^2 \left\{\frac{\lambda_c}{2\lambda}\left[1 + (\gamma\psi)^2\right]^{3/2}\right\}$$

These functions are plotted in Fig. 15 as percentage* of $F_{\parallel}(0)$ vs. $\gamma\psi$ for λ/λ_c ratios ranging from 0.2 to 100. The sum, or variation of total flux vs. $\gamma\psi$, is also shown. Number of photons per sec, ma, mrad θ, mrad ψ at any ψ can then be found by multiplying the ratio of Fig. 15 by the appropriate $N(\lambda,o)$.

If the vertical acceptance angle $\Delta\psi$ is very small and is near $\psi = 0$ the flux is readily obtained as $N(\lambda,o)\,\Delta\psi$. For larger acceptance angles it is necessary to integrate the angular functions.

---

*Note that these percentages are functions of λ/λ_c rather than λ.

II. The Source

The previous section treated the radiation from a current of electrons as if the current were a filament, or for the angular functions, as if the electrons were travelling on parallel orbits. In an alternating gradient ring the electrons will oscillate about the central orbit and the oscillations will cause a spread in position and angle. This distribution of the beam in size and angle is modulated by the magnetic structure of the ring and the modulation produces a rather rapid variation of the transverse dimensions. Photons radiated by the electrons are distributed in angle about the trajectories of the particles and are emitted all along the trajectory. Thus we have a source which is extended in three dimensions in configuration space and in six dimensions in phase space. The properties of the source depend upon a sizeable number of parameters. In order to make the problem somewhat manageable the procedures reduce the description of the source to one in four phase space dimensions. There seems to be no very satisfactory general method. An outline of the source in laboratory space provides no angular information. A four-dimensional phase space solution is general, although very complex, but cannot be drawn. We must then use two two-dimensional diagrams. The curvilinear coordinate s is taken along the central electron orbit, assumed to lie in a plane. Transverse coordinate x is perpendicular to s and in the orbital plane, and $x' = dx/ds$. Since the angles are very small the paraxial approximation $\tan \eta \approx \sin \eta \approx \eta$ is quite good. Similarly, y and $y' = dy/ds$ lie in the plane perpendicular to the orbital plane. It is necessary to keep in mind that there are correlations between the x, x' plane and the y, y' plane and that the figures in these two planes must often be considered together.

The configuration of the electron beam as it goes along s is well known from accelerator orbit dynamics. Emittance of this beam is described by the Courant-Snyder invariant. When the electrons in an element ds emit photons the angular spread increases and the resulting photon distribution can then be characterized by an invariant for succeding optical transformations. If the photon distributions from all elements of a source extended in s are transformed to a single plane the result is a planar optical source which can be described by four phase space dimensions.

1. Source Derivation

The electron beam in a well-behaved storage ring will have an elliptical cross section in configuration space x,y (Fig. 16). Size of the beam is governed by the characteristics of the ring and by the quantum fluctuations of the emitted radiation. Since the latter are random a stabilized beam (e.g. one with small systematic instabilities) will have a normal distribution with probability density

$$P(x,y) = \frac{1}{2\pi\sigma_x\sigma_y} e^{-\left(\frac{x^2}{2\sigma_x^2} + \frac{y^2}{2\sigma_y^2}\right)} \tag{25}$$

The probability functions will be defined as

$$P(z) = \frac{1}{\sigma\sqrt{2\pi}} e^{-\frac{z^2}{2\sigma^2}}$$

$$\text{erf}(x) = \frac{2}{\sqrt{\pi}} \int_0^x e^{-t^2}\, dt \; ; \; \text{erf}\,(x/\sigma\sqrt{2}) = \frac{1}{\sigma\sqrt{2\pi}} \int_{-x}^{x} e^{-\frac{z^2}{2\sigma^2}}\, dz$$

and to normalize

$$\frac{2}{\sqrt{\pi}} \int_o^\infty e^{-t^2}\, dt = \sqrt{\frac{2}{\pi}}\,\frac{1}{\sigma} \int_o^\infty e^{-\frac{z^2}{2\sigma^2}}\, dz = 1 \tag{26}$$

$$\frac{P(o)}{\text{erf}\infty} = \frac{1}{\sqrt{2\pi}\,\sigma}$$

The current in element dx dy at x,y is

$$d^2I = \bar{I}_o\, P(x,y)\, dx\, dy \tag{27}$$

Electrons are distributed in phase space x,x′ and y,y′, and typical examples are shown in Fig. 16. Within the slice dy there is distribution in y′ (y′ = dy/ds is the angle of the electron trajectory to the central axis s). Consider the electron in element dydy′. On succesive transits of the ring it will take various positions indicated by the dotted ellipse in Fig. 16, provided the motion is not on a resonance. A resonance is obviously unallowable in a storage ring. These paths of all elements in the phase

plane are similar and, if y is a normal variate, then y' is also a normal variate. A brief description of particle dynamics of a storage ring is given in Appendix B.

An outline of the beam cross section in the y,y' plane as we proceed along s can be described by the Courant-Snyder invariant

$$\gamma y^2 + 2\alpha y y' + \beta y'^2 = E_y \tag{28}$$

This is an ellipse with coefficients α, β, γ which are functions of s and an area equal to π times the emittance E, a constant of the motion. There are constraints

$$\begin{aligned} \beta\gamma &= 1 + \alpha^2 \\ \alpha &= -\beta'/2 \end{aligned} \tag{29}$$

Figure 17a shows the beam envelope at a waist, or minimum of β, where we will set s = 0. Since $\alpha = 0$ at this s = 0 the emittance ellipse is

$$\gamma\, y^2 + \beta\, y'^2 = E$$

$$\hat{y} = \sqrt{E/\gamma}\ ,\ \hat{y}' = \sqrt{E/\beta}\ ,\ \beta\gamma = 1$$

It is preferable to express the maxima as

$$\hat{y} = \sqrt{E\beta}\ ,\ \hat{y}' = \sqrt{E\gamma}\ \text{ and } \hat{y}/\hat{y}' = \beta \tag{30}$$

(The third relation is not true if the ellipse axes are tilted.)

If the ellipse of Fig. 17a represents the one σ contour of $P(y,y')$ the one σ emittance becomes $\sigma_y \sigma_{y'}$, and the ellipse is described by

$$\frac{\sigma_{y'}}{\sigma_y} y^2 + \frac{\sigma_y}{\sigma_{y'}} y'^2 = \sigma_y \sigma_{y'} \tag{31}$$

At s the transverse coordinates y,y' are transformed by

$$\begin{vmatrix} y_1 \\ y_1' \end{vmatrix} = M_{(o/s)} \begin{vmatrix} y \\ y' \end{vmatrix}$$

and if there is no (magnetic) focussing the transformation matrix is

$$M_{(o/s)} = \begin{vmatrix} 1 & s \\ 0 & 1 \end{vmatrix} \tag{32}$$

Since synchrotron light sources are almost always bending magnets without gradient focussing, this matrix can be used to transform y,y' and x,x' along s rather than the more complex matrices of magnetic focussing systems. The one σ contour at s (Fig. 17b) is now

$$\frac{\sigma_{y'}}{\sigma_y} y^2 - 2\frac{\sigma_{y's}}{\sigma_y} yy' + \left(\frac{\sigma_y}{\sigma_{y'}} + \frac{\sigma_{y's}^2}{\sigma_y}\right) y'^2 = \sigma_y \sigma_{y'} \tag{33}$$

If a bivariate distribution is described by (Ref. 9, Sect. 26.3)

$$P(x,y) = \frac{1}{2\pi\sigma_x\sigma_y\sqrt{1-r^2}} e^{-\frac{1}{2(1-r^2)}\left(\frac{x^2}{\sigma_x^2} - \frac{2r\,xy}{\sigma_x\sigma_y} + \frac{y^2}{\sigma_y^2}\right)} \tag{34}$$

the one σ contour is

$$\frac{x^2}{\sigma_x^2} - \frac{2r\,xy}{\sigma_x\sigma_y} + \frac{y^2}{\sigma_y^2} = (1 - r^2) \tag{35}$$

and

$$\iint_A P(x,y)\,dxdy = 1 - e^{-\frac{1}{2}} = 0.39 \tag{36}$$

where the integral is taken over the area enclosed by (35). If the contour represents $n\sigma$ the integral value is $1 - e^{-\frac{n^2}{2}}$

n	integral
1	0.39
2	0.865
3	0.989
4	0.9997

A general elliptical contour (centered on the axes) is described by

$$gx^2 + 2axy + by^2 = 1 \tag{37}$$

and by equating coefficients to (34) or (35)

$$\begin{aligned} r^2 &= a^2/bg & (1-r^2) &= (bg-a^2)/bg \\ \sigma_x^2 &= bg/g(bg-a^2) & \sigma_y^2 &= bg/b(bg-a^2) \\ \text{area}/\pi &= 1/\sqrt{bg-a^2} \end{aligned} \tag{38}$$

The area is invariant under a linear transformation and it is often useful to set area/π = E, the "emittance" of the beam. Figure 18 lists several useful properties of (37) with the rh side replaced by E. If $(bg-a^2)$ is set equal to 1 (as is usually done in accelerator dynamics) the maxima of the ellipse are simply described

$$\hat{x} = \sqrt{Eb} \qquad \hat{y} = \sqrt{Eg} \tag{39}$$

Rewrite (33) with 1 on the rh side and (38) gives for the electron beam at s:

$$\begin{aligned} \sigma_{y_1}^2 &= \sigma_y^2 + s^2\,\sigma_{y'}^2 \\ \sigma_{y_1'}^2 &= \sigma_{y'}^2 \\ r_1^2 &= s^2\,\sigma_{y'}^2/(\sigma_y^2 + s^2\,\sigma_{y'}^2) \\ (1-r_1^2) &= \sigma_y^2/(\sigma_y^2 + s^2\,\sigma_{y'}^2) \end{aligned} \tag{40}$$

while (34) becomes

$$P_1(y,y') = \frac{1}{2\pi\sigma_y\sigma_{y'}}\, e^{-\frac{1}{2\sigma_y^2}\left[y^2 - 2syy' + (\sigma_y^2 + s^2\sigma_{y'}^2)\,y'^2\right]} \tag{41}$$

To obtain the total current in dy at y (Fig. 16) integrate (27) over all x

$$dI = I_o\, P(y)\, dy$$

and since $I_o \int_{-\infty}^{\infty} P(y)dy = I_o$

renormalize $$d^2I = I_o P_1(y,y')dydy' \tag{42}$$

When an electron at y,y' radiates its position y will not change instantaneously but the radiation will be distributed about its instantaneous direction according to

$$N_{k\parallel}(\psi,\lambda) = \frac{3keIds}{20\pi\rho h}\gamma^2\left(\frac{\lambda_c}{\lambda}\right)^2\left\{(1+\gamma^2\psi^2)^2 K^2_{2/3}\left[\frac{\lambda_c}{2\lambda}(1+\gamma^2\psi^2)^{3/2}\right]\right\}\Delta\psi \tag{43}$$

obtained from (12) and (13) by setting $I\theta = Ids/\rho$ to give number of photons per amp in the element ds. $N_{k\parallel}$ is somewhat arbitarily selected to simplify the expressions, and because the $\parallel$ component is reflected or diffracted most efficiently with vertical dispersion. If we define the radiation angle as Y' then $\psi = Y'-y'$ and the number of photons from ds in dY' from electron current in $dy\,dy'$ is

$$d^4N = I_o P_1(y,y')\frac{N_{k\parallel}}{I}(Y'-y',\lambda)\,dy\,dy'\,dY' \tag{44}$$

The number of photons in dY' at Y' as a function of y is

$$d^3N = I_o\frac{dydY'}{2\pi\sigma_y\sigma_{y'}}e^{-\frac{y^2}{2\sigma_y^2}}\int_{-\infty}^{\infty}\frac{1}{I}N_{k\parallel}(Y'-y',\lambda)\,e^{\frac{1}{2\sigma_y^2}\left[2syy'-(\sigma_y^2+s^2\sigma_{y'}^2)y'^2\right]}dy' \tag{45}$$

for a given value of γ and λ_c/λ.

An optical system can be represented by an optical transformation. If a source is extended along the optical axis the elements of the source can be successively transformed into a surface in the image space in order to compute the image. However, if $M(s_i/s_j)$ is the transformation along the optical axis from s_i to s_j then

$$M(s_o/s_N) = M(s_{N-1}/s_N)\ldots M(s_o/s_1)$$

Then if $M(s_1/s_N)$ transforms a surface in the object space to the desired surface in the image space we can transform all the elements of the orbit to s_1 and create a synthesized object. This can then be transferred to the image space by a single transformation. The synchrotron light source is extended in the direction of the optical axis and it is reasonable to transform all the elements of the source to the transverse plane at its center. The transformation is

$$\begin{vmatrix} y_2 \\ Y_2' \end{vmatrix} \quad \begin{vmatrix} 1 & -s \\ 0 & 1 \end{vmatrix} \quad \begin{vmatrix} y_1 \\ Y_1' \end{vmatrix} \tag{46}$$

and the number of photons at Y' as a function of y_2, in $dy_2 dY'$, can be obtained by integrating (45) over the range of s. Since $N_{k\|}$ was defined as photons per ds

$$d^2N = \frac{dy_2 dY' I_o}{2\pi\sigma_y\sigma_{y'}} \int_{s_1}^{s_1} e^{-\frac{(y_2+sY')^2}{2\sigma_y^2}} \left[\frac{1}{I} \int_{-\infty}^{\infty} N_{k\|}(Y'-y',\lambda)\, e^{\frac{1}{2\sigma_y^2}\left[2s(y_2+sY')y' - (\sigma_y^2+s^2\sigma_{y'}^2)y'^2\right]} dy' \right] ds \tag{47}$$

where y_2, Y' are the y phase coordinates at s = 0, defined as the position of a waist of the electron beam. This would be the situation at the focus in an insertion. If the source lies between s_1 and s_2 and the next waist projected from s_1 is at $s = 0$, the source plane will be at $\bar{s} = (s_1+s_2)/2$. The equation replacing (47) is integrated from s_1 to s_2 and is obtained from (45) by the transformation

$$\begin{vmatrix} 1 & -(s-\bar{s}) \\ 0 & 1 \end{vmatrix}$$

Equation (47) was obtained by assuming that the central orbit lies in the plane y = 0, a condition reasonably well satisfied when a storage ring is in good adjustment. In the x phase plane Eq. (45), with y, Y' replaced by x, X', represents the radiation from arc element ds. But xX' are the coordinates relative to s at ds.

The optical axis projects on the plane s = 0 at (Fig. 19)

$$x^2 = s^2/2\rho \ , \ x_2' = s/\rho$$

and the transformation from s to s = 0 becomes

$$\begin{vmatrix} x_2 \\ x_2' \end{vmatrix} = \begin{vmatrix} 1 & -s \\ 0 & 1 \end{vmatrix} \begin{vmatrix} x \\ x' \end{vmatrix} + \begin{vmatrix} \frac{s^2}{2\rho} \\ \frac{s}{\rho} \end{vmatrix} \tag{48}$$

Eq. (47) expressed in x,x' then becomes, projected on s = 0

$$d^2N = \frac{I_o dx_2 dx_2'}{2\pi\sigma_x\sigma_{x'}} \int_{-s_1}^{s_1} e^{-\frac{1}{2\sigma_x^2}\left[x_2+s(X_2'\frac{s}{\rho})-\frac{s^2}{2\rho}\right]^2} \left[\frac{1}{I}\int_{-\infty}^{\infty} Nk_{\parallel}(x_2' - \frac{s}{\rho} - x', \lambda) \right.$$

$$\left. e^{-\frac{1}{2\sigma_x^2}\left\{2s\left[x_2+s(x_2'-\frac{s}{\rho})-\frac{s^2}{2\rho}\right]x'-(\sigma_x^2+s^2\sigma_{x'}^2)x'^2\right\}_{dx'}} \right] ds \tag{49}$$

2. Approximation of the Source

The expressions of the preceeding sections can be systematized and numerically integrated, but they are too unwieldy for estimating the effects of the several parameters. The electron distribution is described by a normal probability function and, since the manipulation of these functions is well known, approximation of the radiation distribution by a probability function is indicated. From (17)(19)(20)(21)

$$N_k(\lambda) = 1.256 \times 10^{16}\ k\theta I\gamma G_1$$

$$N_{k\parallel}(\psi,\lambda) = 3.461 \times 10^{15}\ k\theta I\gamma^2 F_{\parallel}(\psi) \quad \text{per rad}$$

$$N_{k\parallel}(0,\lambda) = 3.461 \times 10^{15}\ k\theta I\gamma^2 H_2$$

If we set $$N_{k\parallel}(\psi,\lambda) = g(\lambda) \times \frac{1}{\sqrt{2\pi}\,\sigma} e^{-\frac{\psi^2}{2\sigma^2}}$$

then $$N_{k\parallel}(0,\lambda) = g(\lambda) \times \frac{1}{\sqrt{2\pi}\,\sigma}$$

and $$g(\lambda) = 3.461 \times 10^{15}\, k\theta I\gamma^2 H_2 \times \sqrt{2\pi}\,\sigma \tag{50}$$

But $$\int_{-\infty}^{\infty} N_{k\parallel}(\psi,\lambda)d\psi = g(\lambda) = f\, N_k(\lambda) = 1.256 \times 10^{16}\, k\theta I\gamma f G_1 \tag{51}$$

where f is the fraction of total radiation at λ which is $\parallel$ polarized, and is plotted in Fig. 14.

From (50)(51)

$$\gamma\sigma = 1.448 \frac{fG_1}{H_2} \quad \text{(rad)}$$

and is a function only of λ_c/λ, plotted in Fig. 20. It is approximately

$$\gamma\sigma = 0.565(\lambda/\lambda_c)^{0.425} \tag{52}$$

and $$N_{k\parallel}(\psi,\lambda) = 3.461 \times 10^{15}\, k\theta I\gamma^2 H_2 e^{-\frac{\psi^2}{2\sigma^2}} \quad \text{(per rad)} \tag{53}$$

The exponential of (53) is compared in Fig. 21 with the Bessel function curves of Fig. 15. The agreement is good up to $\lambda/\lambda_c = 10$ and is fair at 100.

If we again start at an electron beam minimum, the current in dydy′ is given by

$$d^2I = I_o P(y,y')\, dy\, dy' \tag{54}$$

and the one σ contour of the beam at s = 0 by (31). When transformed to s the electron beam is described by (33) and (40). In the y,y′ plane at s=s the current in dy dy′ is

$$d^2I = I_o P_1(y,y')\, dy\, dy' \tag{55}$$

with P_1 given by (41). Let the electrons radiate from arc $\theta = ds/\rho$ and (53) becomes

$$dN_{k\parallel}(\psi,\lambda) = AI\ ds\ \frac{1}{\sqrt{2\pi}\,\sigma}\ e^{-\frac{\psi^2}{2\sigma^2}}\ d\psi \tag{56}$$

$$A = 3.46 \times 10^{15}\ k\ \frac{\gamma^2}{\rho}\sqrt{2\pi}\,\sigma\ H_2 \tag{57}$$

The radiation angle, referred to s, is Y′ so $\psi = Y' - y'$. Substitute I from (55) in (56) to determine photon flux in dY′ from element dy dy′ ds

$$d^4N_k = AI_o ds\ \frac{1}{(2\pi)^{3/2}\sigma\sigma_y\sigma_{y'}}\ \exp\left[-\frac{1}{2(1-r_1^2)}\left(\frac{y^2}{\sigma_{y_1}^2} - \frac{2r_1yy'}{\sigma_{y_1}\sigma_{y_1'}} + \frac{y'^2}{\sigma_{y_1'}^2}\right)\right] \times$$

$$\times \exp\left[-\frac{1}{2\sigma^2}(Y'-y')^2\right] dy\ dy'\ dY' \tag{58}$$

and to find the photon flux in dy dY′ integrate (58) over all y′

$$d^3N_k = AI_o ds\ \frac{dy\ dY'}{(2\pi)^{3/2}\sigma\sigma_y\sigma_{y'}}\ \exp\left[-\frac{1}{2}\left(\frac{y^2}{\sigma_{y_1}^2(1-r_1^2)} + \frac{Y'^2}{\sigma^2}\right)\right] \times$$

$$\times \int_{-\infty}^{\infty} \exp\left\{-\left[\left(\frac{1}{2(1-r_1^2)\sigma_{y_1'}^2} + \frac{1}{2\sigma^2}\right)y'^2 - \left(\frac{r_1y}{(1-r_1^2)\sigma_{y_1}\sigma_{y_1'}} + \frac{Y'}{\sigma^2}\right)y'\right]\right\}dy' \tag{59}$$

but[9] $\int_{-\infty}^{\infty} e^{-(ax^2+2bx)}\,dx = \sqrt{\frac{\pi}{a}}\ e^{\frac{b^2}{a}}$ so (59) becomes

$$d^3N_k = AI_o\ \frac{ds\ dy\ dY'}{2\pi\sqrt{\sigma_y^2\sigma_{Y'}^2 + s^2\sigma^2\sigma_{y'}^2}}\ e^{-\frac{1}{2[\sigma^2+\sigma_{y_1'}^2(1-r_1^2)]}\left[\frac{\sigma_{Y'}^2}{\sigma_{y'}^2}y^2 - \frac{2r_1\sigma_{y_1'}}{\sigma_{y_1}}y\,Y' + Y'^2\right]} \tag{60}$$

$$\sigma_{Y'}^2 = \sigma_{y_1'}^2 + \sigma^2$$

If the exponential is put in the format of (34)

$$e^{-\frac{1}{2(1-r_2^2)}\left(\frac{y^2}{\sigma_{y_2}^2}-\frac{2r_2yY'}{\sigma_{y_2}\sigma_{y_2'}}+\frac{Y'^2}{\sigma_{y_2'}^2}\right)} \tag{61}$$

The coefficients are

$$\sigma_{Y'}^2=\sigma_{y_2'}^2=\sigma_{y_1'}^2+\sigma^2=\sigma_{y'}^2+\sigma^2$$

$$\sigma_{y_2}^2=\sigma_{y_1}^2=\sigma_y^2+s^2\sigma_{y'}^2 \tag{62}$$

$$r_2^2=r_1^2\sigma_{y_1'}^2/(\sigma_{y_1'}^2+\sigma^2)$$

$$(1-r_2^2)=\left[\sigma^2+\sigma_{y_1'}^2(1-r_1^2)\right]\Big/(\sigma_{y_1'}^2+\sigma^2)$$

This flux in dy dY′ from ds must now be transformed back to s = 0 by

$$\begin{vmatrix} 1 & -s \\ 0 & 1 \end{vmatrix}$$

The exponential of (60) then becomes

$$\exp\left\{-\frac{1}{2(1-r_2^2)}\left[\frac{y^2}{\sigma_{y_2}^2}+\left(\frac{2s}{\sigma_{y_2}^2}-\frac{2r_2}{\sigma_{y_2}\sigma_{y_2'}}\right)yy'+\left(\frac{s^2}{\sigma_{y_2}^2}-\frac{2r_2s}{\sigma_{y_2}\sigma_{y_2'}}+\frac{1}{\sigma_{y_2'}^2}\right)y'^2\right]\right\} \tag{63}$$

and equating coefficients to the form of (34), plus (62)

$$\sigma_{y_3}^2=s^2\sigma^2+\sigma_y^2$$

$$\sigma_{y_3'}^2=\sigma_{y_2'}^2=\sigma_{y'}^2+\sigma^2=\sigma_{Y'}^2 \tag{64}$$

$$(1-r_3^2) = \frac{\sigma_y^2\sigma_{y_3}^2+\sigma^2\sigma_y^2}{\sigma_{y_3}^2\sigma_{Y'}^2} = \frac{\sigma_y^2\sigma_{Y'}^2+s^2\sigma^2\sigma_{y'}^2}{\sigma_{y_3}^2\sigma_{Y'}^2} \tag{64}$$

$$= \frac{\sigma_{y'}^2(\sigma_y^2+s^2\sigma^2) + \sigma^2\sigma_y^2}{(\sigma_y^2+s^2\sigma^2)(\sigma_{y'}^2+\sigma^2)}$$

then from (63) and (64), (60) transforms to

$$d^3N_k = AI_o \frac{ds\ dy\ dY'}{2\pi\sqrt{\sigma_y^2\sigma_{Y'}^2+s^2\sigma^2\sigma_{y'}^2}}\ e^{-\frac{1}{2(1-r_3^2)}\left[\frac{y^2}{\sigma_{y_3}^2} - \frac{2r_3yy'}{\sigma_{y_3}\sigma_{y_3'}} + \frac{y'^2}{\sigma_{y_3'}^2}\right]} \tag{65}$$

or substituting from (64)

$$d^3N_k = AI_o \frac{ds\ dy\ dY'}{2\pi\sqrt{\sigma_y^2\sigma_{Y'}^2+s^2\sigma^2\sigma_{y'}^2}} \times e^{-\frac{1}{2(\sigma_y^2\sigma_{Y'}^2+s^2\sigma^2\sigma_{y'}^2)}\left[(\sigma_{y'}^2+\sigma^2)y^2 - 2s\sigma^2yY' + (\sigma_y^2+s^2\sigma^2)Y'^2\right]} \tag{66}$$

This d^3N_k is the number of photons in dy dY′ in the "source plane" s = 0, which come from radiation along ds at s = s.

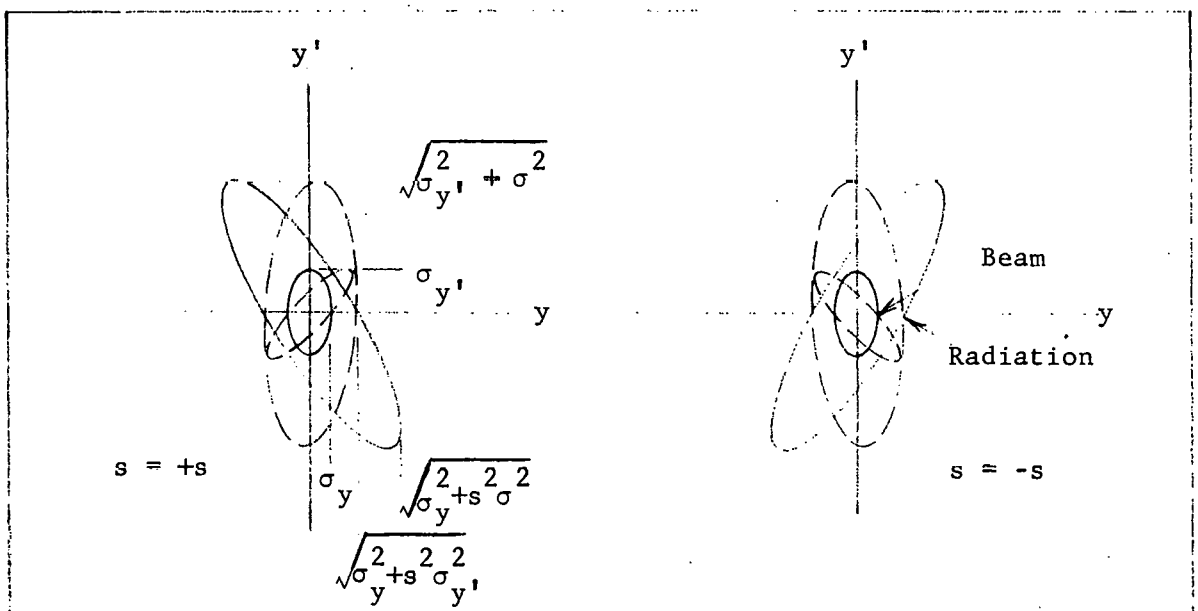

Fig. 22 Successive transmations in vertical (y,y') phase space

These successive transformations are shown graphically in Fig. 22 in which the example is exaggerated, as if from the end of a very long source. Most real sources, fortunately, have less rotation of the ellipses. The contours are σ (or $n\sigma$) ellipses. The electron beam ellipse at s = 0 is upright, by arbitrary definition. It transforms, without magnetic focussing, to a slanted ellipse in which the angles y' are preserved but the size y increases. The radiation then increases the angles to form the real source and, at s, the density of this source will be less than at s = 0. In order to synthesize the optical source the radiation is then transformed to s = 0 with angles preserved but with increase in apparent size. Once established, the radiation area in phase space is an invariant but its shape can be changed and distorted.

The radical in (65) is $\sigma_{y_3}\sigma_{y_3'}\sqrt{1-r_3^2}$ and we can integrate over y, using the properties of bivariate distributions[9,10]

$$d^2N_k = AI_o\, dsdy' \frac{1}{\sqrt{2\pi}\,\sigma_{y_3'}} e^{-\frac{y'^2}{2\sigma^2_{y_3'}}}$$

$$= AI_o dsdy' \frac{1}{\sqrt{2\pi}\sqrt{\sigma^2_{y'}+\sigma^2}} e^{-\frac{1}{2}\frac{y'^2}{(\sigma^2_{y'}+\sigma^2)}} \qquad (67)$$

and since s occurs only as ds this integrates over s as

$$dN_k(y') = \int_{-s}^{s} \frac{d^2N_k}{ds}\, ds = 2AI_o\, dy' \frac{s}{\sqrt{2\pi}\sqrt{\sigma^2_{y'}+\sigma^2}} e^{-\frac{1}{2}\frac{y'^2}{(\sigma^2_{y'}+\sigma^2)}} \qquad (68)$$

Similarly integrate (65) over y' to obtain

$$d^2N_k = AI_o \frac{dy\, ds}{\sqrt{2\pi}\sqrt{\sigma^2_y+s^2\sigma'^2}} e^{-\frac{1}{2}\frac{y^2}{(\sigma^2_y+s^2\sigma'^2)}} \qquad (69)$$

Integration of (69) over s can be done by means of a function which I will call ef(a,Y), defined as

$$ef(a,Y) = \int_0^Y \frac{1}{\cos t} e^{-\frac{a^2}{2}\cos^2 t}\, dt \qquad (70)$$

and normalized by

$$\int_{-\infty}^{\infty} ef(a,Y)da = \sqrt{2\pi}\tan Y$$

at $a = 0$ $\qquad ef(0,Y) = \frac{1}{2}\ell n\left(\frac{1+\sin Y}{1-\sin Y}\right)$

and for $Y < 0.1$ $\qquad ef(a,Y) \simeq Y\, e^{-\frac{a^2}{2}}$

Appendix C has a description of the function together with a graph and short table of values.

If we set $\cos t = \sigma_y/\sqrt{\sigma_y^2+s^2\sigma^2}$ and $a = y/\sigma_y$, then limit Y is given by $\tan Y = \sigma s/\sigma_y$

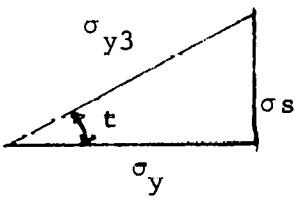

The integral of (69) over s then becomes (Appendix C)

$$dN_k(y) = AI_o \frac{dy}{\sqrt{2\pi}\,\sigma}\int_0^Y \frac{1}{\cos t} e^{-\frac{a^2}{2}\cos^2 t}\, dt$$

and the distribution of photons over y in the plane s = 0 is

$$dN_k(y) = AI_o \frac{dy}{\sqrt{2\pi}\,\sigma} ef\left(\frac{y}{\sigma_y}, \tan^{-1}\frac{\sigma s}{\sigma_y}\right) \qquad (71)$$

while the probability that a photon is in dy′ at y′ is, from (68)

$$P = \frac{dy'}{\sqrt{2\pi}\sqrt{\sigma_y^2+\sigma^2}} e^{-\frac{1}{2}\frac{y'^2}{(\sigma_y^2+\sigma^2)}} \qquad (72)$$

The distribution over s = 0 with equal contributions from negative s and positive s is symmetrical about the y′ axis, and is from (72) symmetrical about the y axis. There will be no cross terms of the independent variates of (71) and (72) and the equi-intensity contours will be symmetrical about the axes. We can then combine (71) and (72) to give the y,y′ intensity in the synthesized source in the transverse plane s = 0 with (71)×2

$$d^2N_k(y,y') = AI_o \frac{dy\,dy'}{\pi\sigma\sqrt{\sigma_{y'}^2+\sigma^2}}\, ef\left(\frac{y}{\sigma_y}, \tan^{-1}\frac{\sigma s}{\sigma_y}\right) e^{-\frac{1}{2}\frac{y'^2}{(\sigma_{y'}^2+\sigma^2)}} \tag{73}$$

At $y = y' = 0$ (66) can be integrated from -s to s by[11]

$$\int \frac{dx}{\sqrt{x^2+a^2}} = \sinh^{-1}\frac{x}{a}$$ to give the central yy′ density

$$d^2N_k(0,0) = AI_o \frac{dy\,dy'}{\pi}\frac{1}{\sigma\sigma_{y'}} \sinh^{-1}\left(\frac{s\sigma\sigma_{y'}}{\sigma_y\sigma_{Y'}}\right) \tag{74}$$

If $A = \sqrt{2\pi}\,\sigma B$

$$B = 3.46 \times 10^{15}\, k\, \frac{\gamma^2}{\rho}\, H_2 \tag{75}$$

and we can rewrite the y densities at $s = 0$;

(71)×2 $$dN_k(y) = 2BI_o dy\, ef(a,Y)$$

$$a = \frac{y}{\sigma_y}\ , \quad \tan Y = \frac{\sigma s}{\sigma_y}$$

(68) $$dN_k(y') = 2BI_o dy' \frac{\sigma s}{\sqrt{\sigma_{y'}^2+\sigma^2}}\, e^{-\frac{1}{2}\frac{y'^2}{(\sigma_{y'}^2+\sigma^2)}} \tag{76}$$

(73) $$d^2N_k(y,y') = \sqrt{\frac{2}{\pi}}\, BI_o \frac{dy\,dy'}{\sqrt{\sigma_{y'}^2+\sigma^2}}\, ef(a,Y)\, e^{-\frac{1}{2}\frac{y'^2}{(\sigma_{y'}^2+\sigma^2)}}$$

(74) $$d^2N_k(0,0) = \sqrt{\frac{2}{\pi}}\, BI_o \frac{dy\,dy'}{\sigma_{y'}} \sinh^{-1}\left(\frac{s\sigma\sigma_{y'}}{\sigma_y\sigma_{Y'}}\right)$$

In the x,x′ plane the central orbit of the electron beam will project on the plane $s = 0$ along the parabola (Fig. 19)

$$x'^2 - 2x/\rho = 0\ , \quad s = \rho x' \tag{77}$$

Radiation from element ds at s will transform to s = 0 centered at $x' = s/\rho$, $x = s^2/2\rho$. The one σ contour of x is, using (64), $\sigma_{x_3}^2 = \sigma_x^2 + s^2\sigma^2$ and since $s = \rho x'$ we obtain the contour

$$x = s^2/2\rho \pm \sqrt{\sigma_x^2+s^2\sigma^2} = \rho x'^2/2 \pm \sqrt{\sigma_x^2+\sigma^2\rho^2x'^2} \tag{78}$$

which is shown in Fig. 23.
The contour of (78) is an approximation based on the assumption that the contours have small curvature in the region considered. Since the radiation emitted by a single electron is parallel to the x′ axis, a radiation distribution large compared to the curvature vs. x′ would enlarge the contour.

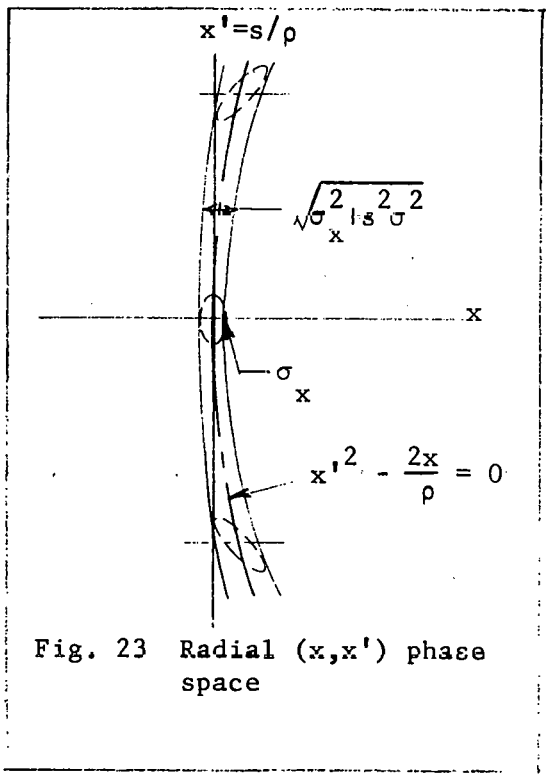

Fig. 23 Radial (x,x') phase space

The radiation is distributed uniformly along the arc so we can obtain the uniform x′ density from (17) multiplied by f to obtain the number of ∥ polarized photons;

$$N_{k\parallel}(\lambda)=1.26\times10^{13}\ kI\gamma G_1 f \ \text{ per sec, mrad } \theta \tag{79}$$

The probability that a photon from s will be in dx is

$$P = \frac{dx}{\sqrt{2\pi}\sqrt{\sigma_x^2+s^2\sigma^2}}\, e^{-\frac{1}{2}\frac{(x-s^2/2\rho)^2}{(\sigma_x^2+s^2\sigma^2)}} \tag{80}$$

and the number of photons in dx dx′ is the product of (79) and (80) times dx′. At x = x′ = 0 the central x density is

$$d^2N_k(0,0) = 1.26 \times 10^{13}\ kI\gamma f G_1 \frac{dx\ dx'}{\sqrt{2\pi}\ \sigma_x} \tag{81}$$

Selection of the source center at a waist, or minimum, or focus of the electron beam made the derivation of the equations manageable. This type of source center is found at the center of a double focussing insertion in a ring and sometimes in the general lattice. However, the source center is often at a location $\bar{s}$ where the beam phase space ellipse is tilted and described by (28)

$$\gamma y^2 + 2\alpha\, yy' + \beta y'^2 = E_y \tag{28}$$

The α, β, γ at the desired $\bar{s}$ and E are obtained from the calculations of the ring lattice dynamics. (See Appendix B). If the one σ emittance is $\sigma_y\sigma_{y'}$, then, by comparing (28) and (33)

$$\sigma_y = \sqrt{E\beta} \quad , \quad \sigma_{y'} = \sqrt{E\gamma} \tag{30}$$

The values at s_1, related to those at $\bar{s}$ are given by

$$\begin{aligned} \beta_1 &= \beta - 2\alpha(s_1-\bar{s}) + \gamma(s_1-\bar{s})^2 \\ \alpha_1 &= \alpha - \gamma(s_1-\bar{s}) \\ \gamma_1 &= \gamma \end{aligned} \tag{82}$$

(provided there is not magnetic focussing). Alternatively (33) can be transformed by (32) with s replaced by $(s_1-\bar{s})$. However, from (82)

$$\alpha(s) = \alpha_o - \gamma(s)s$$

measured from the location of α_o. Set $\alpha_o = 0$ at $s = 0$ and the projected waist will be at

$$\alpha(s) = -\gamma(s)s$$

If we measure from this zero (33) and (34) need only to have s replaced by s_1, and similarly (60) and (62) have s replaced by s_1. The transformation to the forms of (63), (64) and (66) must be done with

$$\begin{vmatrix} 1 & -(s_1-\bar{s}) \\ 0 & 1 \end{vmatrix}$$

and the result is complex expressions and difficult integration which are beyond the scope of this paper. The symmetry assumption incorporated in (76) is no longer exact. The modification of the x,x' procedure is obvious, and is considerably simpler.

The values of the source parameters can be examined and if $\sigma_{y'} < \sigma$, $s\sigma < \sigma_y$ and $s\sigma_{y'} < \sigma_y$ (preferably less than half) the approximations given above are reasonably good for a source not centered at a waist. For extreme cases the source length can be divided into a few Δs, the flux calculated for each, and the results summed.

It is important to note that no allowance has been made for spread of x by momentum dispersion. Ring dynamics calculations provide a momentum compaction function X_p defined by

$$\Delta x = X_p \frac{\Delta p}{p}$$

where Δp is the semi-momentum spread of the beam. In an insertion the X_p can be very small and need not be included. If Δx is appreciable, compared to the betatron oscillation σ_x, then the σ_x of (80) and (81) is replaced by $(\sigma_x^2 + \Delta x^2)^{\frac{1}{2}}$. The X_p amplitude function usually does not vary rapidly with s. As a result the modulation of angle x' by dX_p/ds is small and has only a small effect on the assumption that the radiation is uniform with θ.

In sum, the synchrotron light source is characterized by general parameters

$$\gamma,\ \rho,\ (\lambda_c/\lambda),\ I_o\ ,$$

by specific parameters

$$\sigma_x,\ \sigma_y,\ \sigma_{x'},\ \sigma_{y'},\ s,$$

and in some configurations also by

$$\alpha,\ \beta,\ \gamma,\ X_p\ .$$

III. Radiation Beam Power

The power which can be encountered in a synchrotron radiation beam has an important influence on optical design. Cooling and thermal distortion of the first optical element may well limit the flux which can be gathered from electron storage rings. It is always advantageous, with respect to beam power, to work near λ_c. Figure 10 shows the percentage of power at wavelengths greater than λ vs. λ/λ_c, and it will be noted that half the power is radiated below λ_c.

The total radiated power is current times the volts/turn (Table I)

$$P = 88.5\ E^4 I/\rho \quad \text{kw/amp or w/ma} \tag{83}$$

or multiplying by $10^{-3}/2\pi$

$$\begin{aligned} P &= 0.01409\ E^4 \theta I/\rho \qquad \text{w/ma mrad} \\ &= 9.61 \times 10^{-16}\ \gamma^4 \theta I/\rho \quad " \quad " \end{aligned} \tag{84}$$

is the total power intecepted from arc θ.
By combining (84) and (16), E in GeV and λ_c in Å, $P = 0.0787\ E/\lambda_c$ w/ma mrad θ

The power radiated as a function of the vertical angle ψ is, from (9) (24)

$$\begin{aligned} P &= 1.44 \times 10^{-18} \frac{\gamma^5}{\rho} F(\gamma\psi) \quad \text{w/ma mrad } \theta, \psi \\ &- 0.413 \frac{E^5}{\rho} F(\gamma,\psi) \qquad " \qquad " \end{aligned} \tag{85}$$

Function $F(\gamma\psi)$ is shown in Fig. 12 as well as $F_7(\gamma\psi)$ defined by (24). $F(\gamma\psi)$ can be approximated closely by a normal distribution

$$F(\gamma\psi) = \frac{k}{\sqrt{2\pi}\,\sigma} e^{-\frac{1}{2}\frac{(\gamma\psi)^2}{\sigma^2}} \tag{86}$$

which can be normalized by the total power from (84)

$$\int_{-\infty}^{\infty} F(\gamma\psi)\,d(\gamma\psi) = \gamma \int_{-\infty}^{\infty} F(\gamma\psi)\,d\psi = k \quad (\gamma\psi \text{ in rad})$$

and since the integral of (86) is k,

so $$\int P d\psi = 1.44 \times 10^{-15} \frac{\gamma^4 k}{\rho} = 9.61 \times 10^{-16} \frac{\gamma^4}{\rho} \; ; \quad k = 0.667$$

and at 0

$$F(\gamma\psi) = \frac{k}{\sqrt{2\pi}\,\sigma} = 0.4375$$

$$\sigma_\psi = 0.608 \text{ rad of } \gamma\psi$$

and
$$F(\gamma\psi) = 0.4375\, e^{-\frac{1}{2}\frac{(\gamma\psi)^2}{(0.608)^2}} \qquad (\psi \text{ in rad}) \tag{87}$$

It is often convenient to represent the power distribution by a rectangle of "width" $\psi = 2/\gamma$. If in (85)

$$\int_0^\infty F(\gamma\psi) d\psi = k_1/\gamma$$

$$2 \times 1.44 \times 10^{-15} \frac{\gamma^4}{\rho} k_1 = 9.61 \times 10^{-16} \frac{\gamma^4}{\rho} \tag{88}$$

$$k_1 = 0.334 \text{ rad of } \gamma\psi$$

The rectangle is shown in Fig. 12. If this approximation is used it is sometimes necessary to remember that the peak power is larger in the ratio 1.31.

If we assume the beam is very small there is an approximation useful for estimating. At one meter from the source one mrad θ subtends 10^{-3} m and $\psi = 2/\gamma$ subtends $2/\gamma$ m so the radiation falls on $2 \times 10^{-3}/\gamma$ m^2. But the power from one mrad θ is (84)

$$P = 9.61 \times 10^{-16} \gamma^4/\rho \text{ w/ma mrad } \theta$$

and the specific power

$$P/A = 4.80 \times 10^{-13} \gamma^5/\rho \text{ w/ma m}^2 \text{ at 1 m}$$

If D is the distance from the source in m

$$P/A = 1.38\, E^5/\rho D^2 \text{ w/ma cm}^2 \tag{89}$$

If the angular spread of the electron beam is appreciable this power will be reduced by the approximate ratio (see (93))

$$\gamma^{-1}/\sqrt{\gamma^{-2} + \alpha^2} \tag{90}$$

where α is the angular divergence of the beam.

The preceeding relations apply to an electron beam which is a filament. Distribution of the beam in y and y′ will reduce the power density, often by a significant factor. In the vertical coordinates the electron beam is described (55) by

$$d^2I = \frac{I_o}{2\pi\sigma_y\sigma_{y'}} e^{-\frac{1}{2}\left(\frac{y^2}{\sigma_y^2} + \frac{y'^2}{\sigma_{y'}^2}\right)} dy\, dy' \tag{91}$$

and the current in element dy dy′ will radiate power in angle element $d\psi$ at ψ, using (85) in radians of ψ and (87)

$$d^3P = d^2I(1.44\times10^{-15}\,\frac{\gamma^5}{\rho})\,\frac{k_2}{\sqrt{2\pi}\,\sigma_\psi} e^{-\frac{1}{2}\frac{\psi^2}{\sigma_\psi^2}} d\psi \quad \text{per mrad } \theta \tag{92}$$

at $\psi = 0$ $\qquad k_2/\sqrt{2\pi}\,\sigma_\psi = 0.4375$ and $\sigma_\psi = 0.608/\gamma$

so

$$d^3P = d^2I(9.61\times10^{-16}\,\frac{\gamma^4}{\rho})\,\frac{1}{\sqrt{2\pi}\,\sigma_\psi} e^{-\frac{1}{2}\frac{\psi^2}{\sigma_\psi^2}} \tag{93}$$

but if the radiation angle is Y′, $\psi = Y' - y'$, and the power in element dy dY′ radiated from current in dy dy′ is

$$d^3P = (9.61\times10^{-16}\,\frac{\gamma^4}{\rho})\,\frac{I_o\, dy\, dy'\, dY'}{(2\pi)^{3/2}\sigma_\psi\sigma_y\sigma_{y'}} e^{-\frac{1}{2}\left(\frac{y^2}{\sigma_y^2} + \frac{y'^2}{\sigma_{y'}^2}\right) - \frac{1}{2\sigma_\psi^2}(Y'-y')^2} \tag{94}$$

If we integrate over all y′ the power radiated from element dy dY′ of the source is (assuming one mrad θ and I_o in ma)

$$d^2P = (9.61\times10^{-16}\,\frac{\gamma^4}{\rho})\,\frac{I_o dy\, dY'}{2\pi\,\sigma_y\sigma_o} e^{-\frac{1}{2}\left(\frac{y^2}{\sigma_y^2} + \frac{Y'^2}{\sigma_o^2}\right)} \tag{95}$$

and $\sigma_o^2 = \sigma_y^2, + \sigma_\psi^2$ $\qquad\qquad$ $\sigma_\psi = 0.608/\gamma$ rad

If the beam height y is small, integrate over y to obtain the angular distribution

$$d^2P = (9.61\times10^{-16}\,\frac{\gamma^4}{\rho})\,\frac{I_o\,dY'}{\sqrt{2\pi}\,\sigma_o}\,e^{-\frac{1}{2}\frac{Y'^2}{\sigma_o^2}} \qquad (96)$$

Units of (94) and (95) are watts per mrad θ per ma.

Equations (95) and (96) describe the source. The power density can be transformed to surfaces by using the methods of Sect. II2.

IV. Optical Transformations

The characteristics of sources can be most readily examined with linear paraxial transformations. These transformations map the elements of phase space and represent the best conditions that can be achieved. Aberrations and losses are beyond the scope of this section, but source properties and comparisons can be examined with idealized assumptions.

1. Non-Focusing Optics

The optical axis, s, is the central ray of the system. Deviations from s are, in the horizontal and vertical planes, specified by x, x' and y, y'. If there is no refraction or change of momentum the s phase space (and time) are preserved and can be ignored.* The four dimensional phase space x, x', y, y'' is invariant but, if there is no xy coupling, the x, x' and y, y' phase spaces are independently invariant.

A ray at y_o, y'_o propagating through free space from D = 0 will be at D = D_1, at

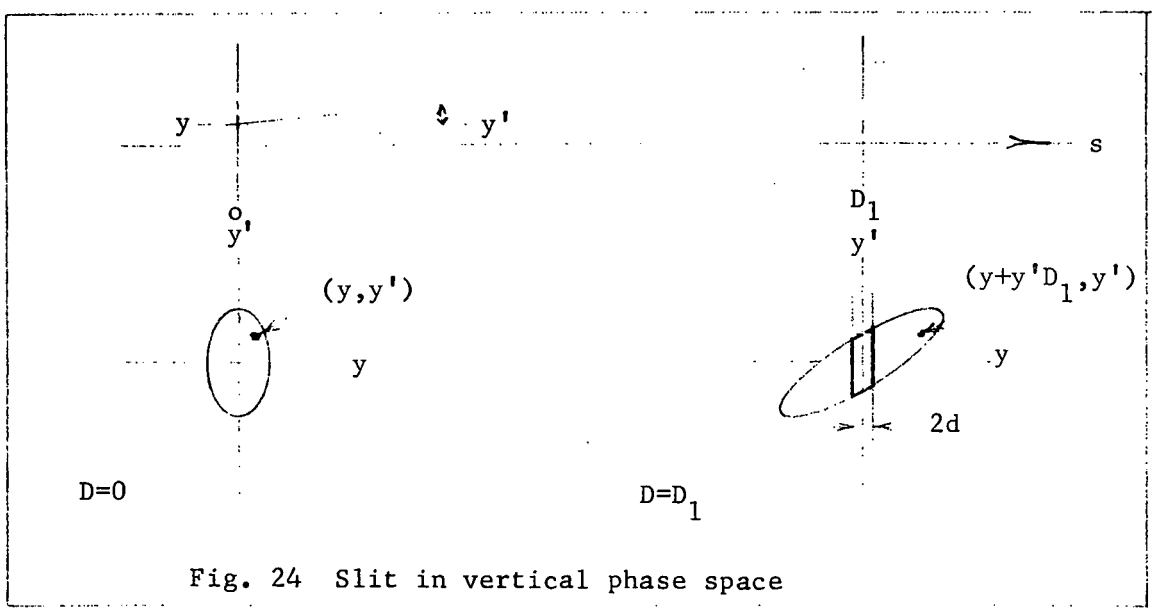

Fig. 24 Slit in vertical phase space

$$y = y_o + y' D_1, \quad y' = y'_o$$

and the free space transformation is

$$\begin{vmatrix} y \\ y' \end{vmatrix} = \begin{vmatrix} 1 & D_1 \\ 0 & 1 \end{vmatrix} \begin{vmatrix} y_o \\ y'_o \end{vmatrix}$$

*The effects of s are folded into x and y.

Suppose a source at D = 0 (Fig. 24) with contour

$$\frac{\Sigma_{y'}}{\Sigma_y} y^2 + \frac{\Sigma_y}{\Sigma_{y'}} y'^2 = \Sigma_y \Sigma_{y'}$$

To avoid utter chaos in nomenclature, Σ will be used as the variance, or equivalent variance, of the synthesized optical source; σ will be reserved for the variance of the electron beam. The emittance of this source is $\Sigma_y \Sigma_{y'}$ and the phase space area is $\pi \Sigma_y \Sigma_{y'}$. Maxima are the axial intercepts $\hat{y} = \Sigma_y$, $\hat{y}' = \Sigma_{y'}$. If this source is transformed by (96) to D_1 the contour will be

$$\frac{\Sigma_{y'}}{\Sigma_y} y^2 - \frac{2\Sigma_{y'} D}{\Sigma_y} yy' + \left(\frac{\Sigma_y}{\Sigma_{y'}} + \frac{\Sigma_{y'} D^2}{\Sigma_y}\right) y'^2 = \Sigma_y \Sigma_{y'} \quad . \tag{97}$$

Area and emittance are preserved but the maxima are no longer the intercepts. They are (Fig. 18)

$$\hat{y} = \sqrt{\Sigma_y^2 + \Sigma_{y'}^2 D^2} \quad , \quad \hat{y}' = \Sigma_{y'} \tag{98}$$

and this shows, as expected, that the angular distribution is unaltered but the size increases.

One of the most common, and important, optical instruments is the slit. It will be considered here in vertical dispersion. Suppose a slit of width 2d at D_1 (Fig. 24). We can examine the properties by transforming the slit back onto the source or by transforming the source onto the slit. The latter seems preferable. The intercept of the source contour on y′ is

$$y = 0, \; y' = \frac{\Sigma_y \Sigma_{y'}}{\sqrt{\Sigma_y^2 + \Sigma_{y'}^2 D^2}} \tag{99}$$

and the minimum angular resolution (semi-angle) as the slit width goes to 0 is $\Sigma_y \Sigma_{y'} / \sqrt{\Sigma_y^2 + \Sigma_{y'}^2 D^2}$. Slope of the contour at y = 0 is, by differentiating (97)

$$\frac{d_{y'}}{d_y} = \frac{D}{(\Sigma_y/\Sigma_{y'})^2 + D^2} \tag{100}$$

and the maximum angle through the slit is approximately

$$\frac{\Sigma_y \Sigma_{y'}}{\sqrt{\Sigma_y^2 + \Sigma_{y'}^2 D^2}} + \frac{Dd}{(\Sigma_y/\Sigma_{y'})^2 + D^2} \tag{101}$$

The area outlined in Fig. 24 is, in most practical situations, nearly a parallelogram of area

$$\frac{4d\Sigma_y \Sigma_{y'}}{\sqrt{\Sigma_y^2 + \Sigma_{y'}^2 D^2}} \tag{102}$$

and since the emittance area is $\pi\Sigma_y\Sigma_{y'}$, the fraction of flux passed by the slit is

$$\frac{4d}{\pi\sqrt{\Sigma_y^2 + \Sigma_{y'}^2 D^2}} \tag{103}$$

Eq. 103 assumes uniform density, which may be a poor approximation. A somewhat better approximation is obtained by the ratio of slit width to emittance width

$$\frac{d}{\sqrt{\Sigma_y^2 + \Sigma_{y'}^2 D^2}}$$

It is sometimes desirable to integrate (76) over 2d.

In the radial or x, x′ space the radiation beam will be distributed

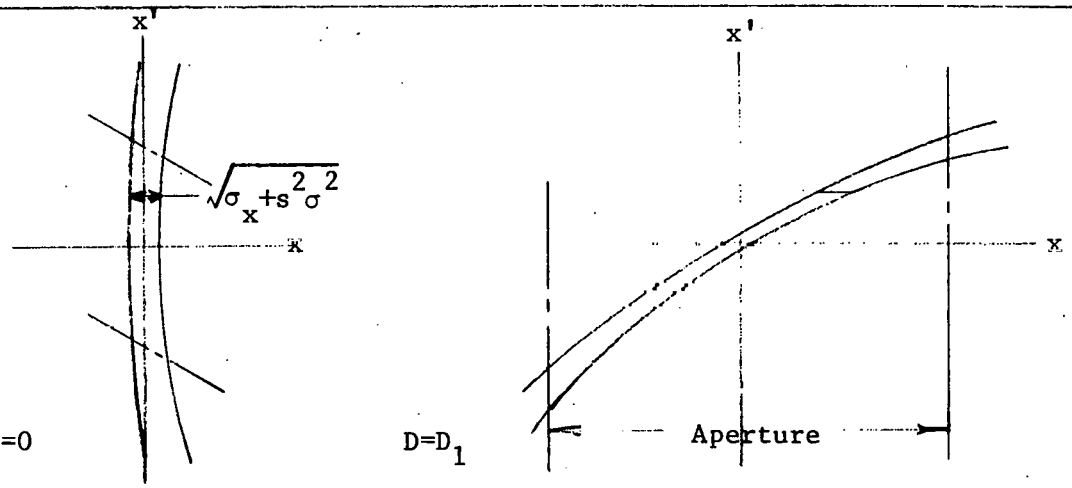

Fig. 25 Slit in radial phase space

along the length of the slit and will be cut off by the ends of the slit or by the aperture of the instrument illuminated. There will be a systematic variation of x′, the horizontal angle, along the slit. The xx′ density (Fig. 25) will vary as $\sqrt{\sigma_x^2 + s^2\sigma^2}$, transformed to $D = D_1$ (see (78) and Fig. 23). In the vertical direction the angular distribution is given by $dN_k(y')$ of (76) and, if the slit width $2d \ll \hat{y}$ of (98) this distribution will be uniform across the width of the slit. However, the $dN_k(y)$ of (76) has been integrated over s and represents the sum of the source. Since the yy′ density is correlated with the xx′ density through s, the y distribution given by (69) will vary over the length of the slit. For relatively short sources and moderate values of the various σ the variations are small and in many, if not most, synchrotron light applications the slit is rather uniformly illuminated. Extreme cases can be analyzed by dividing the source length s into a few Δs and transforming the parts piecewise in order to maintain the correlation between x and y.

One important application of the slit occurs with the double crystal monochromator in the parallel position, now usually a channel cut crystal. The angular distribution passing the slit determines the resolution (if the angles are greater than the crystal angular window) and the resolution is limited by (100) or perhaps (101). With the extended source the resolution $\Delta\lambda/\lambda = \cot\theta\Delta y'$ (Bragg angle θ) is limited by the characteristics of the source and the distance to the slit, but not by the slit width. The distance to the slit and crystal are determined by the geometry. Flux is collected from orbit arc approximately $\theta = x/D$, where x is the usable face width of the crystal. Flux at the shorter x-ray wavelengths will often be limited by the power the first elements can tolerate.

The double crystal spectrometer in the anti-parallel position is unique in that it is an angular slit in phase space.

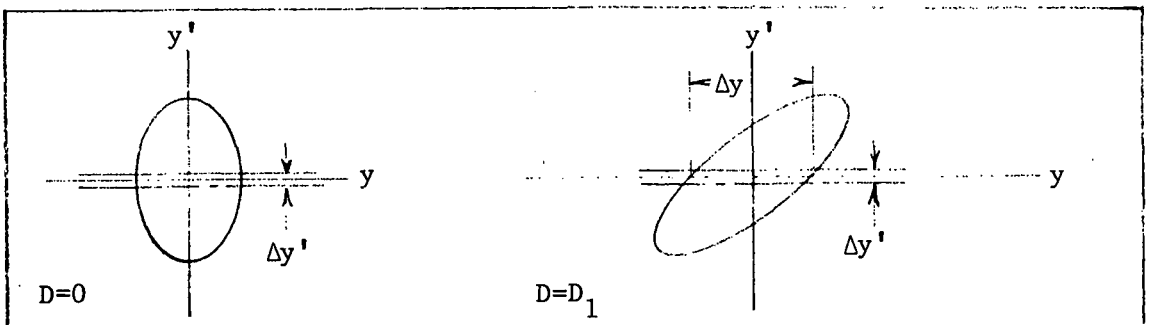

Fig. 26 Double crystal monochromator angular slit

Assuming vertical dispersion, the acceptance at the crystals is $\Delta y'$ (Fig. 26) and this transforms back to the source as $\Delta y'$. Angular acceptance is very small, with good crystals only a few seconds, so Δy is nearly the same at D - 0 and D_1. Usable Δy is determined by the projected vertical height of the crystals and this will set one limit to source length s by (73) or (76). The other limit is given by the width w of the crystals which limits the source arc to $\theta = w/D = s/\rho$ The smaller of these limits applies. However, the diffraction angle

to the crystal planes is changed by the off axis angle x' in the amount $\frac{1}{2} x'^2 \tan\theta$ (this θ is the Bragg angle) which must be less than the crystal acceptance $\Delta y'$. For this application the source angle $\theta/2 = x'$ will seldom be limiting since it can be a few mradians for good crystals at Bragg angle of say 20^o. $\Delta y'$ is very small so the exponential in $dN_k(y')$ of (76) is approximately one and

$$dN_k(y') \simeq 7 \times 10^{15}\ k I_o \gamma^2 H_2 \theta \cdot \frac{\sigma}{\sqrt{\sigma_{y'}^2 + \sigma^2}}\ \Delta y'$$

with θ determined by the size of the crystals and the distance D_1.

Diffraction studies such as those using Laue patterns or topography depend critically upon source size and source brightness. A specific study will require a specified angular spread across the sample. The situation is shown in Fig. 27 for two typical synchrotron light sources which can be used for x-ray diffraction. The slit may be either a pinhole or the edges of the crystal. If we rewrite (99)

$$y' = \frac{\Sigma_y}{\sqrt{(\Sigma_y/\Sigma_{y'})^2 + D^2}} \qquad (104)$$

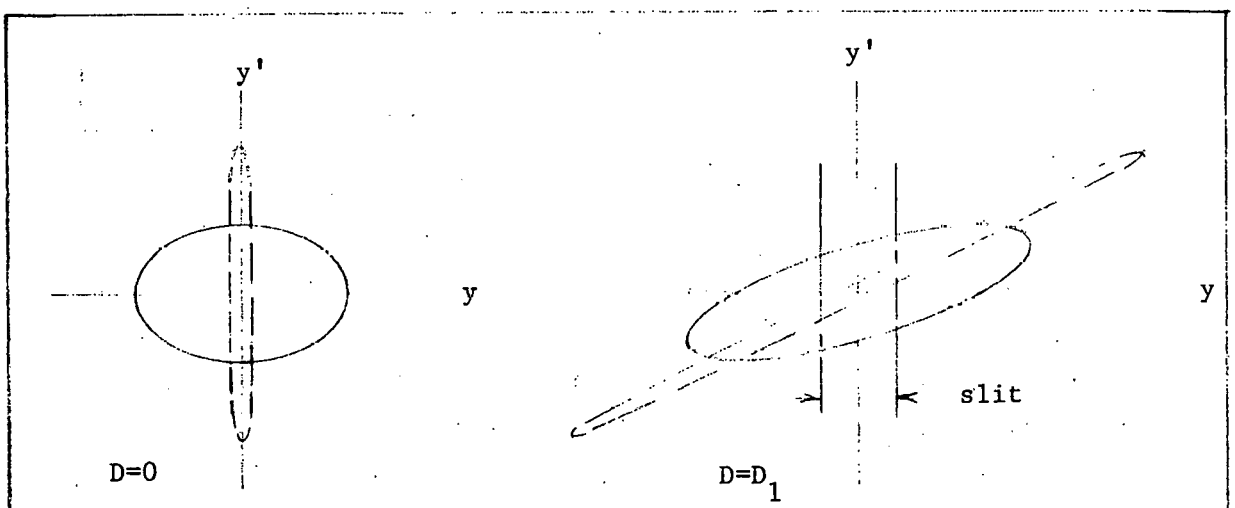

Fig. 27 Two typical sources, from different emittance beams, transformed to slit in y,y' space

The maximum semi-angle is roughly Σ_y/D, but Σ_y for short sources is largely determined by σ_y. A similar situation obtains in xx' (see Fig. 25). The σ_x and σ_y of various synchrotron light sources will take values in a range of more than an order of magnitude, and this can force a corresponding range of D_1. (One must of course retreat far enough to illuminate most of the sample and to prevent thermal decomposition of the material).

The flux passed through the small aperture at D_1, and the exposure of the detector, depend upon the central brightness of the source. The central density functions in x, x' and y, y' are given by (81) and (76). These cannot simply be multiplied because we would then be counting the same photons twice. By the analogy of (65) or (66) to (76), the probability that a photon will lie in element $dydy'$ (at $y = y' = 0$) of the source is, from (74)*

$$P = \frac{dydy'}{\pi} \frac{1}{\sigma\sigma_{y'}} \sinh^{-1}\left(\frac{s\sigma\sigma_{y'}}{\sigma_y\sigma_{Y'}}\right) \quad . \tag{105}$$

and this times (81) gives the central brightness

$$d^4N_k(0) = 1.26\times10^{13}\, kI\gamma f G_1 \frac{dx\, dx'\, dy\, dy'}{\pi\sqrt{2\pi}\sqrt{\sigma_x^2+s^2\sigma^2}(\sigma\sigma_{y'})} \sinh^{-1}\left(\frac{s\sigma\,\sigma_{y'}}{\sigma_y\,\sigma_{Y'}}\right) \tag{106}$$

For diffraction sources the argument of $\sinh^{-1}$ is less than 1 and $\sinh^{-1} x \approx x$; $s\sigma$ tends to be small compared to σ_x. Eq. (106) can then be approximated as:

$$d^4N_k = k_2\gamma \left(\frac{s}{\sigma_x\sigma_y\sigma_{Y'}}\right) \Delta x\Delta x'\Delta y\Delta y' \tag{107}$$

with k_2 a numerical constant involving k, I_o and functions of (λ_c/λ). The phase space area subtended by the diffraction sample will almost always be small so dx . . . can be replaced by Δx. . . and we can avoid integrating. Good x-ray sources will have $\sigma_{Y'} \approx \sigma$ and this varies as γ^{-1} at a fixed (λ_c/λ). The brightness is thus proportional to γ^2 and inversely to $\sigma_x\sigma_y$, the electron beam size. Although source length s is in the numerator, its magnitude is limited by the sample size and distance to $s = w\rho/D$. Increasing s and ρ together has no influence on flux, which is proportional to $\theta = s/\rho$ and such increase will

*Constant A of (74) contains a σ

enlarge Σ_x and Σ_y.

2. Focusing Optics

An optical system can be reduced, in first order, to a focal length f and the location of two principal planes.

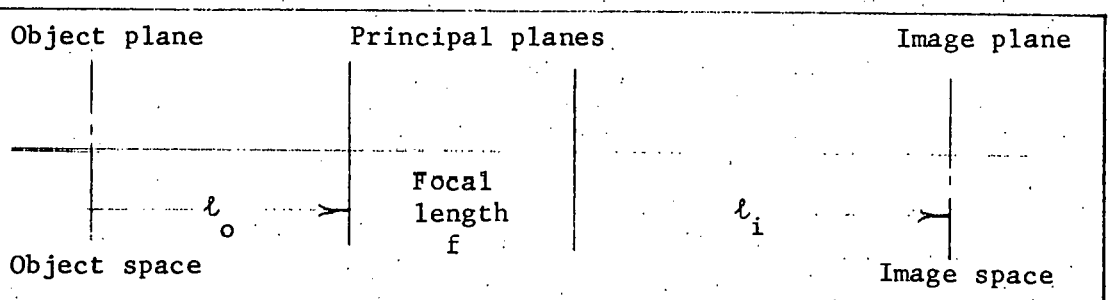

Fig. 28 Optical system definitions

The transformation from the first to the second principal plane is

$$\begin{vmatrix} 1 & 0 \\ -\frac{1}{f} & 1 \end{vmatrix}$$

and to transform from y_o, y'_o in the object space to y_i, y'_i in the image space

$$\begin{vmatrix} y_i \\ y'_i \end{vmatrix} = \begin{vmatrix} 1 & \ell_i \\ 0 & 1 \end{vmatrix} \begin{vmatrix} 1 & 0 \\ -\frac{1}{f} & 1 \end{vmatrix} \begin{vmatrix} 1 & \ell_o \\ 0 & 1 \end{vmatrix} \begin{vmatrix} y_o \\ y'_o \end{vmatrix}$$

or

$$\begin{vmatrix} y_i \\ y'_i \end{vmatrix} = \begin{vmatrix} 1 - \frac{\ell_i}{f} & \left(\ell_o - \frac{\ell_i \ell_o}{f} + \ell_o\right) \\ -\frac{1}{f} & \left(-\frac{\ell_o}{f} + 1\right) \end{vmatrix} \begin{vmatrix} y_o \\ y'_o \end{vmatrix}$$

$$y = \left(1 - \frac{\ell_i}{f}\right) y_o + \left(\ell_o - \frac{\ell_i \ell_o}{f} + \ell_i\right) y'_o$$

and for image formation, e.g. conjugate planes in the object and image spaces

$$\ell_o - \frac{\ell_i \ell_o}{f} + \ell_i = 0 \text{ or } \frac{1}{\ell_o} + \frac{1}{\ell_i} = \frac{1}{f}$$

also

$$\ell_o = -\ell_i \frac{f}{f - \ell_i} \quad , \quad \ell_i = \ell_o \frac{f}{f - \ell_o} \tag{108}$$

and linear magnification $M = \dfrac{f - \ell_i}{f} = \dfrac{f}{f - \ell_o} = -\dfrac{\ell_i}{\ell_o} = \dfrac{y_i}{y_o}$

angular magnification is 1/M and the transformation between conjugate planes is

$$\begin{vmatrix} y_i \\ y'_i \end{vmatrix} = \begin{vmatrix} M & 0 \\ -\frac{1}{f} & \frac{1}{M} \end{vmatrix} \begin{vmatrix} y_o \\ y'_o \end{vmatrix} \tag{109}$$

(Matrix optics[12,13] are usually formulated with historical sign and coefficient conventions. I find the above formulation in which distance proceeds from left to right and the column vectors have position on top to be more convenient.)

If a source is focused on a y slit the contours transform as in Fig. 29, which shows magnification arbitrarily set at 1½.

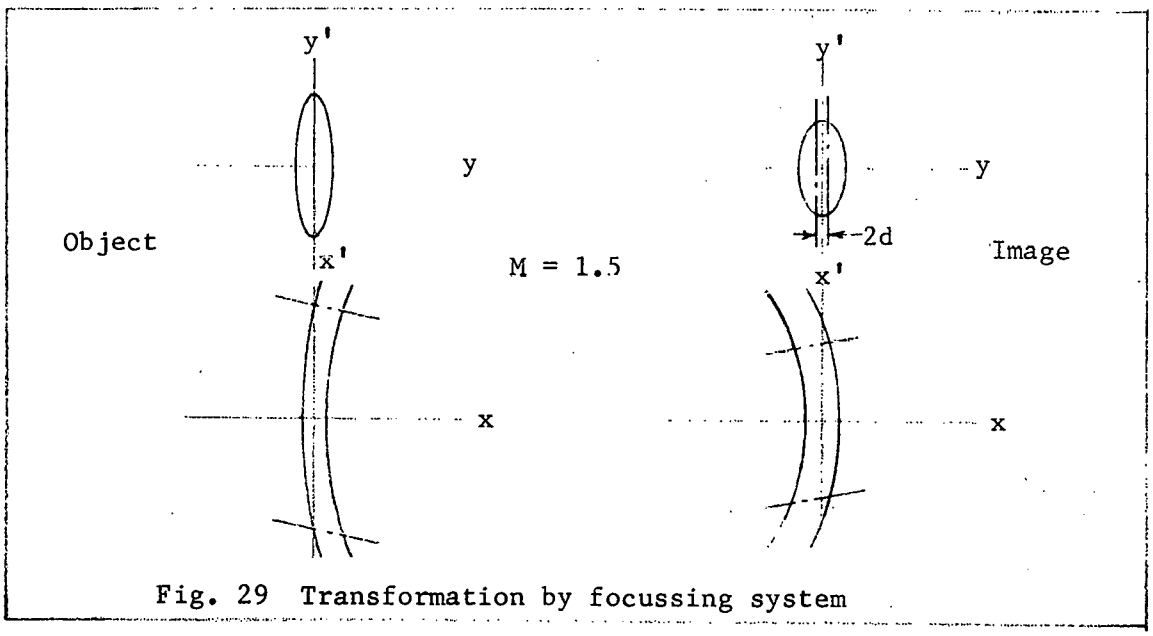

Fig. 29 Transformation by focussing system

The x, x′ figure is transformed to the system aperture stop (Fig. 25) and the stop then transformed back to the dashed line in Fig. 29. This determines θ and s, and the resulting source transforms to the image as shown in Fig. 29. The vertical, or y, source transforms as shown in Fig. 29 and it is assumed for this example that all y′ are passed by the system. (See Refs. 12, 13 for transformation of aperture stops.) Since the radial aperture has determined s the flux passing the slit is from (76)

$$N_k = \int_{-d}^{d} 2BI_o \, ef\left(\frac{y}{\sigma_y} , \tan^{-1}\frac{\sigma s}{\sigma_y}\right) d_y \quad . \tag{110}$$

Note on the curves of ef(a, Y) in Appendix C that if $y/\sigma_y = d$ is not larger than 2 or 3, the usual case, we can approximate this integral by a trapezoid

$$N_k = 4BI_o d \; ef\left(\frac{d}{2\sigma_y} , \tan^{-1}\frac{\sigma s}{\sigma_y}\right) \quad . \tag{111}$$

(If the magnification is M the d of (110) and (111) is replaced by d/M.) On the curve of ef(0,Y) in Appendix C it will be seen that for $\tan Y = \sigma s/\sigma_y$ greater than 1 or 2 the proportionate increase of flux density with increase of s diminishes rapidly. The y′ distribution is given by

$$dN_k(y') = 2BI_o dy' \frac{\sigma s}{\sqrt{\sigma_{y'}^2 + \sigma^2}} \, e^{-\frac{1}{2} y'^2/(\sigma_{y'}^2 + \sigma^2)} \tag{76}$$

and will be magnified by 1/M. In the example this has all been passed by the slit; the angular variation is determined by $\sigma_{y'}$ and σ. We can usually make $\sigma_{y'} < \sigma$. The radiation angle σ is roughly proportional to $(1/\gamma)\,(\lambda/\lambda_c)^{\frac{1}{2}}$ from (52) and $\lambda_c = 4\pi\rho/3\gamma^3$. Combining these, at a given λ, σ is approximately proportional to $(\gamma/\rho)^{\frac{1}{2}}$ or to $B^{\frac{1}{2}}$ (this B is magnetic field). Flux constant B is (75) proportional to γ^2/ρ and to H_2 which is slowly varying from λ/λ_c ranging from say 0.3 to 20.

In general we need to keep σ_y and $\sigma_{y'}$ small (small emittance) and to work with γ and B as high as feasible, without encountering serious beam power problems. Angular variation in the slice through the slit of Fig. 29 can be reduced by diaphragming further on in the system, but this of course reduces the flux.

In the x direction, along the slit, the angular density is given by (79) multiplied by 1/M. The x' extent is simply equal to the orbital arc subtended $\times$ 1/M. The size x has a one σ width (80) of $(\sigma_x^2 + s^2\sigma'^2)^{\frac{1}{2}} \times M$, and this indicates the desirability of keeping σ_x and s small.

There are many different focusing systems that can precede or follow the slit. They are all subject to the unfortunate restriction that we cannot compress phase space; we cannot reduce both size and angle without slicing off flux. Interaction with the numerous source parameters is complex and analysis is probably best done numerically.

REFERENCES

1. J. Schwinger, Phys. Rev. 75, 1912 (1949).
2. A.A. Sokolov and I.M. Ternov, "Synchrotron Radiation", Pergamon Press (1968).
3. D.H. Tomboulian and P.L. Hartman, Phys. Rev. 102, 1423 (1956).
4. R.A. Mack, "Spectral and Angular Distributions of Synchrotron Radiation". Internal report CEAL-1027, Cambridge Electron Accelerator (1966).
5. K. Codling, Rep. Prog. Phys. 36, 541 (1973).
6. E.M. Rowe, IEEE Trans. on Nuc. Sci. NS-20, 973 (1973).
7. Orsay LURE Group, Ann. de Phys. 9, 9 (1975).
8. H.Ellis and J.R. Stevenson, "Computer Calculation and Numerical Tabulations of Some MacDonald Functions", School of Physics, Georgia Institute of Technology.
9. M. Abramowitz and Irene Stegun, "Handbook of Mathematical Functions", Dover (1972).; also U.S. Government Printing Office (1972).
10. A. Blanc-Lapierre and R. Fortet, "Theory of Random Functions", Gordon and Breach (1965); C.E. Weatherburn, "Mathematical Statistics", Cambridge Univ. Press (1949).
11. B.O. Peirce, "A Short Table of Integrals", Ginn and Co. (1929).
12. J.W. Blaker, "Geometric Optics", Marcel Dekker (1971).
13. W. Brouwer, "Matrix Methods in Optical Instrument Design", Benjamin (1964).
14. A.P. Sabersky, Particle Accelerators 5, 199 (1973).
15. A.P. Banford, "Transport of Charged Particle Beams", Spon (1966).
16. E.D. Courant and H.S. Snyder, Annals of Phys. 3, 1 (1958);
    G.K. Green and E.D. Courant, "The Proton Synchrotron", Handbuch der Physik XLIV, Springer (1959);
    H. Bruck, "Accelerateurs Circulaires de Particules", Presses Universitaires de France (1966);
    M. Sands, "Physics of Electron Storage Rings", SLAC Report 121 (1970).

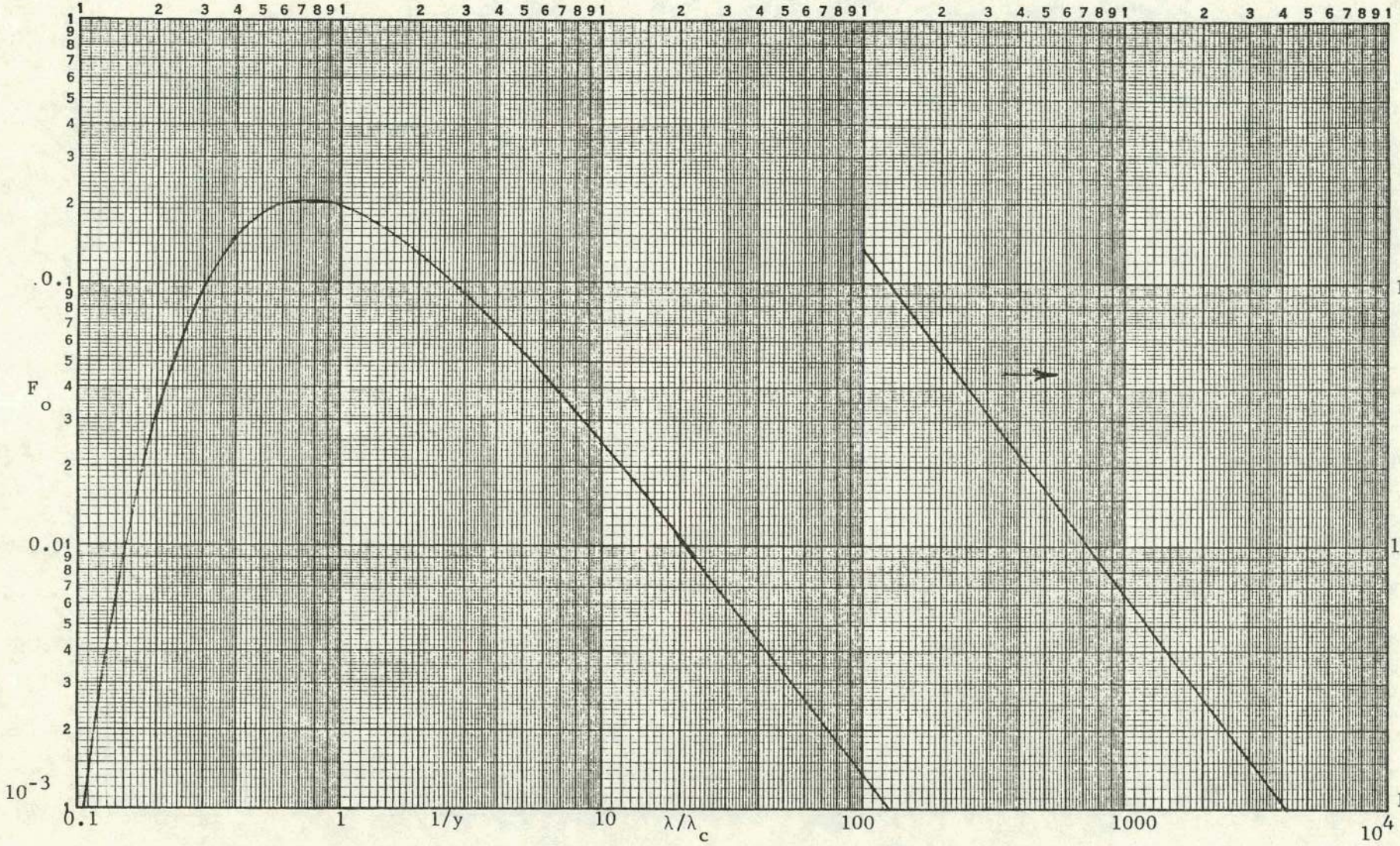

Fig. 1 $F_o(\lambda/\lambda_c)$ $N(\lambda)=(\gamma^4/\rho)F_o$ photons/Å, sec, ma, mrad θ

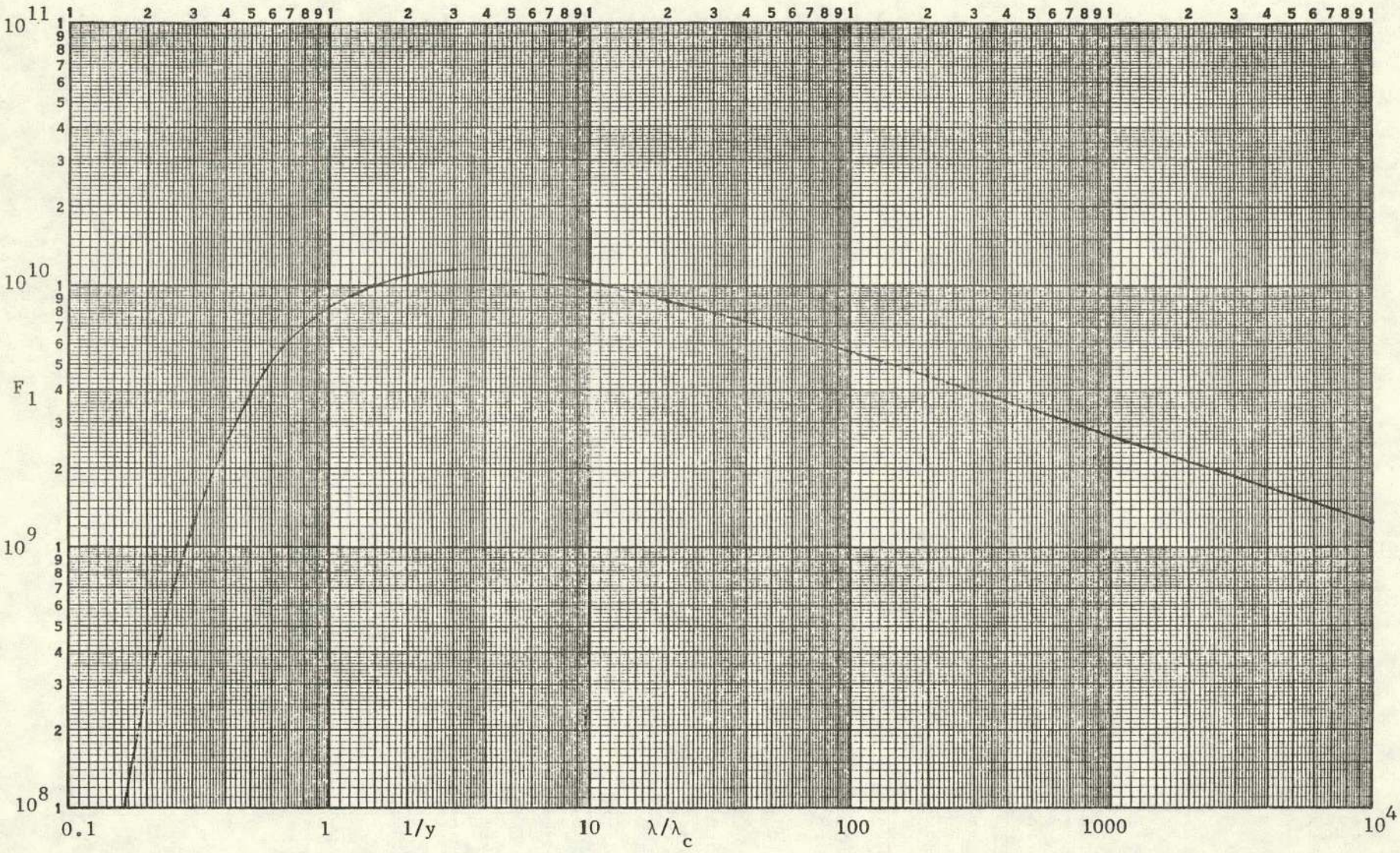

Fig. 2 $F_1(\lambda/\lambda_c)$ $N_k(\lambda) = k\gamma F_1$ photons/kλ, sec, ma, mrad θ

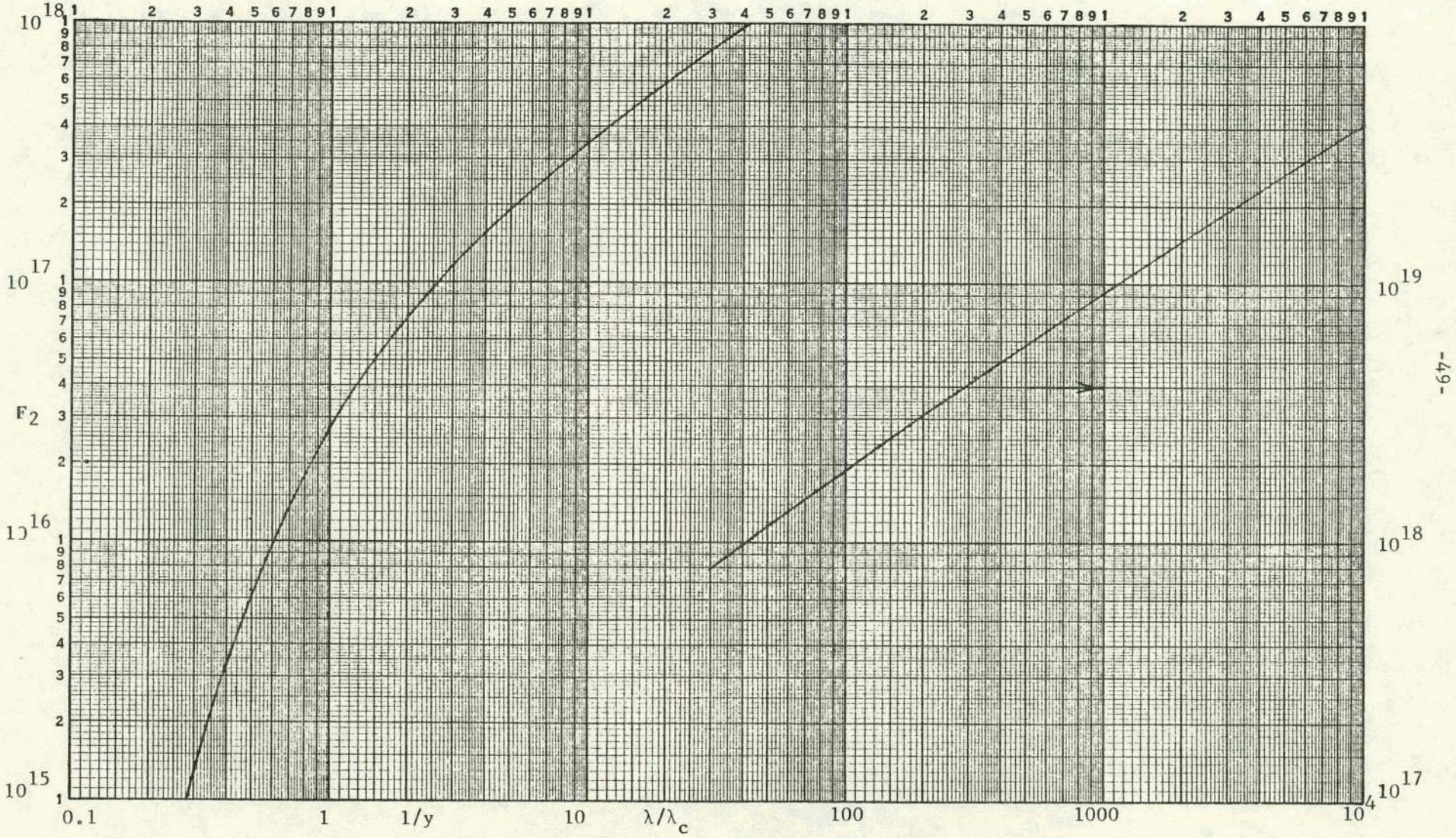

Fig. 3 $F_2(\lambda/\lambda_c)$ $N_{\Delta\epsilon}(\lambda)=(\rho/\gamma^2)F_2$ photons/eV, sec, ma, mrad θ

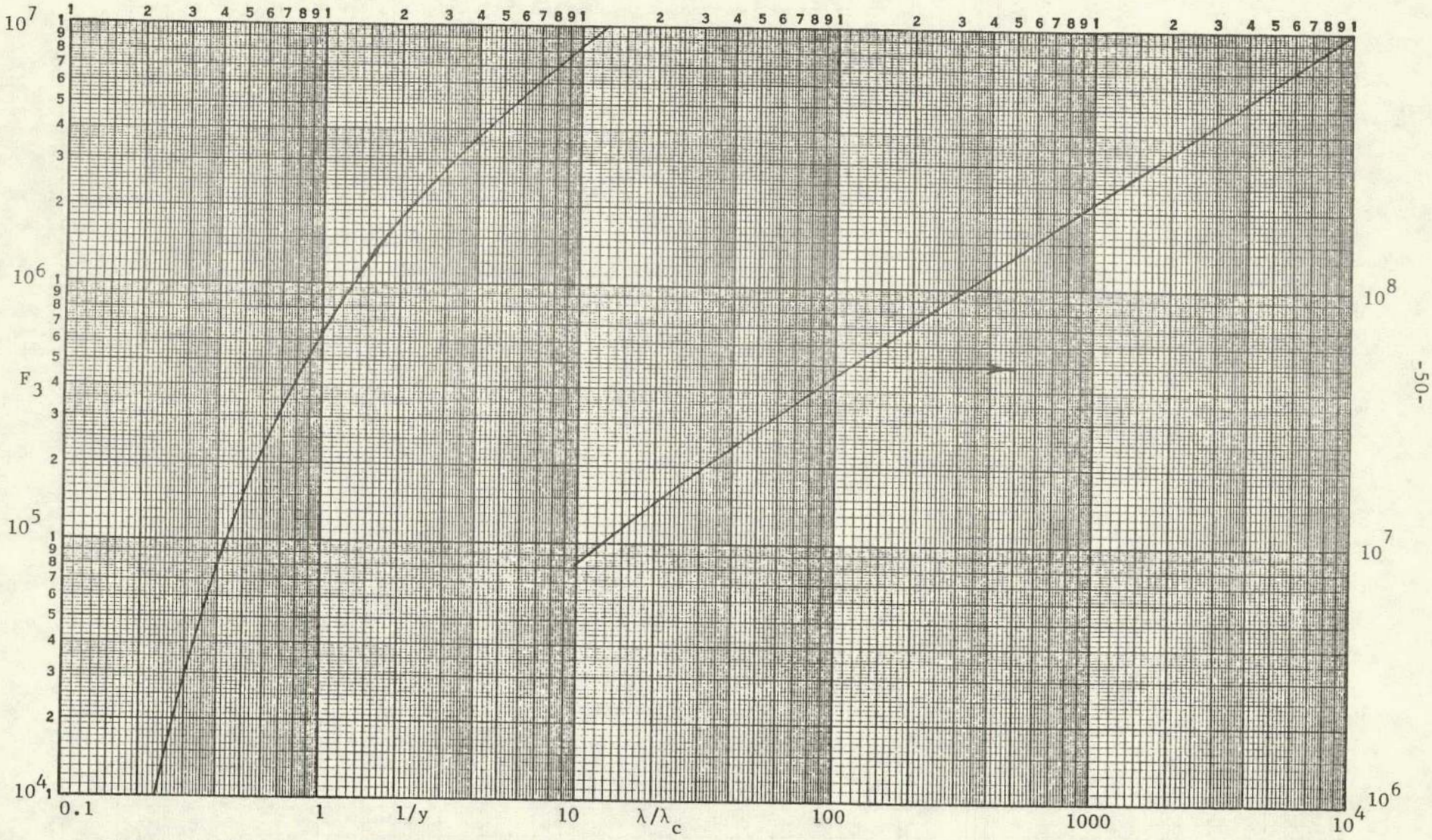

Fig. 4 $F_3(\lambda/\lambda_c)$ $N_{\Delta\varepsilon}(\lambda)=\gamma\lambda_c F_3$ photons/eV, sec, ma, mrad θ

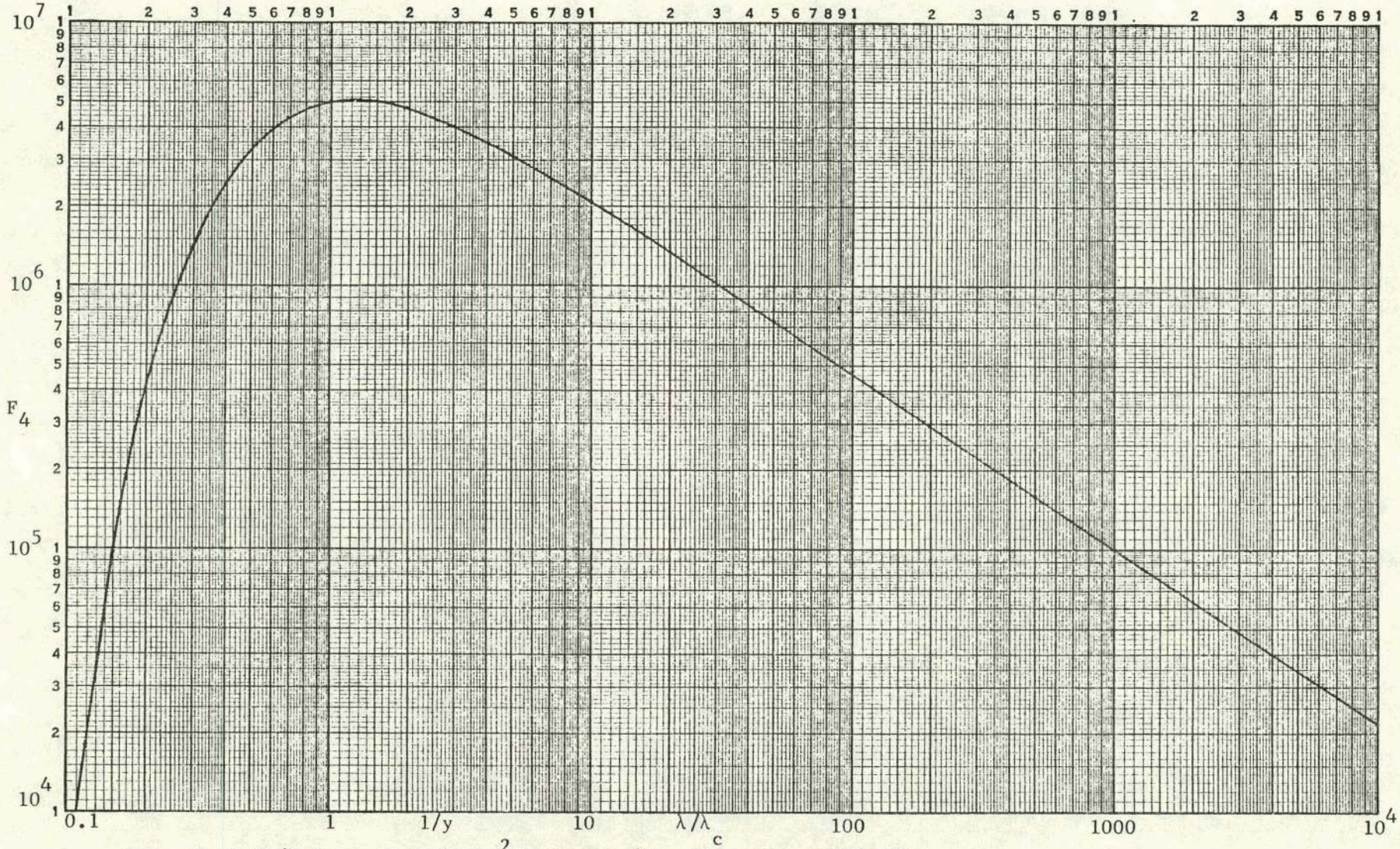

Fig. 5 $F_4(\lambda/\lambda_c)$ $N_k(\lambda,0)=k\gamma^2 F_4$ photons/kλ, sec, ma, mrad θ, ψ

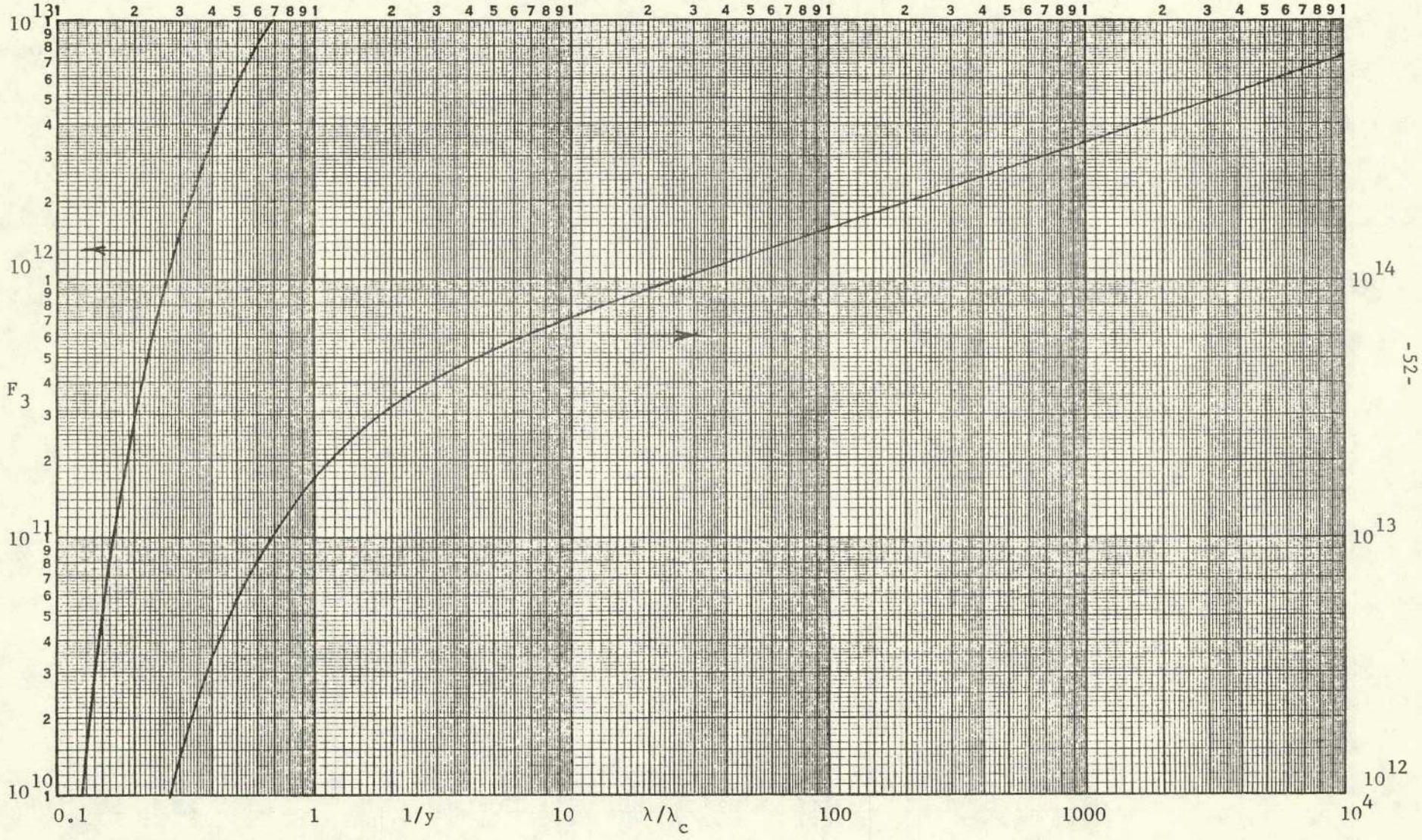

Fig. 6 $F_5(\lambda/\lambda_c)$ $N_{\Delta\epsilon}(\lambda,0)=(\rho/\gamma)F_5$ photons/eV, sec, ma, mrad θ, ψ

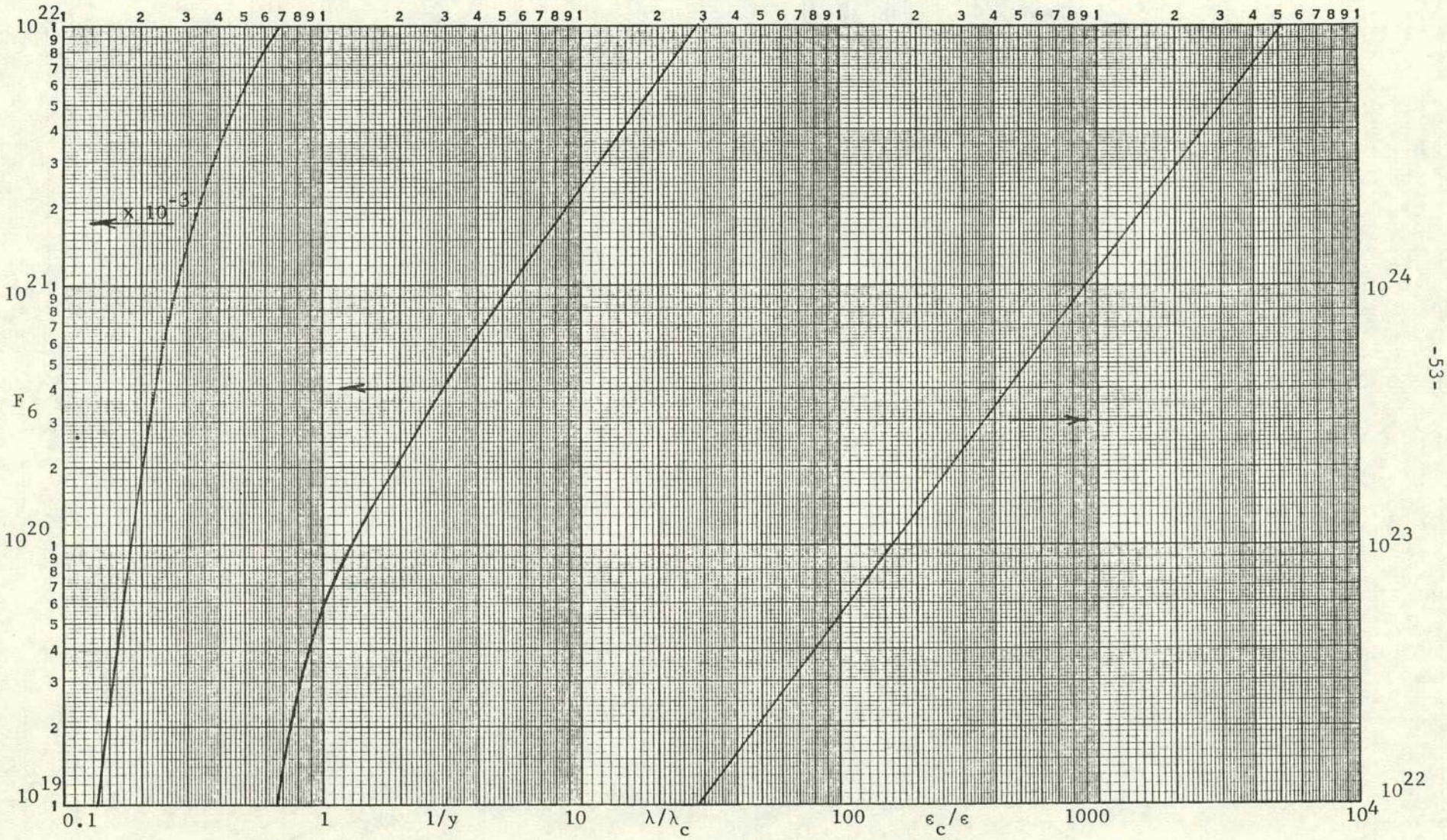

Fig. 7. $F_6(\lambda/\lambda_c)$ $N_{\Delta\varepsilon}(\varepsilon,0)=(\varepsilon_0^2/\gamma^4)F_6$ photons/eV, sec, ma, mrad θ, ψ

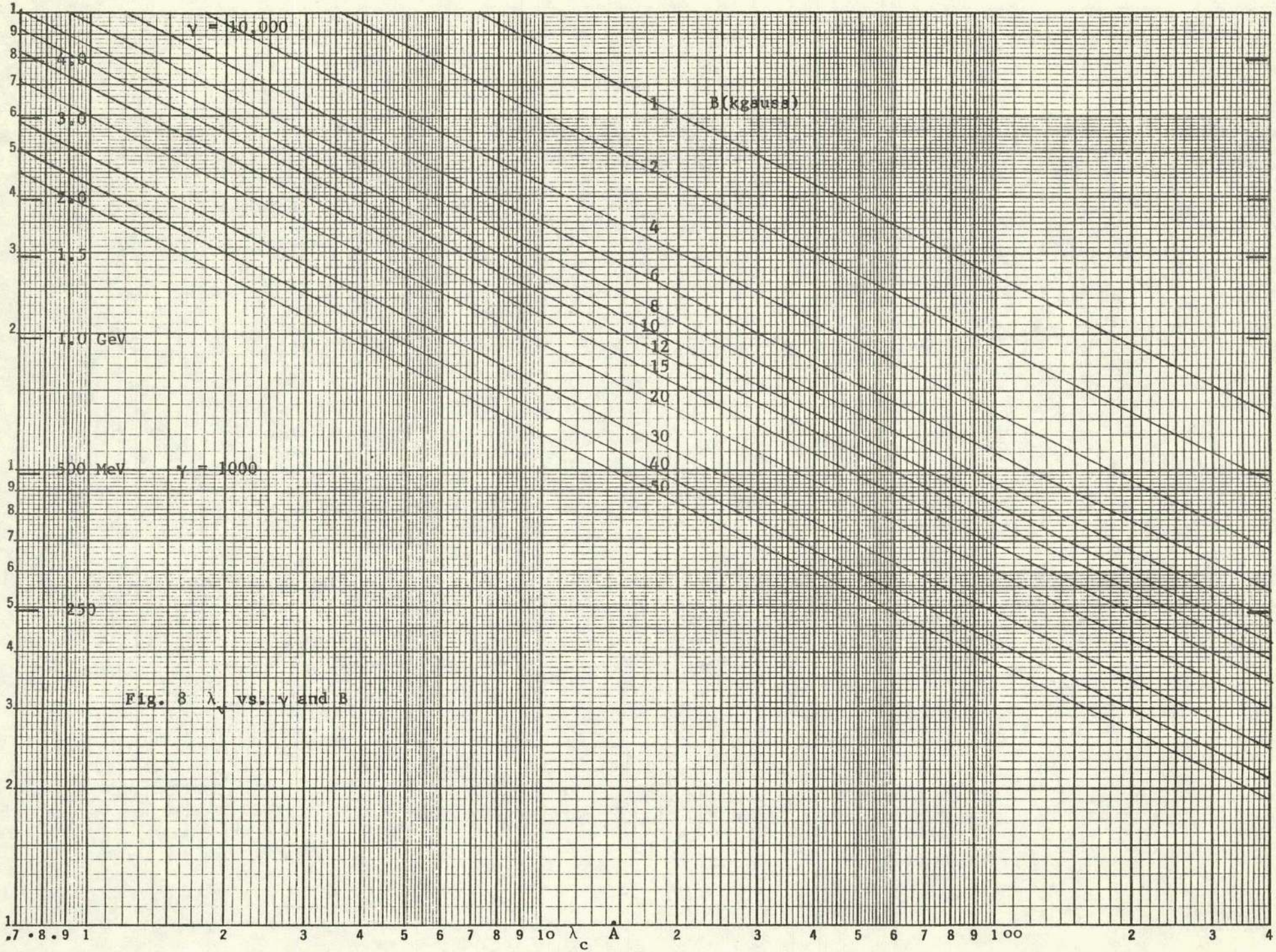

Fig. 8 λ_c vs. γ and B

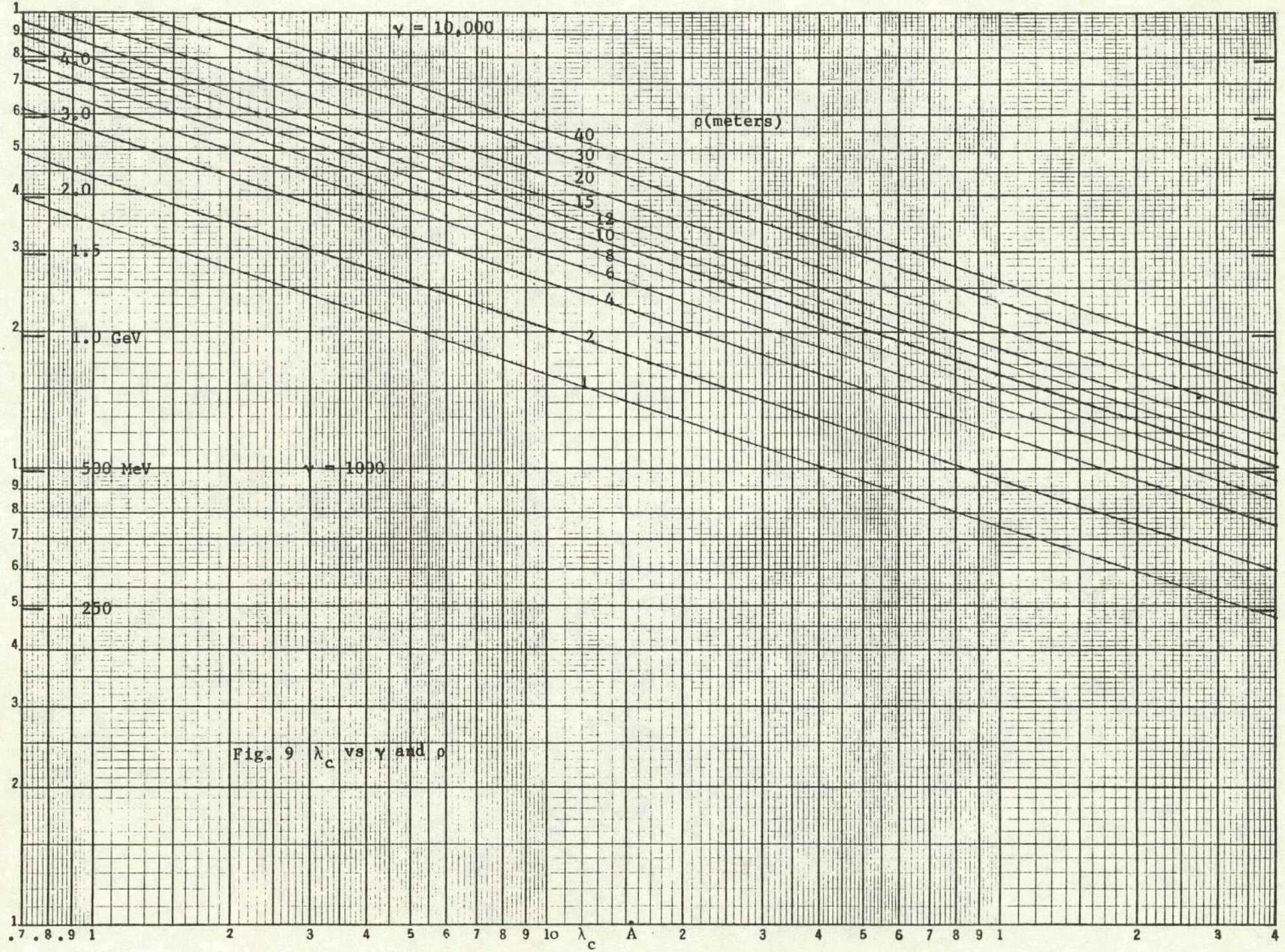

Fig. 9 λ_c vs γ and ρ

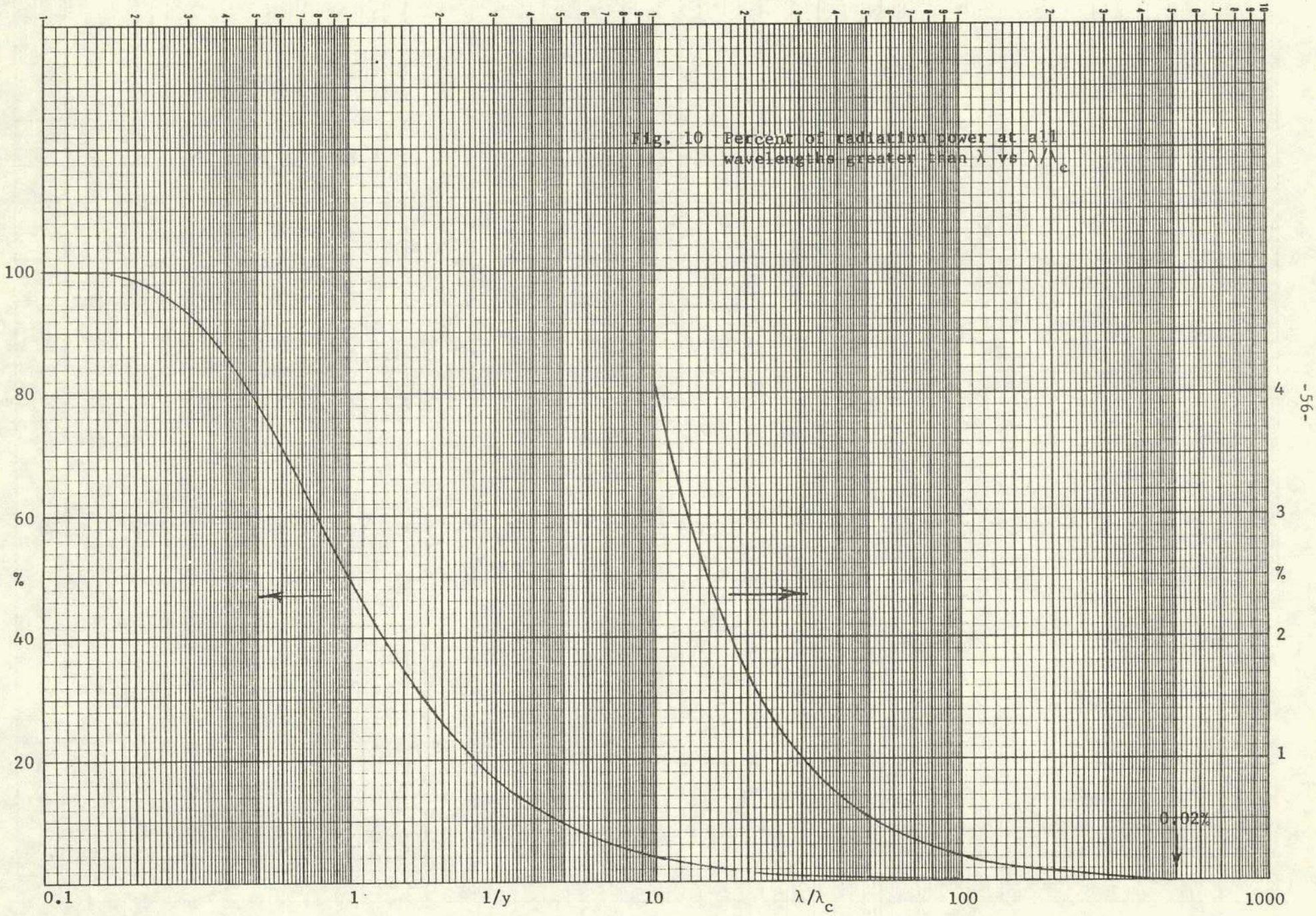

Fig. 10 Percent of radiation power at all wavelengths greater than λ vs λ/λ_c

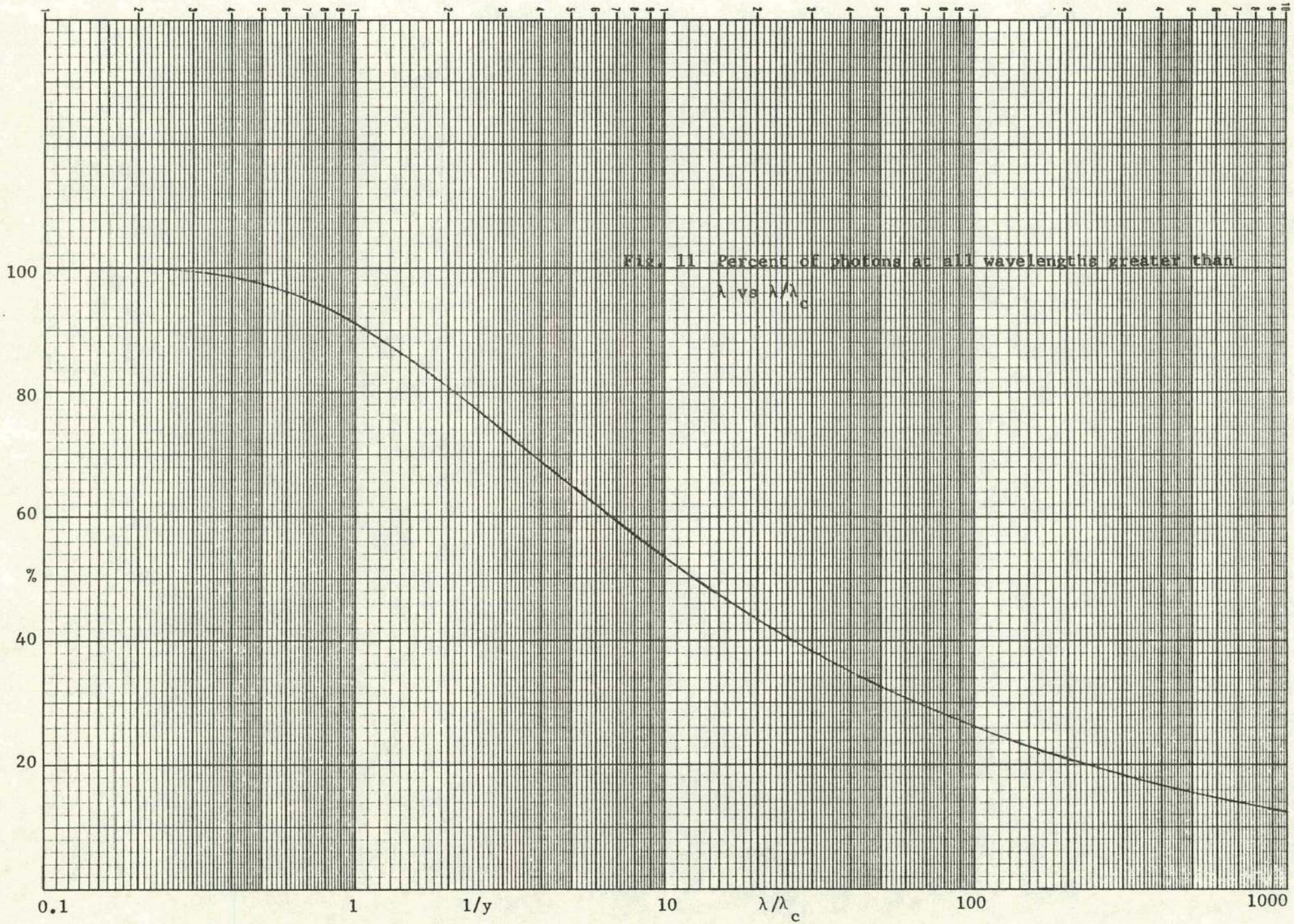

Fig. 11 Percent of photons at all wavelengths greater than λ vs λ/λ_c

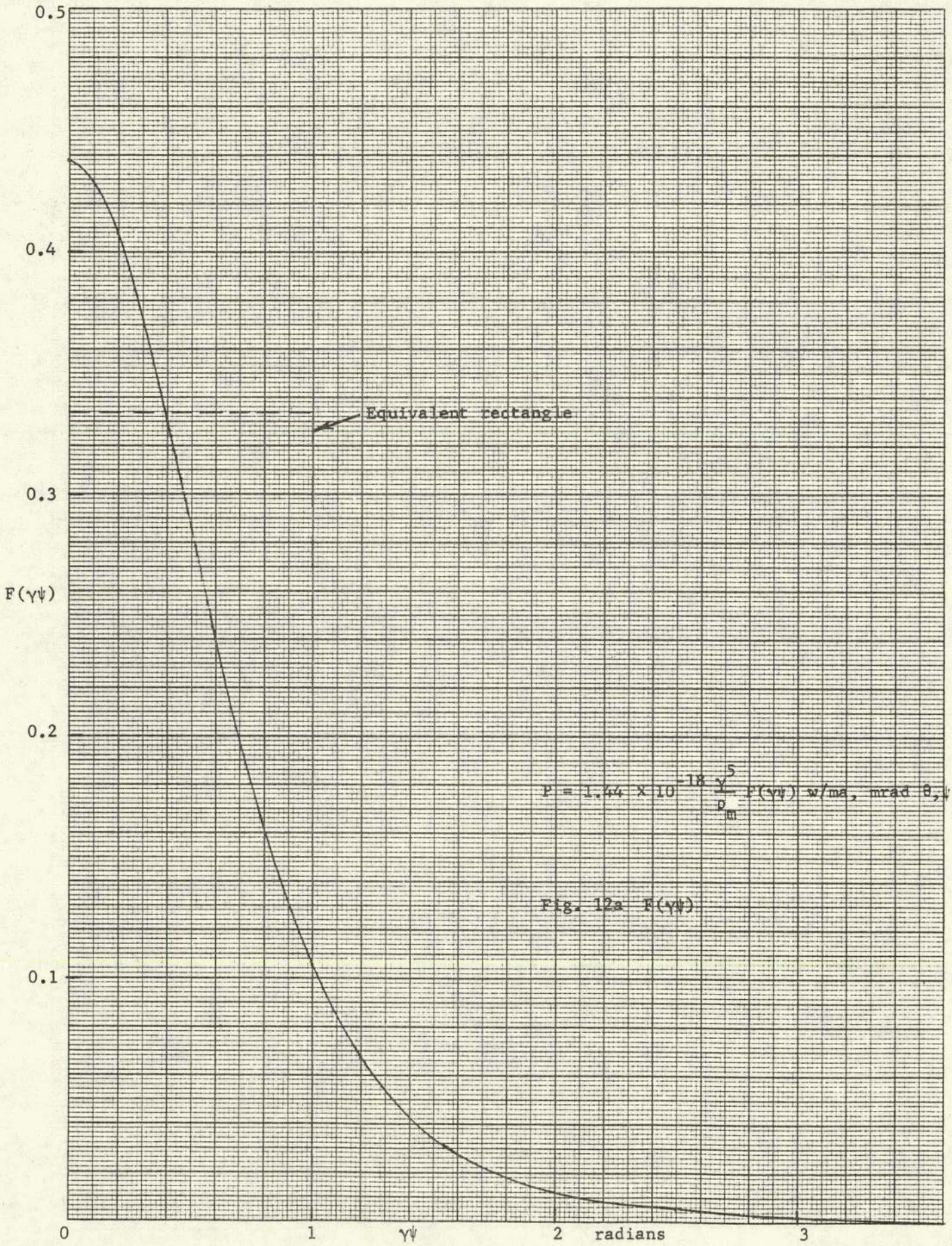
0.5
0.4
0.3
0.2
0.1
0
1
2
3
radians
Equivalent rectangle
F(γψ)
γψ
P = 1.44 × 10^-18 (γ^5/ρ_m) F(γψ) w/ma, mrad θ,ψ

Fig. 12a F(γψ)

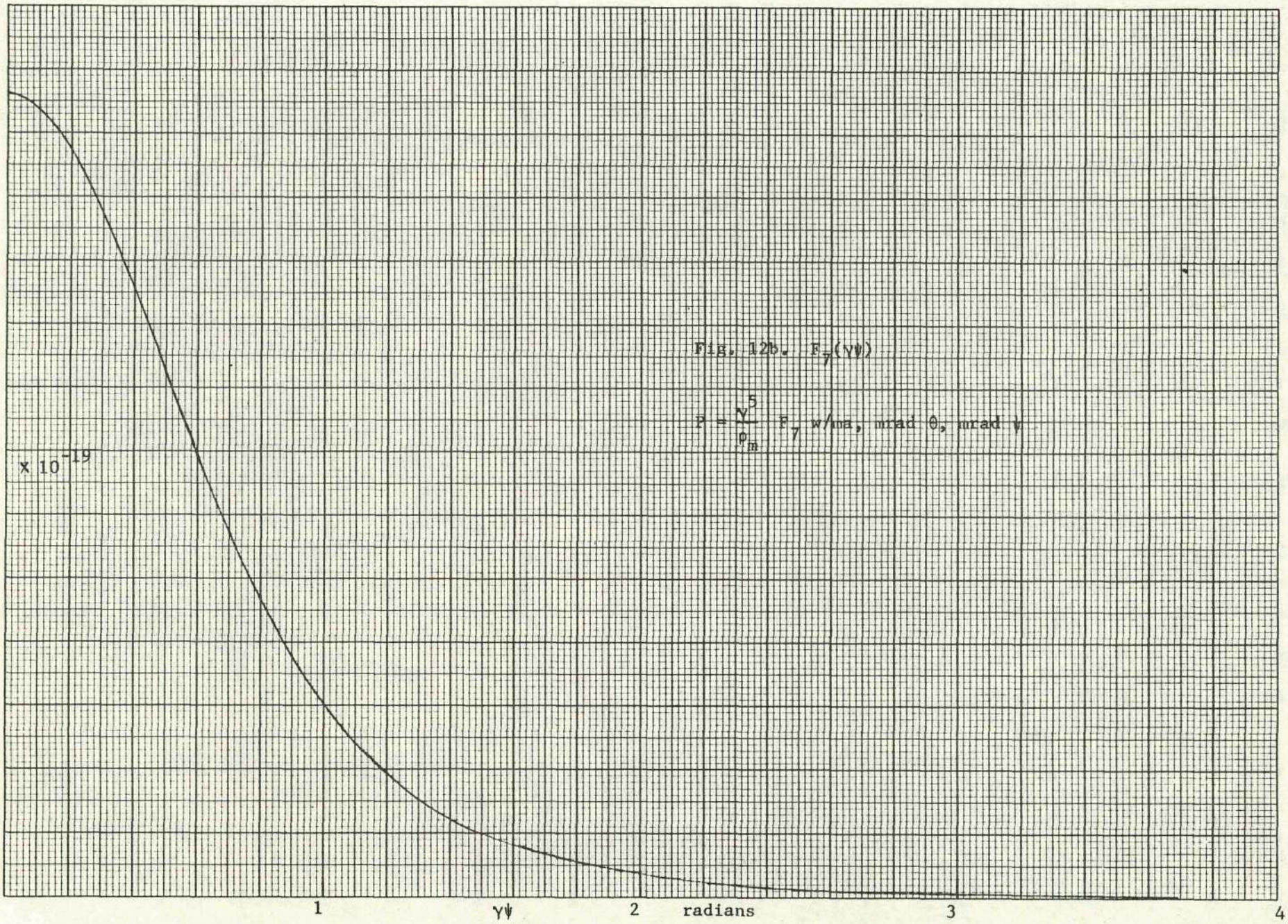

Fig. 12b. $F_7(\gamma\psi)$

$P = \frac{\gamma^5}{\rho_m} F_7$ w/ma, mrad θ, mrad ψ

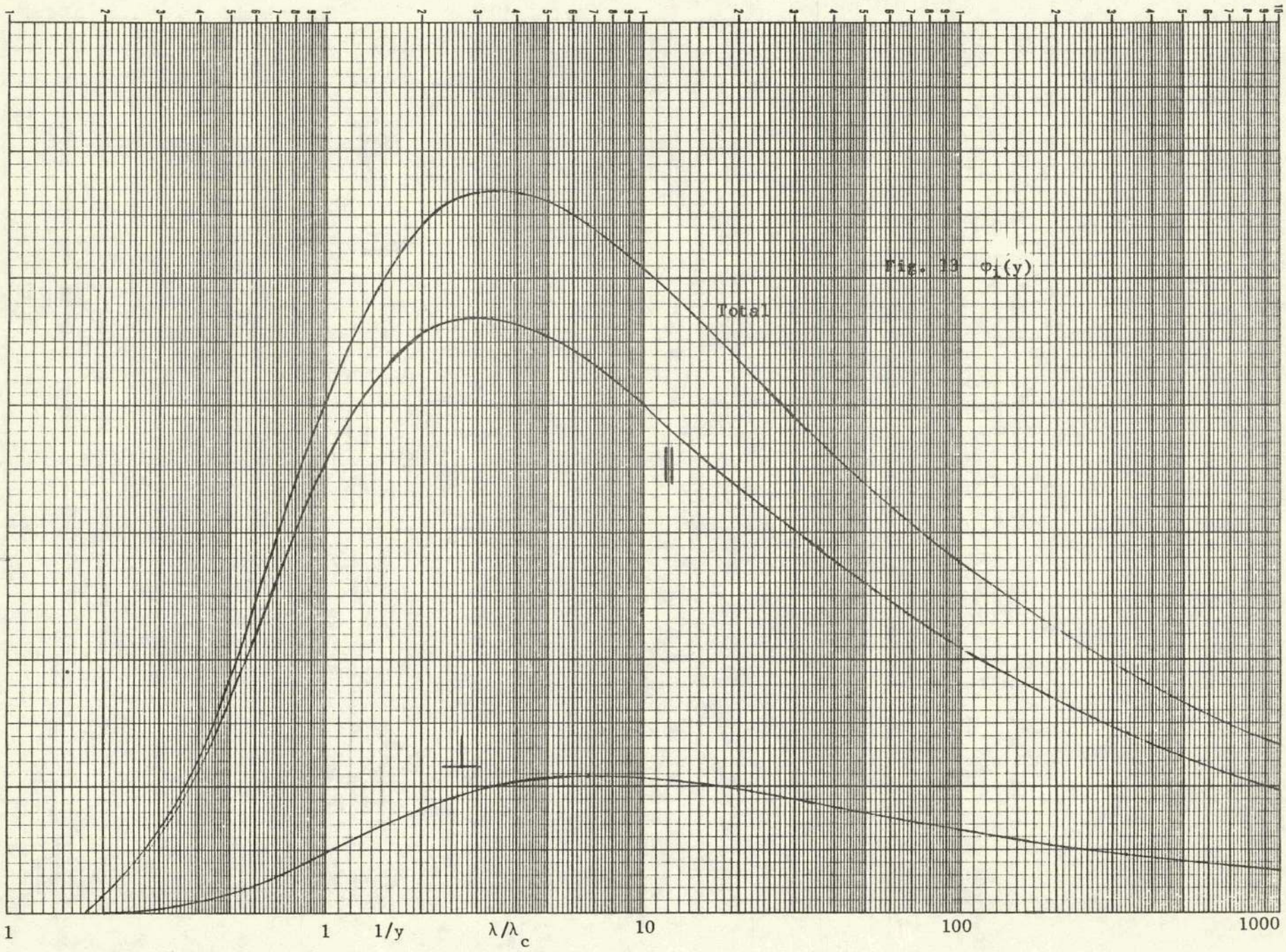

Fig. 13 $\Phi_i(y)$

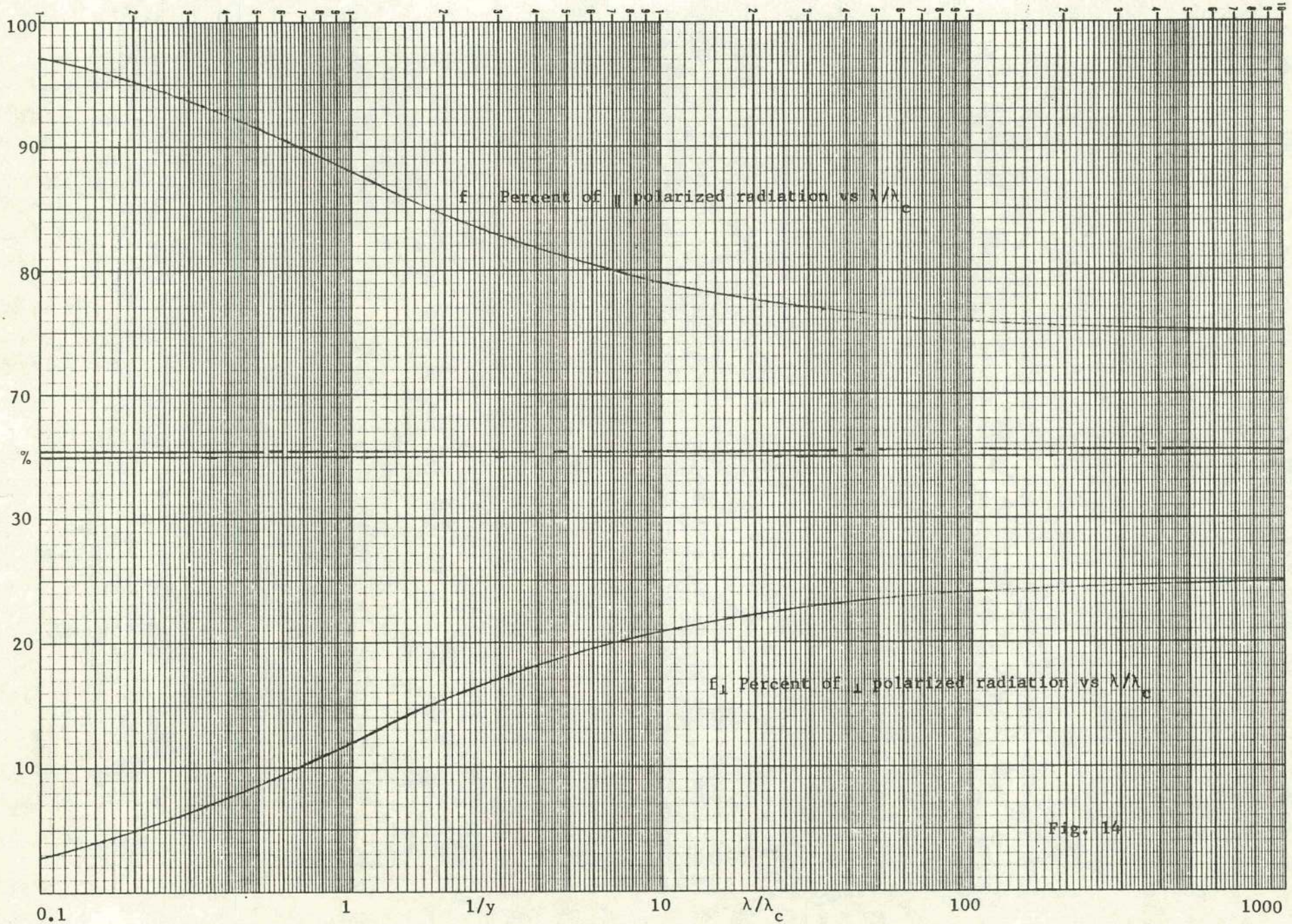
100
90
80
70
%
30
20
10
f ∥ Percent of ∥ polarized radiation vs λ/λc
f⊥ Percent of ⊥ polarized radiation vs λ/λc
0.1
1
1/y
10
λ/λc
100
1000

Fig. 14

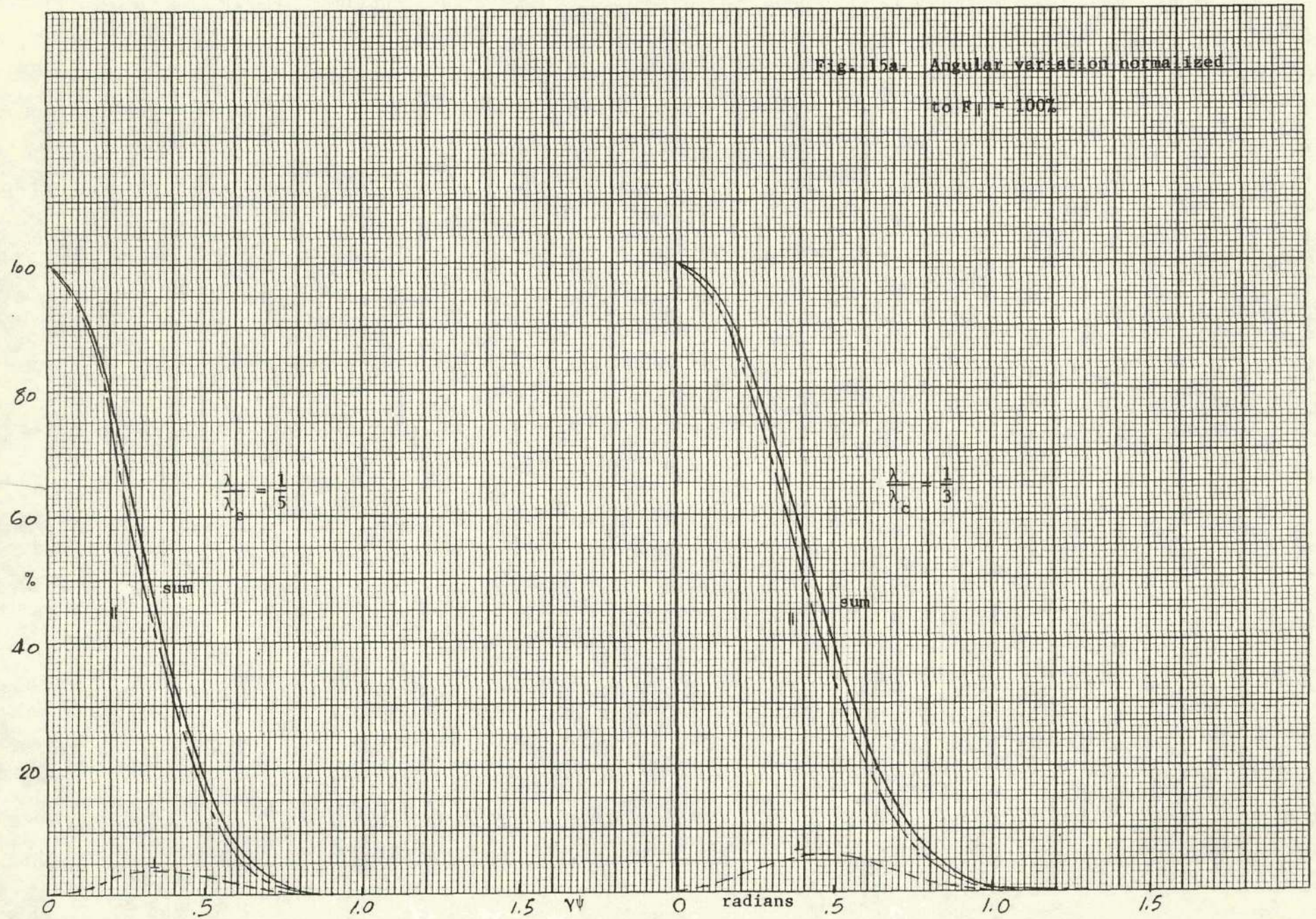

Fig. 15a. Angular variation normalized to $F_{\parallel} = 100\%$

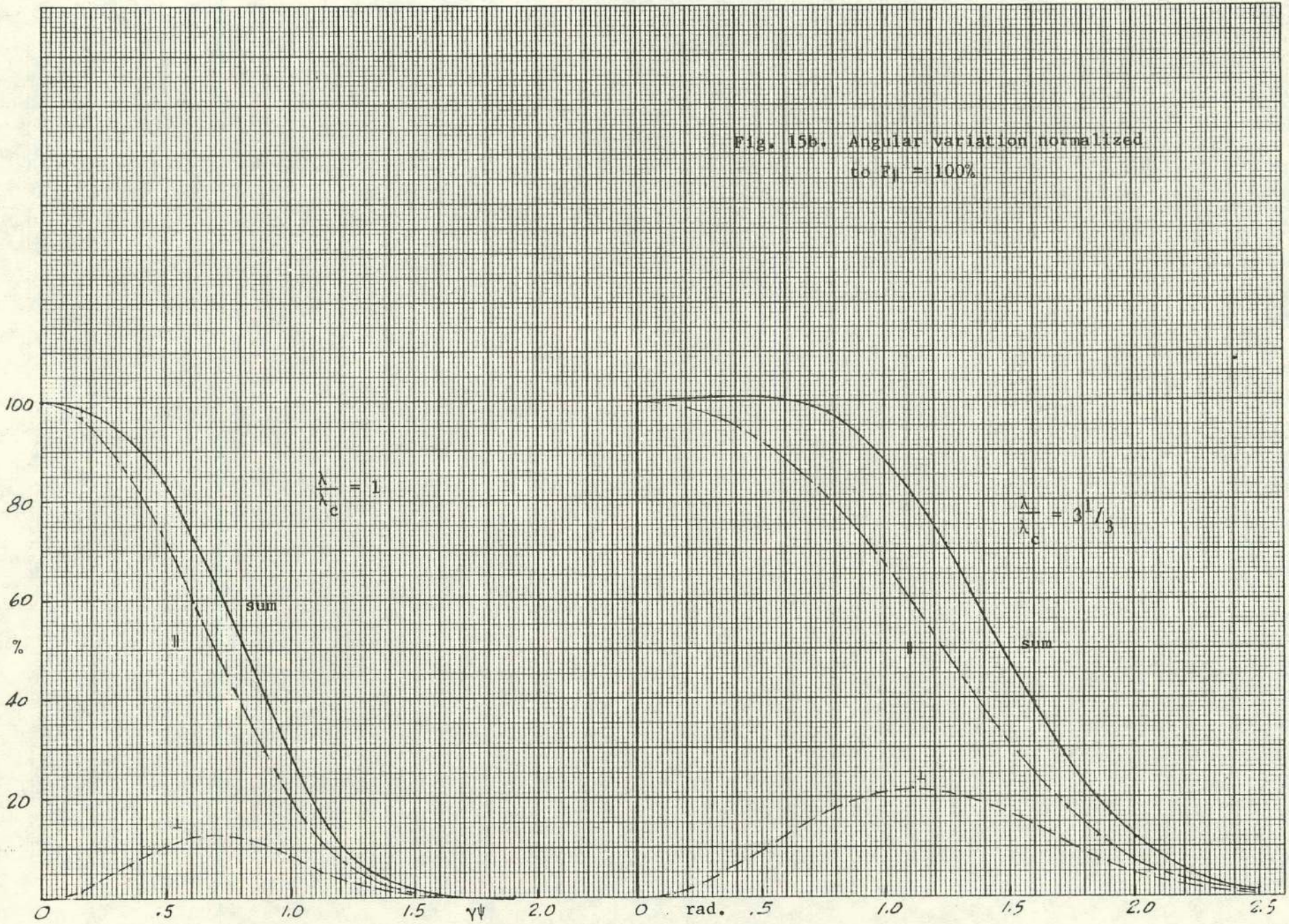

Fig. 15b. Angular variation normalized to $F_{\parallel} = 100\%$

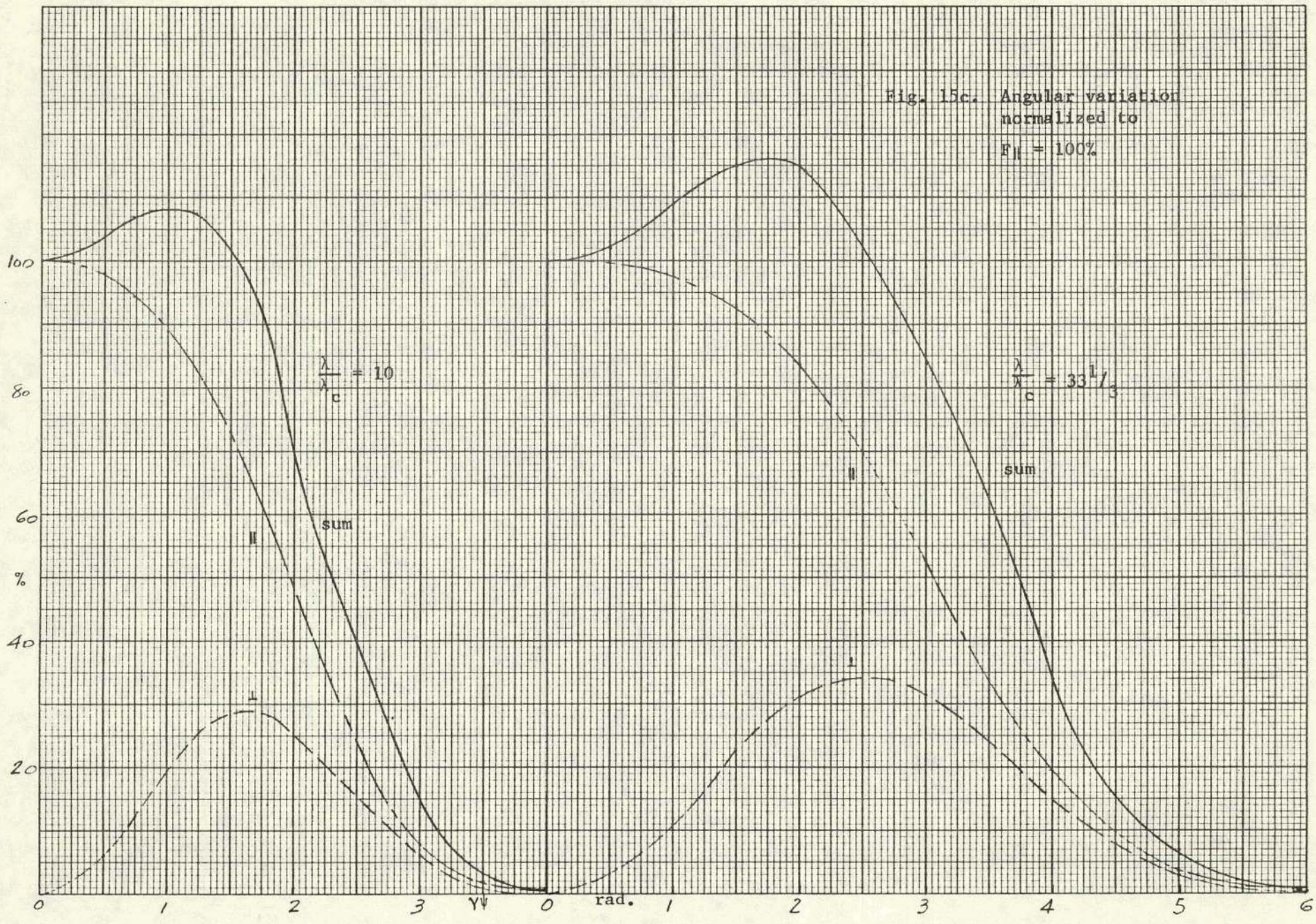

Fig. 15c. Angular variation normalized to $F_{\parallel} = 100\%$

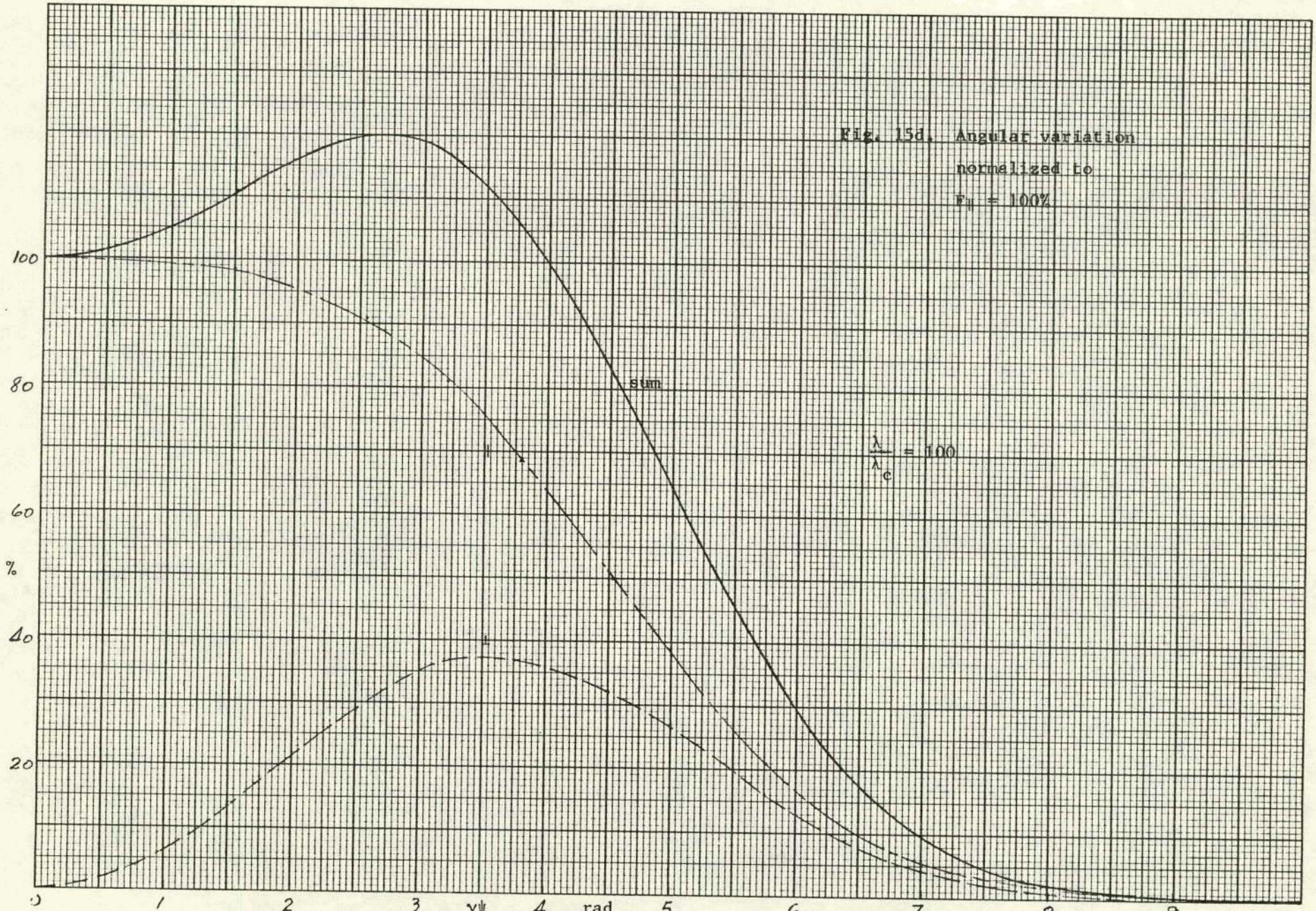

Fig. 15d. Angular variation normalized to $F_{\parallel} = 100\%$

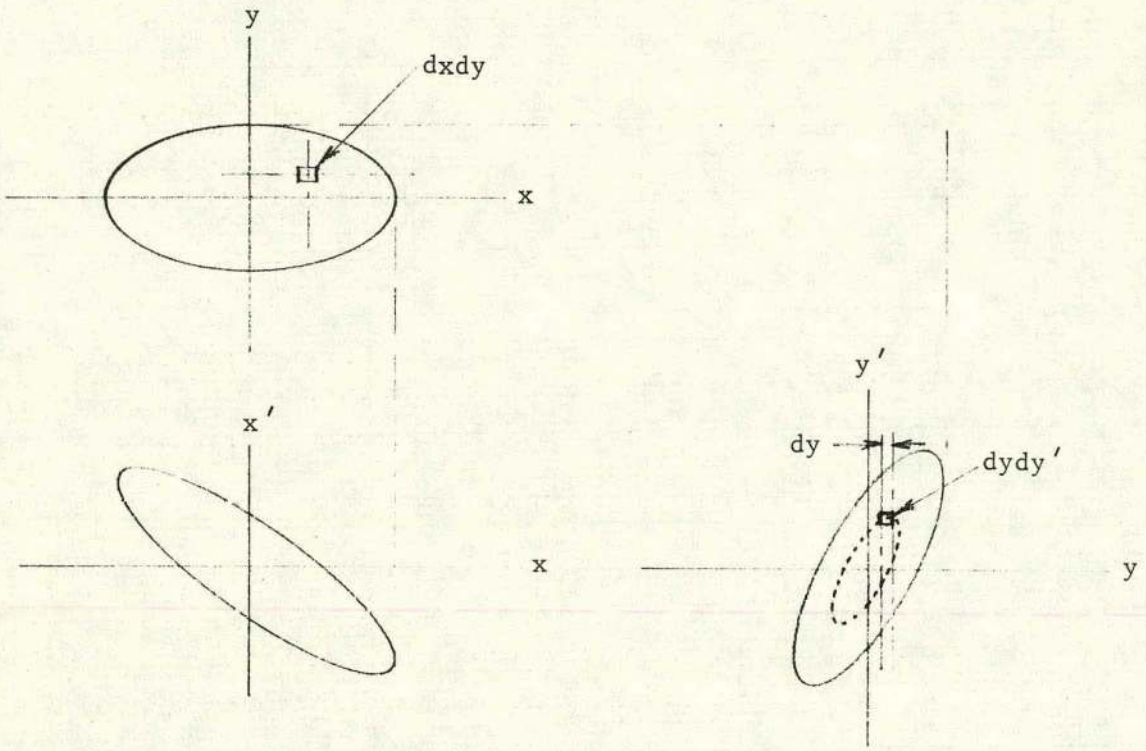

Fig. 16 Electron beam cross section in configuration and phase space

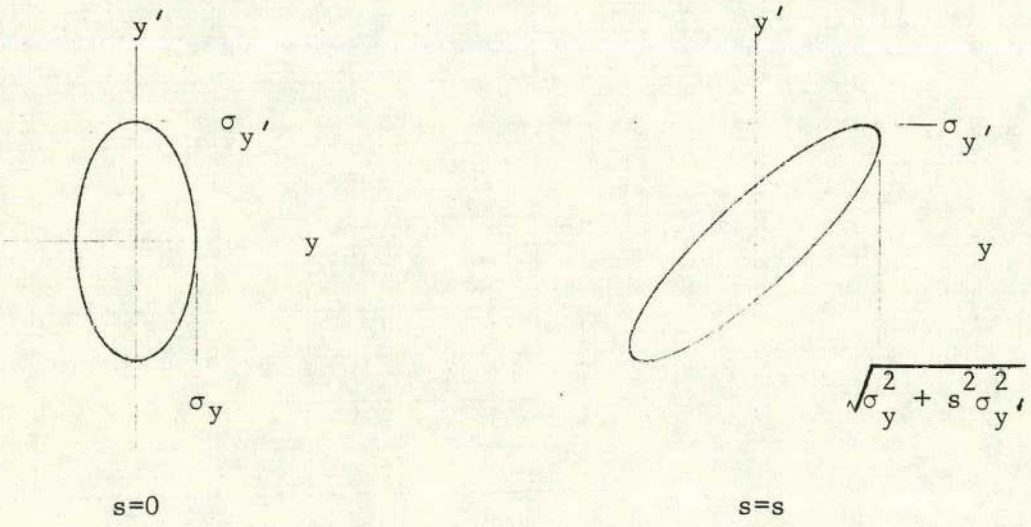

Fig. 17a. Envelope at waist, s=0. b. Envelope at s.

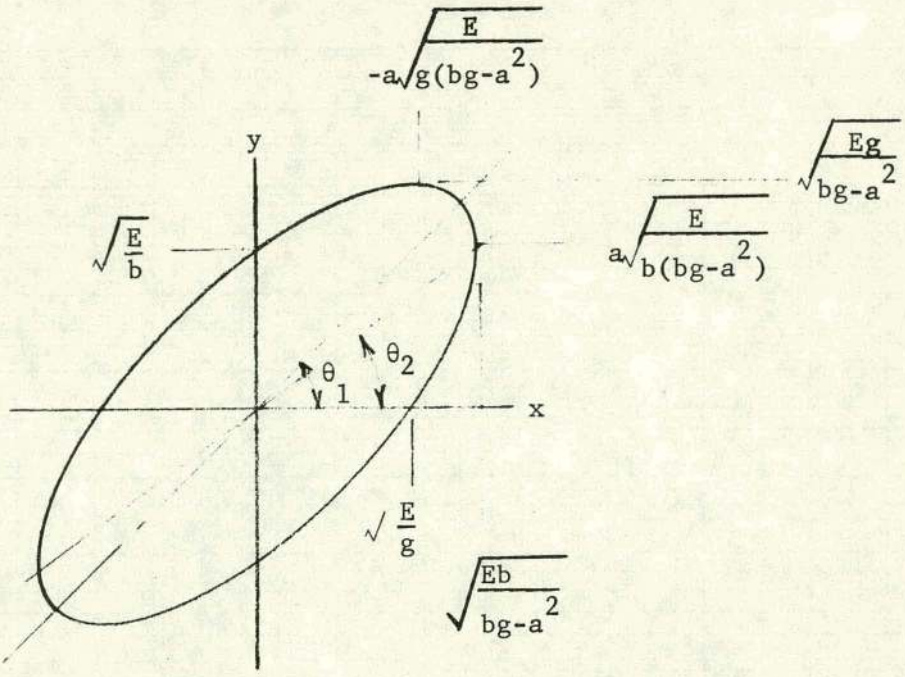

Ellipse

$gx^2 + 2axy + by^2 = E$

$\text{area}/\pi = \hat{xy}(o) = E/\sqrt{bg-a^2}$

$\tan 2\theta_1 = 2a/(g-b)$ (axis)

$\tan \theta_2 = -a/b$ (diameter)

Fig. 18 Properties of ellipse

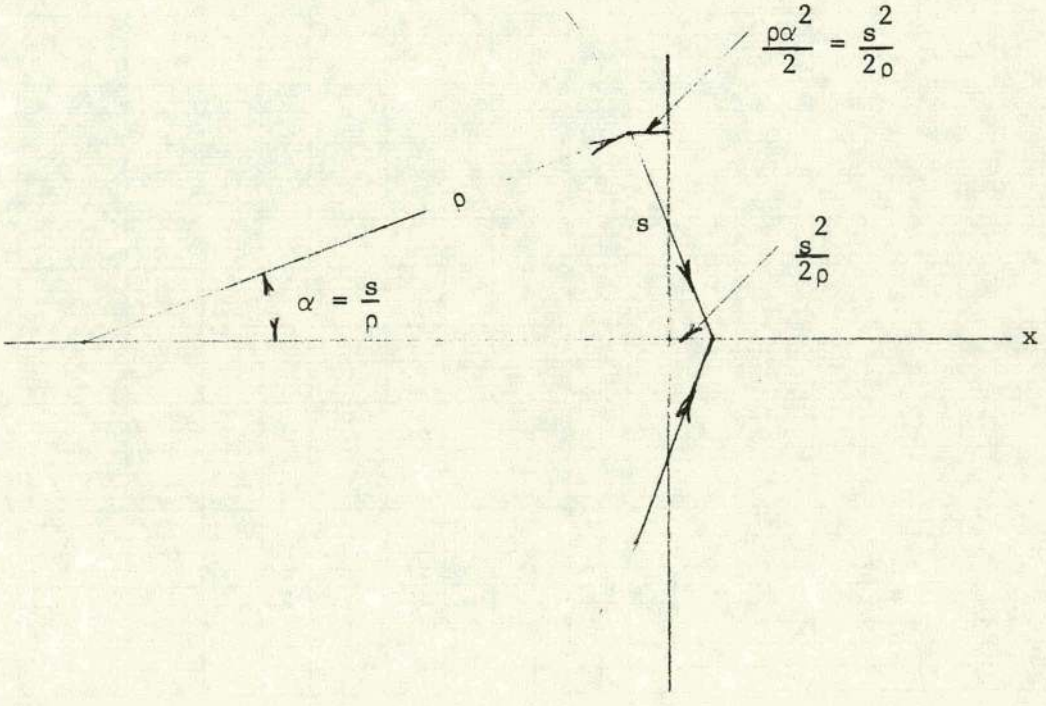

Fig. 19 Arc in x-s plane

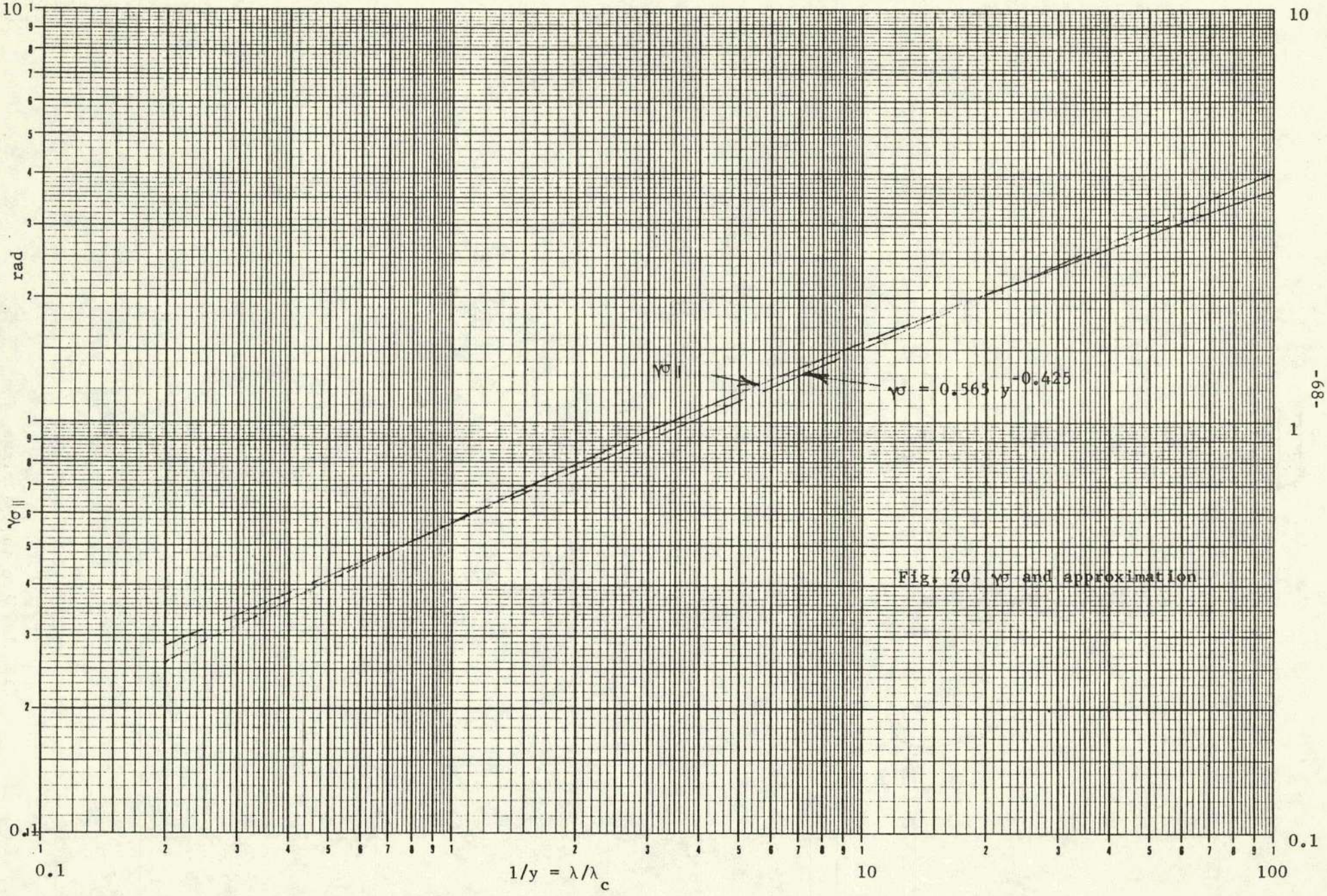

Fig. 20 $\gamma\sigma$ and approximation

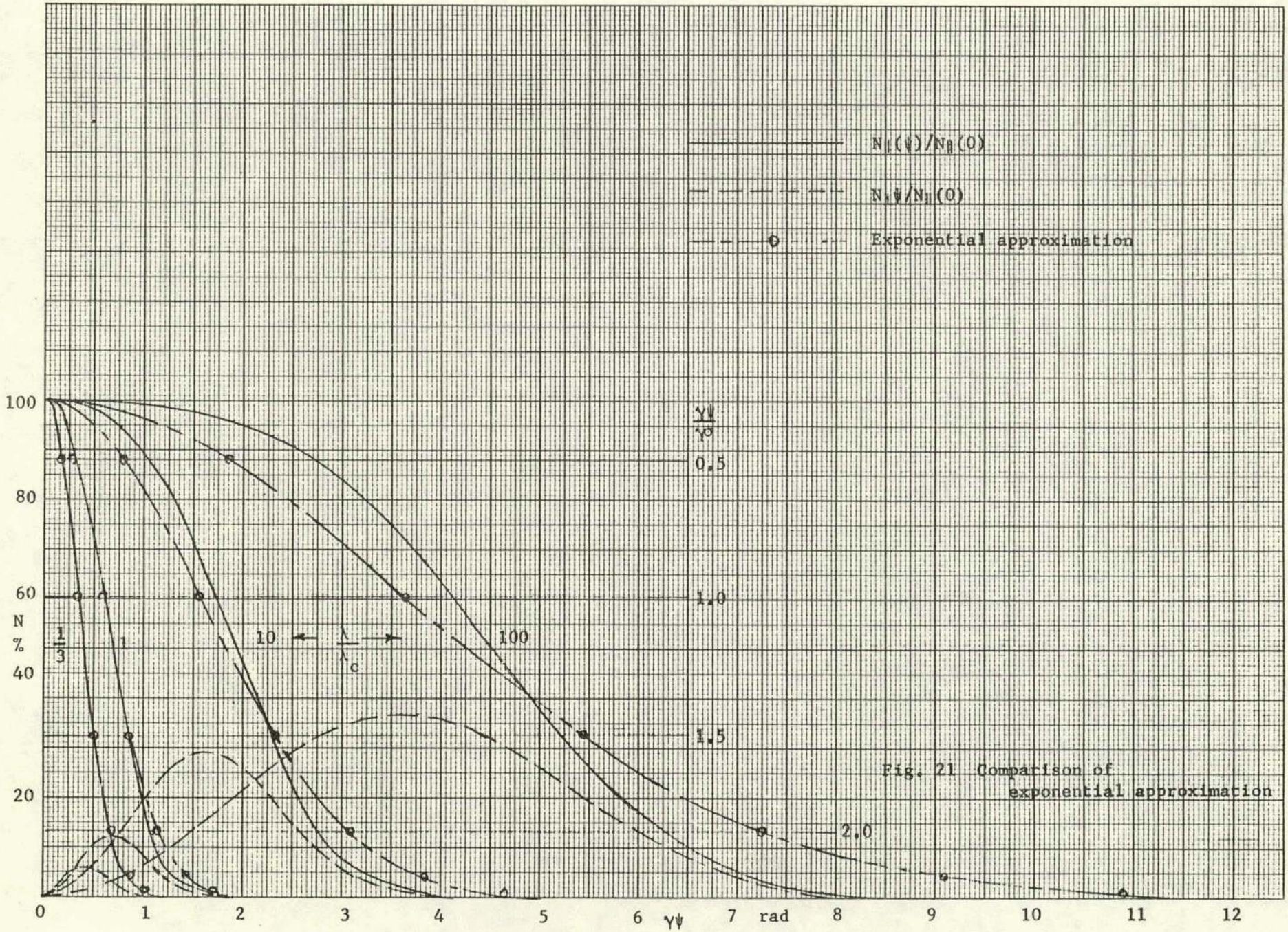

Fig. 21 Comparison of exponential approximation

APPENDIX A

Computation of synchrotron radiation spectra requires the modified Bessel functions $K_{1/3}(x)$, $K_{2/3}(x)$, $K_{5/3}(x)$ and the integral $\int_x^\infty K_{5/3}(\eta)\, d\eta$, or the Tomboulian and Hartman $G = x^3 \int_x^\infty K_{5/3}(\eta)\, d\eta$. The most accurate tables are probably the "Tables of Bessel Functions of Fractional Order," Vol. II, Computation Lab., National Bureau of Standards, Columbia University Press, New York, 1948. However, the K_ν functions must be computed from the I_ν, which are tabulated, using;

$$K_\nu(x) = \frac{\pi}{2 \sin \pi\nu} \left[I_{-\nu}(x) - I_\nu(x) \right]$$

To obtain $K_{5/3}(x)$ from these tables it would be necessary to use a recurrence relation such as

$$K_{5/3}(x) = K_{1/3}(x) + \frac{4}{3x} K_{2/3}(x)$$

These tables give $x^{\pm\nu} I_{\mp\nu}(x)$ for small arguments and since this product converges as $x \to 0$ the values of K for arguments less than 0.002 (less than 0.005 for four figure accuracy) can be calculated by

$$K_{1/3}(x) = 1.81380 \, (0.930437 \, x^{-1/3} - 0.888823 \, x^{1/3})$$

$$K_{2/3}(x) = 1.81380 \, (0.592549 \, x^{-2/3} - 0.697828 \, x^{2/3}) \qquad x<0.002$$

Values of G_o for arguments less than 0.001 can be obtained by use of Schwinger's expansion for $\omega \ll \omega_c$. Equating his II16 and II20

$$G_o = \int_y^\infty K_{5/3}(\eta)\, d\eta = 2.149 \, y^{-2/3} \left[1 - 0.677 \, (y/2)^{1/3} + \ldots \right], \quad y < 0.001$$

The most convenient tables of $K_{1/3}$, $K_{2/3}$, $K_{5/3}$ and G are in an unnumbered and undated report[8] - H. Ellis and J.R. Stevenson, "Computer Calculations and Numerical Tabulations of Some MacDonald Functions," School of Physics, Georgia Tech. (There is a misprint on page 3. The approximation for $x \gg 1$ is $K_{\mu}(x) = \sqrt{\frac{\pi}{2x}}\ e^{-x}$).

The short tables and graphs in the report by R.A. Mack[4] are convenient but the report, issued from the late Cambridge Electron Accelerator, is hard to get. Note that Mack's g(r) is related to G_1 by

$$g(r) = G_1(r)/0.9 \times 2^{2/3}(5/3)! = G_1(r)/2.150$$

The following short Table AI of functions has arguments spaced for reasonable interpolation. $H_o(y,0) = K^2_{2/3}(y/2)$ and $G_o(y) = \int_y^{\infty} K_{5/3}(\eta)\ d\eta$ are tabulated. H_i and G_i can then be obtained by multiplying by y^i.

Figure A1 is a graph of G(y) e.g. $G_3(y)$ vs. y.

TABLE AI

y	$K_{1/3}(y)$	$K_{2/3}(y)$	$K_{5/3}(y)$	$H_o(y,0)$	$G_o(y)$
.0001	36.284	498.86	6.652+6	6.271+5	973
.001	16.715	107.46	1.4330+5	2.910+4	213.6
.002	13.192	67.686	4.514+4	1.155+4	133.6
.004	10.376	42.621	1.422+4	4.581+3	83.49
.006	8.995	32.509	7.233+3	2.677+3	63.29
.008	8.116	26,820	4.478+3	1.817+3	51.92
.010	7.486	23.098	3.087+3	1.348+3	44.50
.020	5.781	14.498	9.723+2	5.335+2	27.36
.030	4.932	11.017	4.946+2	3.096+2	20.45
.040	4.386	9.052	3.0612	2.102+2	16.57
.050	3.991	7.762	2.110+2	1.555+2	14.03
.060	3.685	6.837	1.556+2	1.214+2	12.22
.070	3.437	6.136	1.203+2	98.37	10.85
.080	3.231	5.581	96.25	81.94	9.777
.090	3.054	5.130	79.05	69.69	8.905
.100	2.900	4.753	66.27	60.25	8.182
.150	2.343	3.513	33.57	34.15	5.832
.200	1.979	2.802	20.66	22.59	4.517
.250	1.714	2.329	14.14	16.26	3.663
.300	1.509	1.987	10.34	12.34	3.059
.350	1.343	1.725	7.915	9.713	2.607
.400	1.206	1.517	6.263	7.850	2.225
.450	1.809	1.347	5.082	6.474	1.973
.500	9.890-1	1.206	4.205	5.424	1.742
.550	9.018-1	1.086	3.534	4.602	1.549
.600	8.251-1	9.828-1	3.009	3.947	1.386
.650	7.571-1	8.933-1	2.589	3.414	1.246
.700	6.965-1	8.148-1	2.249	2.975	1.126
.750	6.422-1	7.455-1	1.967	2.610	1.020
.800	5.932-1	6.839-1	1.733	2.302	9.280-1
.850	5.489-1	6.288-1	1.535	2.040	8.465-1
.900	5.086-1	5.794-1	1.367	1.816	7.740-1
1.00	4.384-1	4.945-1	1.098	1.454	6.514-1
1.25	3.079-1	3.406-1	6.712-1	8.771-1	4.359-1
1.50	2.202-1	2.402-1	4.337-1	5.557-1	3.004-1
1.75	1.594-1	1.722-1	2.906-1	3.642-1	2.113-1
2.00	1.165-1	1.248-1	1.998-1	2.445-1	1.508-1
2.25	8.581-2	9.132-2	1.399-1	1.672-1	1.089-1
2.50	6.354-2	6.726-2	9.941-2	1.160-1	7.926-2
2.75	4.727-2	4.981-2	7.142-2	8.145-2	5.811-2

y	$K_{1/3}(y)$	$K_{2/3}(y)$	$K_{5/3}(y)$	$H_o(y,0)$	$G_o(y)$
3.00	3.531-2	3.706-2	5.178-2	5.772-2	4.286-2
3.25	2.645-2	2.767-2	3.781-2	4.123-2	3.175-2
3.50	1.988-2	2.073-2	2.778-2	2.964-2	2.362-2
3.75	1.497-2	1.558-2	2.051-2	2.144-2	1.764-2
4.00	1.130-2	1.173-2	1.521-2	1.558-2	1.321-2
4.25	8.545-3	8.853-3	1.132-2	1.138-2	9.915-3
4.50	6.472-3	6.693-3	8.455-3	8.338-3	7.461-3
4.75	4.909-4	5.069-3	6.332-3	6.132-3	5.626-3
5.00	3.729-3	3.844-3	4.754-3	4.523-3	4.250-3
5.50	2.159-3	2.220-3	2.697-3	2.481-3	2.436-3
6.00	1.255-3	1.287-3	1.541-3	1.373-3	1.404-3
6.50	7.317-4	7.495-4	8.855-4	7.659-4	8.131-4
7.00	4.280-4	4.376-4	5.113-4	4.299-4	3.842-4
7.50	2.509-4	2.562-4	2.965-4	2.426-4	2.755-4
8.00	1.474-4	1.504-4	1.725-4	1.376-4	1.611-4
8.50	8.679-5	8.842-5	1.007-4	7.837-5	9.439-5
9.00	5.118-5	5.209-5	5.890-5	4.480-5	5.543-5
9.50	3.023-5	3.073-5	3.454-5	2.569-5	3.262-5
10.00	1.787-5	1.816-5	2.030-5	1.478-5	1.922-5

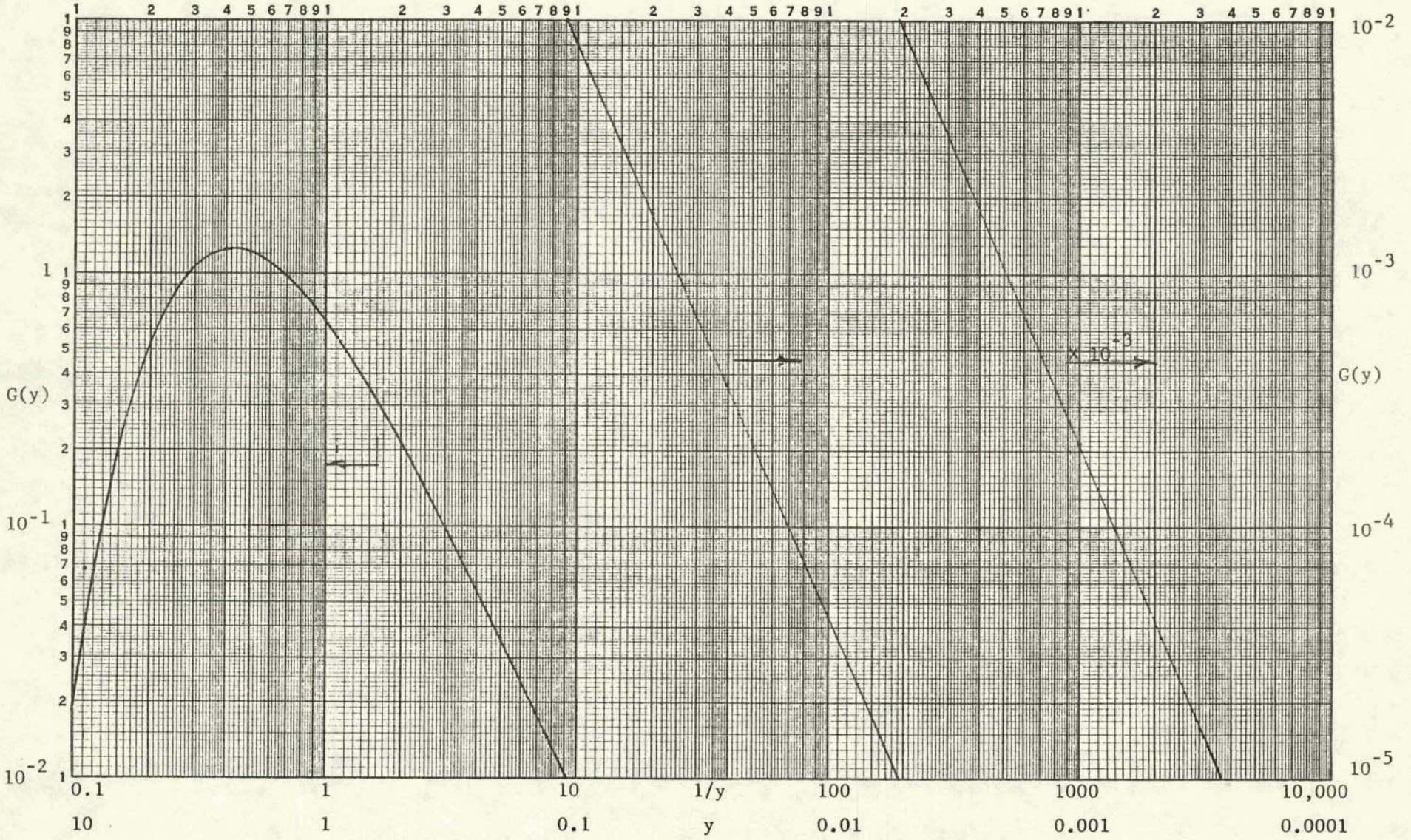

Fig. A1 $G(y) \equiv G_3(y)$

APPENDIX B

Outline of Storage Ring Particle Dynamics

Properties of the synchrotron radiation source depend upon the angular distribution of the radiation process and on the spacial and angular distribution of the electron beam. The radiation angles are a function of λ/λ_c and γ (Section I.2.) and can be controlled to the extent that those parameters can be chosen. Electron beam distributions are a function of the storage ring design and, in an alternating-gradient ring, will vary with circumferential position. In this brief note only the properties of separated-function alternating gradient storage rings will be considered. The separated function ring has dipoles (negligible field gradient) which bend the electron beam a total of 2π and quadrupoles (constant transverse gradient magnets) which supply the restoring forces that keep the beam "focussed". A quadrupole has zero field on its axis and exerts converging, or focussing, forces in one transverse plane and diverging, or defocussing, forces in the normal transverse plane. (Ref. 15, Chap. 6.) A sequence of quadrupoles is normally arranged with focussing and defocussing directions alternating. Such a sequence will then be net focussing over a rather wide range of parameters.

The central orbit of a storage ring is that orbit which will be repetitively traced by a particle of design energy launched precisely on that orbit. The central orbit is constructed by joining circular arcs in the bending magnets to segments of straight lines in the quadrupoles and field free sections ("straight-sections".) Solution of the geometrical problem is done by requiring that the central orbit close on itself. Two examples of very different magnet lattices are shown in Fig. B1 with the central orbit indicated by a dashed line.* In order to ensure that particles will remain indefinitely in the neighborhood of the central orbit when subjected to disturbances and imperfections, strong restoring forces are applied by the quadrupoles inserted in the lattice.

The energy of an electron is continually being changed (in small increments) by photon radiation and by the acceleration system of the ring.

*The examples of this section were selected from a series of orbit studies done by Renate Chasman.

An electron with energy differing from that of the central orbit will then have a different radius of curvature in the bending magnets $\rho = 33.35\ E/B$ (Eq. 16) and will travel on a larger, or smaller, circumference. A closed equilibrium orbit exists for these off-energy particles but the field of the quadrupole is no longer zero off-axis. A recursion function can be written for the motion of an electron through the bending magnets and quadrupoles and this function can be solved, in principle, for the closed equilibrium orbit. Solution is best done numerically by one of the numerous programs used by accelerator designers. If s is the coordinate along the trajectory a momentum function $X_p(s)$ is defined by

$$\Delta x = X_p(s) \frac{\Delta E}{E_o}$$

where Δx is the local setover of the equilibrium orbit for energy change ΔE from the central orbit energy E_o.[16] (The momentum function is also referred to as α_p or η.) In Fig. B2 the X_p is always finite. For this type of FODO lattice the off-axis equilibrium orbit is adjacent to the central orbit but has "wiggle-motion" which is correlated with the focussing periodicity. The triplet lattice functions shown in B3 illustrate the effects of an achromatic bend design. X_p is finite in the bending magnet sectors but is approximately zero in the insertions between sectors.

The radio frequency accelerating waveform has a phase focussing action and the radiation damps the longitudinal motion. This results in the electron beam being compressed into short bunches with energy distribution σ_p which has a minimum value determined by the quantum fluctuations of the photon radiation. (The observed value of σ_p will be increased by intrabeam scattering and by instabilities.) Thus the ensemble of equilibrium orbits in a ring will be a band of width

$$\Delta x(s) = \pm X_p(s)\ \sigma_p$$

about the central orbit.

If an electron is displaced in position and/or angle from its equilibrium orbit it will execute "betatron" oscillations about that orbit. Let s be the distance along the equilibrium orbit and x be the radial and y the vertical displacement from the equilibrium orbit of the electron. A prime will denote the derivative with respect to s. The transverse motion can be described by the phase-amplitude solution

$$x = A_x \beta_x^{\frac{1}{2}} \sin\left(\int \frac{ds}{\beta_x} + \delta_x \right)$$

$$y = A_y \beta_y^{\frac{1}{2}} \sin\left(\int \frac{ds}{\beta_y} + \delta_y \right)$$

Constants A and δ are determined by the initial conditions. β is an amplitude function which can be calculated from the transformation matrix of the ring lattice.[16] Figures B2 and B3 show β as a function of s for the two examples. If β is constant the equations are those of the simple harmonic oscillator with wavelength given by $\beta = \lambda/2\pi$. In an alternating gradient ring the motion is that of an oscillator in which the amplitude multiplier varies while the phase advance speeds up and slows down. One wavelength of betatron oscillation is completed when

$$\int_{s_1}^{s_2} \frac{ds}{\beta} = 2\pi$$

A very important number is the ν value, the number of oscillation cycles per turn

$$\nu = \frac{1}{2\pi} \int_s^{s+C} \frac{ds}{\beta} \quad , \quad C = \text{circumference}$$

In order to avoid resonance effects ν must not be a small rational fraction. One can then visualize the transverse motion as a sinusoid precessing around the ring and superimposed on it a wiggle motion fixed to the magnet lattice and related to $\beta^{\frac{1}{2}}$. If there is a beam circulating with a large number of particles distributed in phase and amplitude the envelope of the betatron oscillations is proportional to $\beta^{\frac{1}{2}}$ vs s.

Define two other variables,

$$\alpha = -\beta'/2$$

$$\gamma = (1 + \alpha^2)/\beta$$

Then α, β, γ are coefficients of the transfer matrices[16] which can be used to transform the position and angle of the betatron motion at any azimuth of the ring to any other azimuth. They are also the coefficients of the Courant-Snyder invariant

$$E_x = \frac{1}{\beta_x}\left[x^2 + (\alpha_x x + \beta_x x')^2\right] = \gamma_x x^2 + 2\alpha_x xx' + \beta_x x'^2$$

(and similarly for y, in uncoupled motion). The right-hand side is the equation of an ellipse in x and x'. Since α, β, γ are functions of s, the shape and inclination of the ellipse in the phase space x, x' will vary with s but the area will remain invariant. A particle with displacement and angle x_1, x_1' at s_o will lie on ellipse

$$E_1 = \gamma(s_o)\, x_1^2 + 2\alpha(s_o)\, x_1 x_1' + \beta(s_o)\, x_1'^2$$

and will transverse the path in phase space defined by E_1 as it goes around the ring. If an ensemble of particles lies within boundary E at s it will lie within E everywhere around the ring. At any s the maximum x of any particle will be

$$\hat{x} = [\beta(s)E]^{\frac{1}{2}}$$

and the maximum angle

$$\hat{x}' = [\gamma(s)E]^{\frac{1}{2}}$$

Enter the ring at a β_{max} or β_{min} where $\alpha = 0$ and consequently $\beta = 1/\gamma$. The ellipse axes lie on x and x' and the area of the ellipse is

$$\pi xx' = \pi E$$

E is the emittance of the beam. There is an E_x and an E_y.

Thus the largest beam size will occur at a β_{max} and the largest divergence at a β_{min}:

$$\hat{x} = [E_x \hat{\beta}_x]^{\frac{1}{2}} \quad ; \quad \hat{x}' = [E_x/\beta_{xmin}]^{\frac{1}{2}}$$

Although the size-angle product of the beam can be considered crudely constant, this is strictly true only at a β_{max} or a β_{min}. Elsewhere the ellipse containing the beam is inclined and the $\hat{x}\hat{x}'$ product will be larger than E.

The foregoing relations are valid for a conservative system or for a radiating system in quasi-equilibrium.

An electron position x_o, x_o' at s_o will be at s_1[16]

$$\begin{vmatrix} x_1 \\ x_1' \end{vmatrix} = \begin{vmatrix} a_{11} & a_{12} \\ a_{21} & a_{22} \end{vmatrix} \begin{vmatrix} x_o \\ x_p' \end{vmatrix}$$

A focussing quadrupole of length ℓ and gradient $G = dB_y/dx$ operating on a particle with magnetic rigity $B\rho$ has transformation matrix;

$$\begin{vmatrix} \cos \ell\sqrt{K} & \frac{1}{\sqrt{K}} \sin \ell\sqrt{K} \\ -\sqrt{K} \sin \ell\sqrt{K} & \cos \ell\sqrt{K} \end{vmatrix}$$

with $K = G/B\rho$

and a defocussing quadrupole has transformation matrix;

$$\begin{vmatrix} \cosh \ell\sqrt{K} & \frac{1}{\sqrt{K}} \sinh \ell\sqrt{K} \\ \sqrt{K} \sinh \ell\sqrt{K} & \cosh \ell\sqrt{K} \end{vmatrix}$$

The same transformations apply to y, y' with focussing and defocussing interchanged, i.e. a focussing quadrupole in the x coordinate is defocussing in the y coordinate and vice versa. A non-focussing section of length ℓ has transformation matrix:

$$\begin{vmatrix} 1 & \ell \\ 0 & 1 \end{vmatrix}$$

(Bending magnets have small focussing effects, especially at their ends, but these effects can be disregarded when examining a source. The axis s in a bending magnet is curvilinear with radius ρ.) Transformation through multiple elements is then a matrix obtained by multiplying the matrices of the elements in succession.

An ellipse

$$\gamma_o x^2 + 2\alpha_o xx' + \beta_o x'^2 = E$$

can be transformed from s_o to s_1 by

$$\begin{vmatrix} \alpha_1 \\ \beta_1 \\ \gamma_1 \end{vmatrix} = \begin{vmatrix} a_{11}a_{22}+a_{12}a_{21} & -a_{11}a_{21} & -a_{12}a_{22} \\ -2a_{11}a_{12} & a_{11}^2 & a_{12}^2 \\ -2a_{21}a_{22} & a_{21}^2 & a_{22}^2 \end{vmatrix} \begin{vmatrix} \alpha_o \\ \beta_o \\ \gamma_o \end{vmatrix}$$

in which the a_{ij} are the elements of the x,x' transformation matrix from s_o to s_1. The determinant of this matrix must be 1 so $a_{11}a_{22} - a_{12}a_{21} = 1$. If there is no focussing this becomes;

$$\begin{vmatrix} \alpha_1 \\ \beta_1 \\ \gamma_1 \end{vmatrix} \quad \begin{vmatrix} 1 & 0 & -\ell \\ -2\ell & 1 & \ell^2 \\ 0 & 0 & 1 \end{vmatrix} \quad \begin{vmatrix} \alpha_o \\ \beta_o \\ \gamma_o \end{vmatrix}$$

or

$$\alpha_1 = \alpha_o - \ell\gamma_o$$

$$\beta_1 = 2\ell\alpha_o + \beta_o + \ell^2\gamma_o$$

$$\gamma_1 = \gamma_o$$

If initial conditions of α, β, γ are known from design tables or from curves such as Figs. B2, B3 then coefficients are readily determined at distance ℓ along s. An important special case begins at the center of an insertion where β_o is a minimum,

$\alpha_o = -\beta'/2 = 0$ and $\gamma_o = (1+\alpha^2)/\beta_o = 1/\beta_o$. Then the equations simplify to

$$\alpha_1 = -\ell\gamma_o = -\ell/\beta_o$$

$$\beta_1 = \beta_o + \ell^2\gamma_o = \beta_o + \ell^2/\beta_o$$

$$\gamma_1 = \gamma_o = 1/\beta_o$$

The electron beam configuration of a source is determined from the ring parameters at the azimuth, or s, of the source. It is usually adequate to assume that the vertical equilibrium orbits lie in the median plane and that there is zero vertical momentum function. The vertical emittance and vertical amplitude functions at the chosen azimuth then give the vertical size and angular distribution.

Radial distribution of the equilibrium orbits is given by $\sigma_p X_p$ with σ_p the variance of energy spread $\Delta E/E$. Betatron oscillations occur about these equilibrium orbits with variance σ_x obtained from the emittance and horizontal amplitude functions. The energy oscillations are at a low frequency, the betatron oscillations are at a high frequency, and the two are uncorrelated. The horizontal width variance is obtained by adding in quadrature

$$\sigma_h^2 = (\sigma_p X_p)^2 + \sigma_x^2$$

It is often sufficient to assume that X_p is constant at the value at the center of the source.

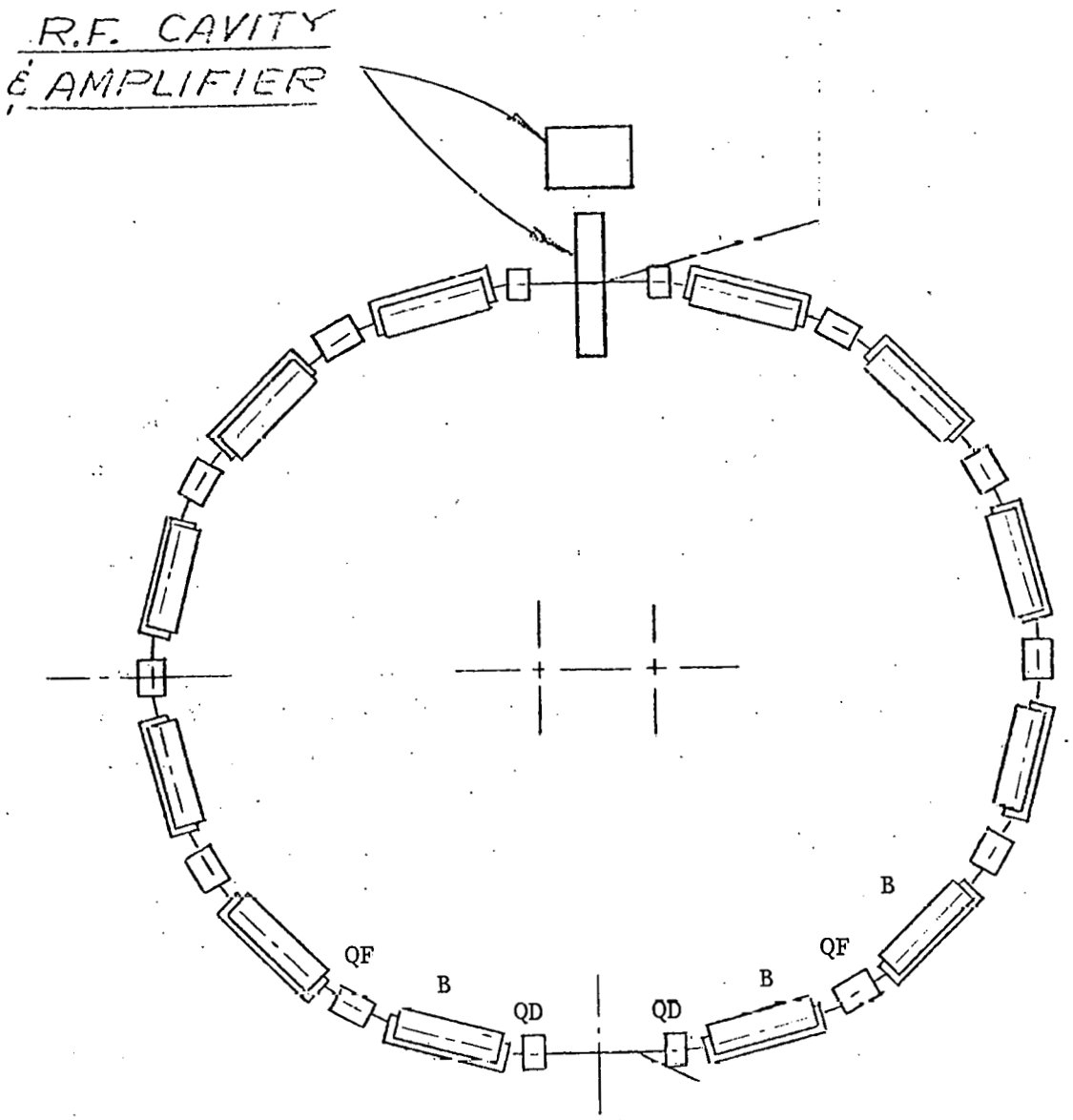

Fig. B1a. Ring with FODO lattice. Q-quadrupole, B-bending magnet.

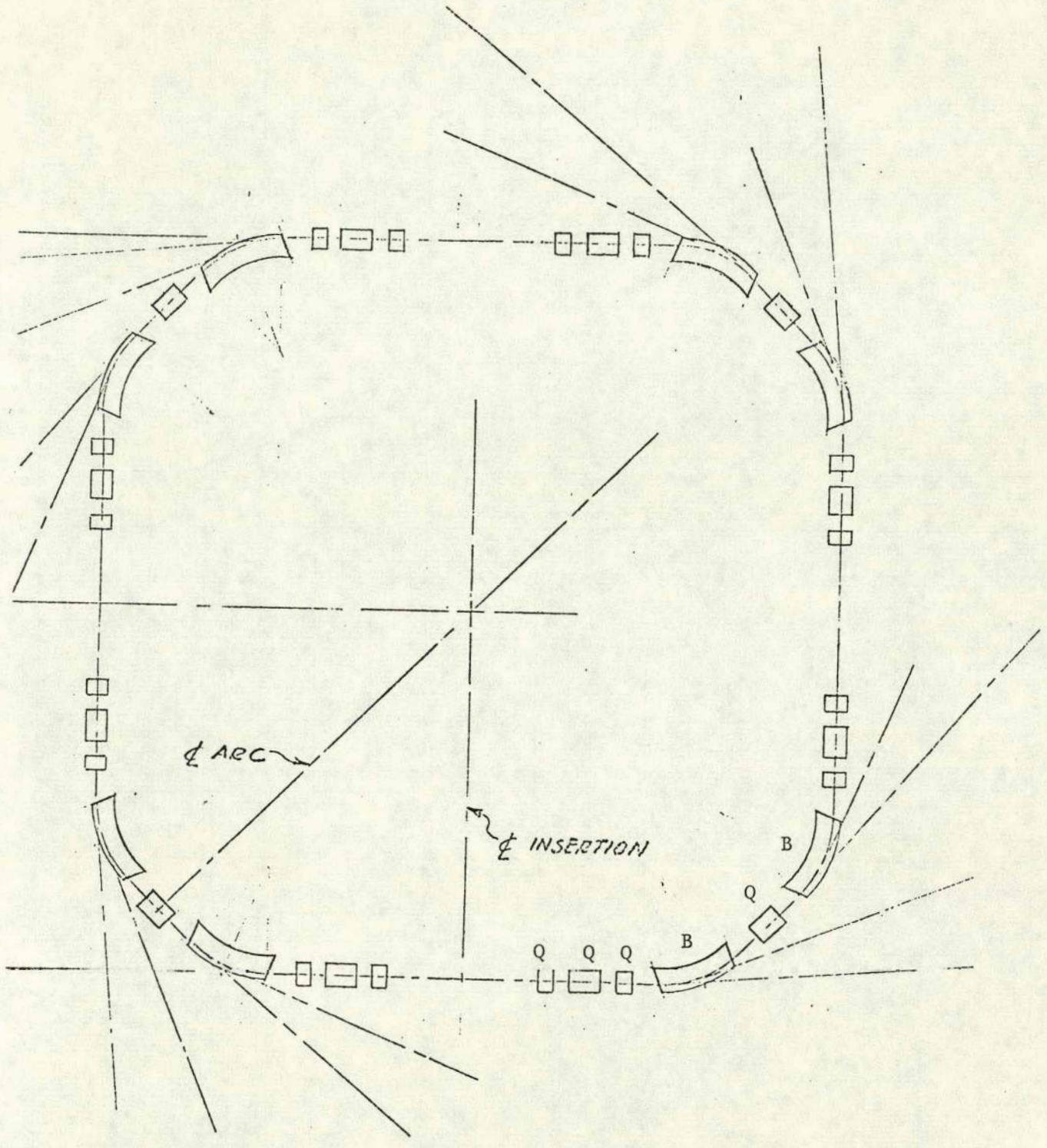

Fig. B1b. Ring with triplett lattice. Q-quadrupole, B-bending magnet.

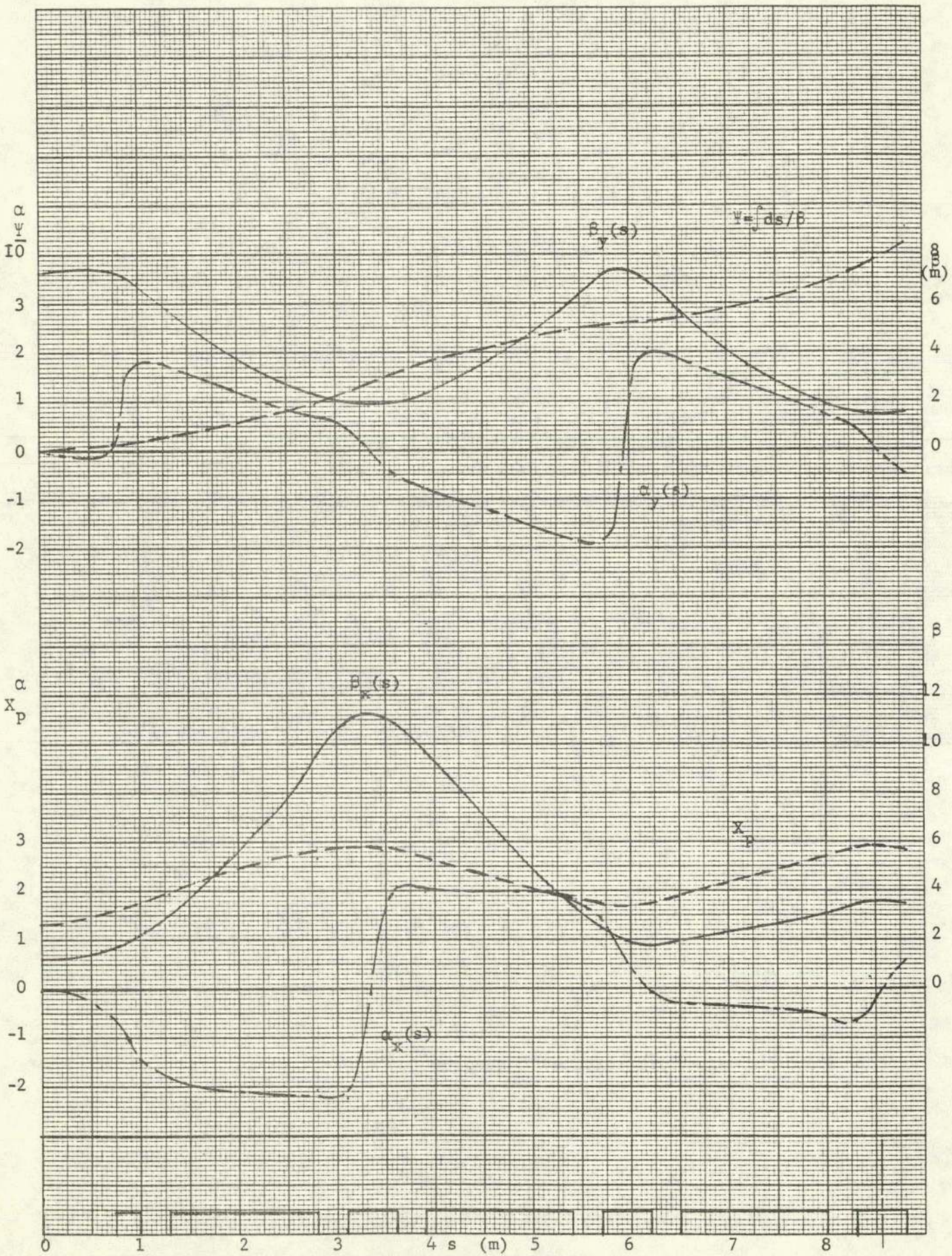

Fig.B 2. FODO amplitude functions and phase advance.

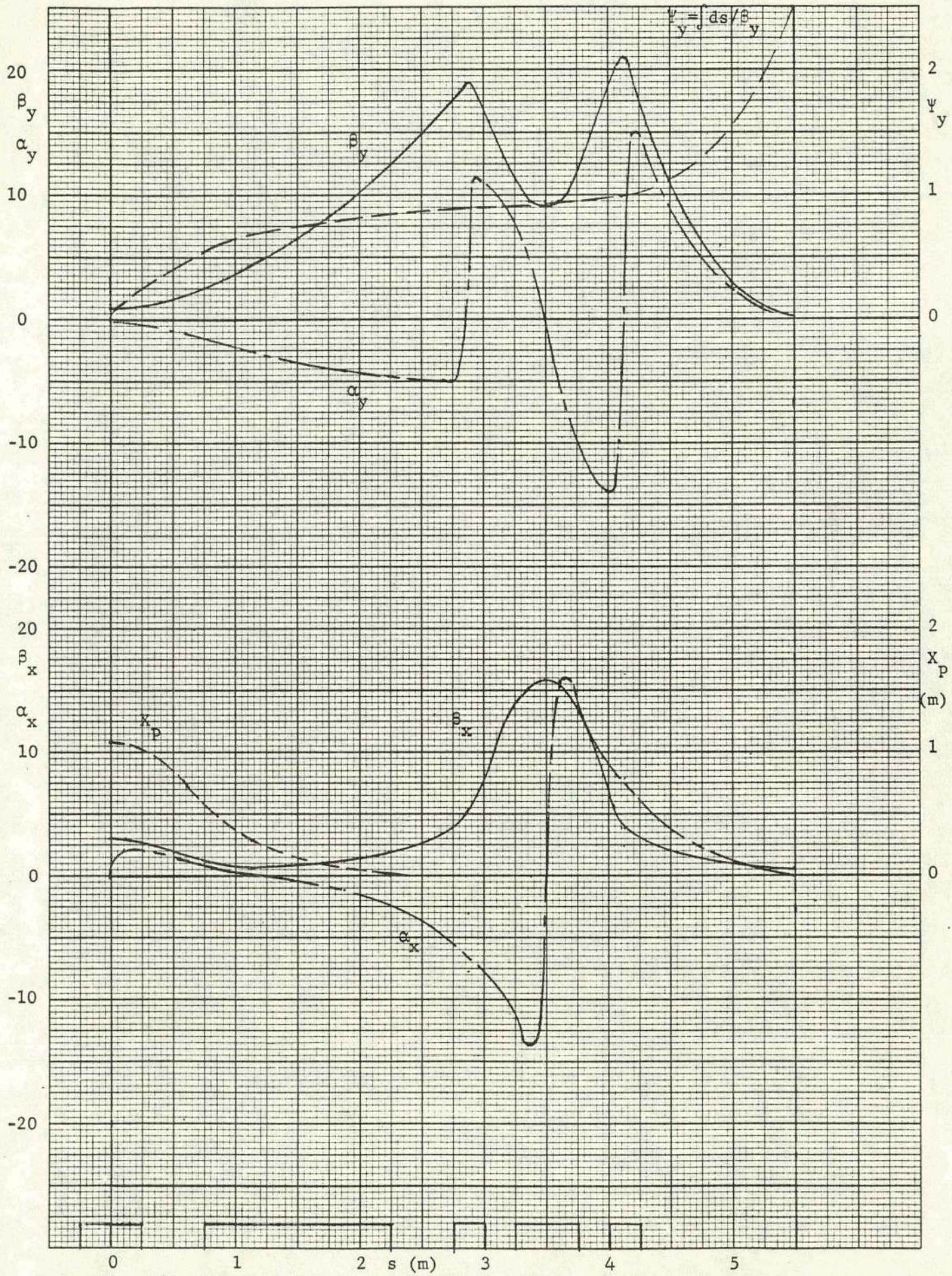

Fig. B3. Triplett lattice amplitude functions and phase advance.

APPENDIX C

Exponential Integrating Function ef(a,Y)

A function of z

$$\int_o^{z_1} \frac{1}{\sqrt{b^2 + c^2 z^2}} e^{-\frac{1}{2}\frac{y^2}{(b^2 + c^2 z^2)}} dz$$

in which b, c, and y are constants can be transformed by

$$\cos t = \frac{b}{\sqrt{b^2 + c^2 z^2}}, \quad \tan t = \frac{cz}{b}, \quad dz = \frac{b}{c} \sec^2 t \, dt$$

to $$\frac{1}{c} \int_0^{\tan^{-1}\frac{cz_1}{b}} \frac{1}{\cos t} e^{-\frac{y^2}{2b^2}\cos^2 t} dt$$

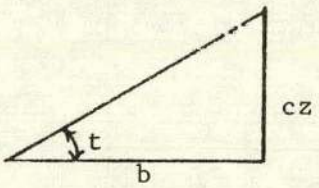

Define $$ef(a,Y) = \int_o^Y \frac{1}{\cos t} e^{-\frac{a^2}{2}\cos^2 t} dt \qquad Y < \frac{\pi}{2}$$

with, for f(z), $a = y/b$, $\tan Y = cz_1/b$

To normalize, Ref. 11 No. 492,

$$\int_o^Y \int_o^\infty \frac{1}{\cos t} e^{-\frac{a^2}{2}\cos^2 t} dt \, da = \sqrt{\frac{\pi}{2}} \int_o^Y \frac{1}{\cos^2 t} dt = \sqrt{\frac{\pi}{2}} \tan Y$$

or $$\int_{-\infty}^{\infty} ef(a,Y) \, da = \sqrt{2\pi} \tan Y$$

At $a = 0$

$$ef(o,Y) = \int_o^Y \frac{dt}{\cos t} = \frac{1}{2} \ell n \left(\frac{1+\sin Y}{1-\sin Y}\right) \qquad \text{(Ref. 11. No. 288)}$$

If $Y < 0.1$ $\cos t \approx 1$

and $$ef(a,Y) \simeq \int_o^Y e^{-\frac{a^2}{2}} dt = Y e^{-\frac{a^2}{2}}$$

$$\int_0^{z_1} \frac{1}{\sqrt{b^2+c^2z^2}} e^{-\frac{1}{2}\frac{y^2}{(b^2+c^2z^2)}} dz = \frac{1}{c} ef(a,Y)$$

with $a = y/b$, $\tan Y = cz_1/b$

Graphs of ef(a,Y) and ef(O,Y) are Figs. C1 and C2. A short table of the function is included as Table CI. This table was kindly programmed and run by Kurt Jellett.

TABLE CI ef(a,Y)

Mantissa following table entry denotes power of ten multiplier.

tan Y	Y \ a	0	0.25	0.5	1.0	1.5	2.0	3.0
.1003	0.1	0.1002	0.9710-1	0.8843-1	0.6086-1	0.3264-1	0.1365-1	1.130-3
.2027	.2	.2013	0.1952	0.1780	0.1229	.6636-1	.2799-1	2.378-3
.3093	.3	.3046	.2955	.2698	.1875	0.1023	.4382-1	3.898-3
.4228	.4	.4111	.3991	.3652	.2561	.1418	.6210-1	5.921-3
.5463	.5	.5222	.5075	.4656	.3302	.1865	.8411-1	8.839-3
.6841	.6	.6396	.6222	.5728	.4119	.2384	0.1116	1.334-2
.8423	.7	.7654	.7455	.6890	.5035	.3001	.1471	2.069-2
1.030	.8	.9022	.8800	.8170	.6082	.3759	.1942	3.314-2
1.260	.9	1.054	1.030	.9607	.7304	.4683	.2579	5.477-2
1.557	1.0	1.226	1.200	1.126	.8759	.5861	.3457	9.277-2
1.965	1.1	1.428	1.400	1.321	1.054	.7389	.4690	1.596-1
2.572	1.2	1.674	1.645	1.562	1.280	.9430	.6456	2.766-1
3.010	1.25	1.821	1.792	1.708	1.420	1.073	.7631	3.649-1
3.602	1.30	1.993	1.964	1.878	1.585	1.229	.9082	4.824-1
4.455	1.35	2.200	2.169	2.083	1.785	1.422	1.091	6.406-1
5.798	1.40	2.458	2.428	2.340	2.039	1.670	1.331	8.588-1
8.238	1.45	2.806	2.775	2.687	2.383	2.009	1.665	1.175
14.101	1.50	3.341	3.310	3.221	2.915	2.539	2.190	1.689
16.428	1.51	3.493	3.462	3.373	3.067	2.691	2.341	1.839
19.670	1.52	3.673	3.642	3.553	3.247	2.870	2.520	2.016

Blank indicates value less than 10^{-6}

Y \ a	4.0	5.0	6.0	7.0	8.0	10	20
0.1	3.452-5						
.2	7.547-5						
.3	1.327-4	1.744-6					
.4	2.259-4	3.536-6					
.5	3.992-4	8.171-6					
.6	7.594-4	2.232-5					
.7	1.574-3	7.124-5	1.957-6				
.8	3.526-3	2.540-4	1.229-5				
.9	8.334-3	9.592-4	8.119-5	4.918-6			
1.0	2.019-2	3.643-3	5.261-4	5.944-5	5.190-6		
1.1	4.874-2	1.332-2	3.142-3	6.289-4	1.057-4	1.725-6	
1.2	1.149-1	4.529-2	1.646-2	5.432-3	1.615-3	1.024-4	
1.25	1.741-1	8.077-2	3.547-2	1.456-2	5.545-3	6.319-4	
1.30	2.615-1	1.407-1	7.325-2	3.652-2	1.733-2	3.316-3	
1.35	3.903-1	2.396-1	1.451-1	8.578-2	4.929-2	1.473-2	3.336-6
1.40	5.817-1	4.014-1	2.770-1	1.895-1	1.280-1	5.557-2	2.365-4
1.45	8.760-1	6.695-1	5.162-1	3.988-1	3.076-1	1.804-1	7.444-3
1.50	1.374	1.148	9.724-1	8.297-1	7.111-1	5.258-1	1.100-1
1.51	1.521	1.293	1.113	9.668-1	8.439-1	6.487-1	1.745-1
1.52	1.697	1.466	1.283	1.133	1.007	8.027-1	2.714-1

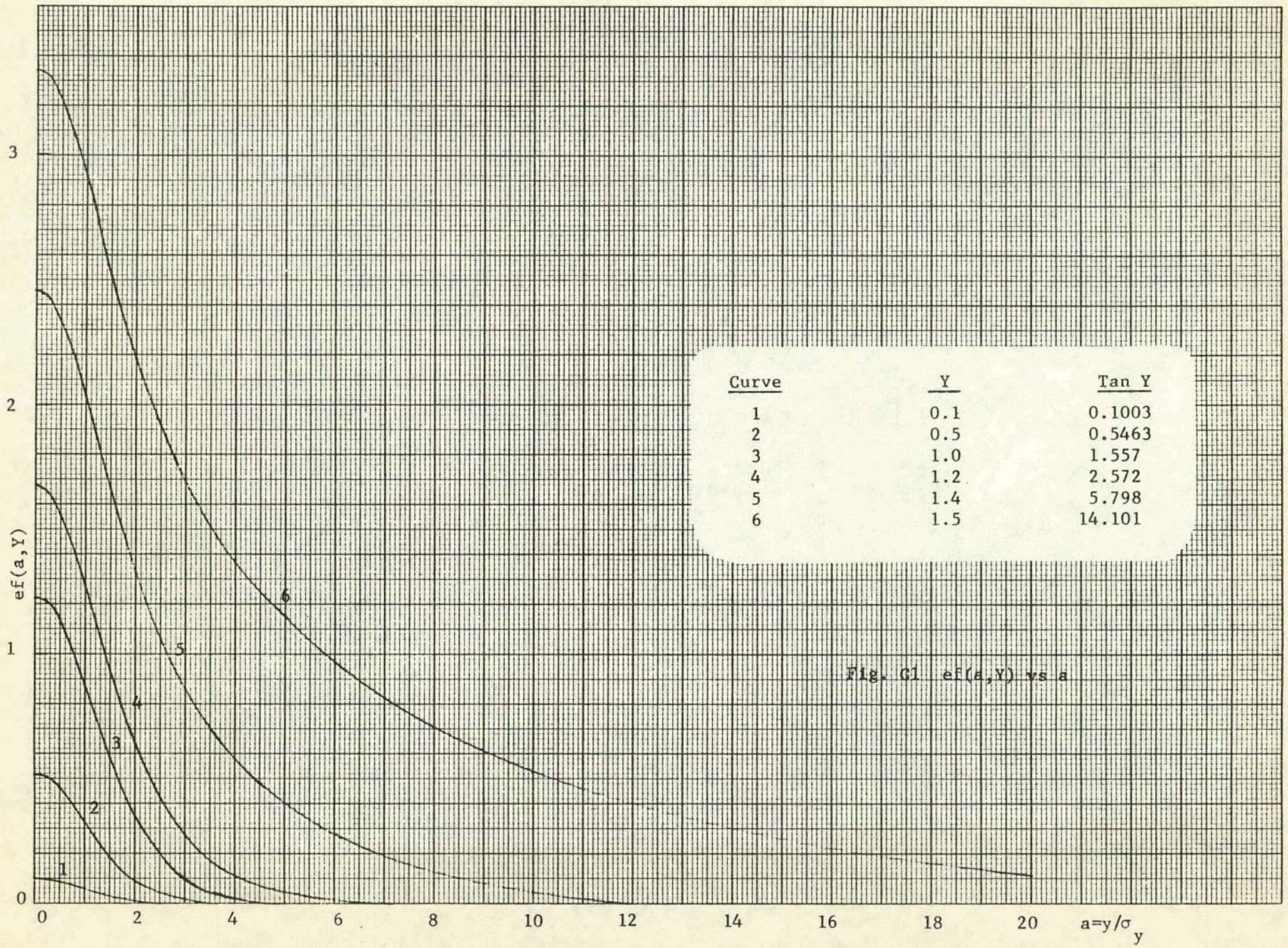

Curve	Y	Tan Y
1	0.1	0.1003
2	0.5	0.5463
3	1.0	1.557
4	1.2	2.572
5	1.4	5.798
6	1.5	14.101

Fig. C1 ef(a,Y) vs a

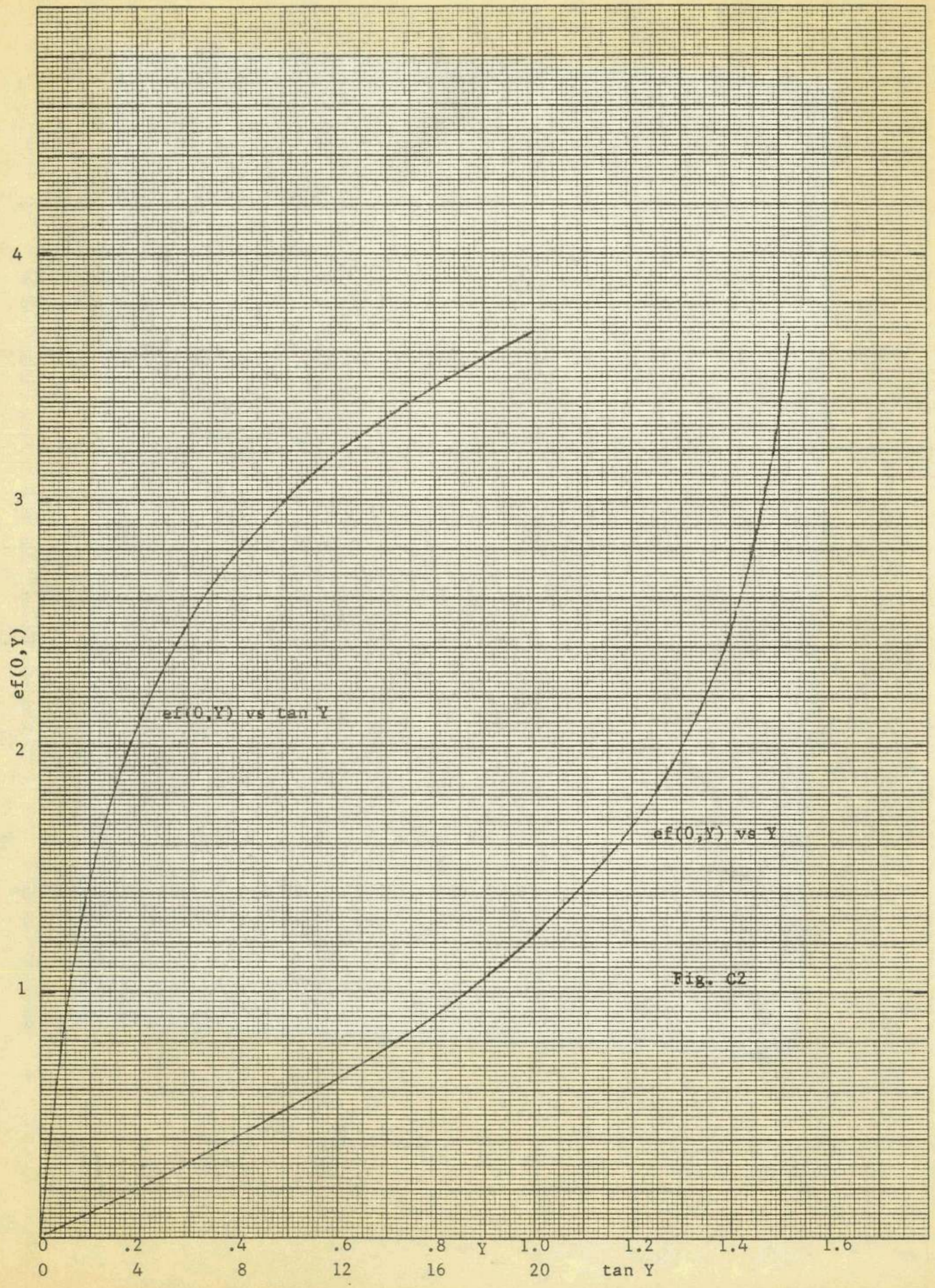
4
3
2
1
ef(0,Y)
ef(0,Y) vs tan Y
ef(0,Y) vs Y
0
.2
.4
.6
.8
Y
1.0
1.2
1.4
1.6
0
4
8
12
16
20
tan Y

Fig. C2